FATIGUE BEHAVIOUR ANALYSIS OF DIFFERENTLY HEAT TREATED MEDIUM CARBON STEEL

A THESIS SUBMITTED IN PARTIAL FULFILLMENT

OF THE REQUIREMENTS FOR THE DEGREE OF

Master of Technology (Res.)

in

Metallurgical and Materials Engineering

By

Sweta Rani Biswal

Roll No- 608MM301

Department of Metallurgical and Materials Engineering

National Institute of Technology

Rourkela

FATIGUE BEHAVIOUR ANALYSIS OF DIFFERENTLY HEAT TREATED MEDIUM CRABON STEEL

A THESIS SUBMITTED IN PARTIAL FULFILLMENT

OF THE REQUIREMENTS FOR THE DEGREE OF

Master of Technology (Res.)

in

Metallurgical and Materials Engineering

By

Sweta Rani Biswal

Roll No- 608MM301

Under the Guidance of

Dr. SUDIPTA SEN

Asso. Professor

Department of Metallurgical and Materials Engineering

National Institute of Technology

Rourkela

Department of Metallurgical and Materials Engineering
National Institute of Technology
Rourkela

CERTIFICATE

*This is to certify that the work in this thesis report entitled "***Fatigue Behaviour Analysis of Differently Heat Treated Medium Carbon Steel***" which is being submitted by* ***Ms. Sweta Rani Biswal*** *(Roll no: 608MM301) of Master of Technology(Res.), National Institute of Technology, Rourkela has been carried out under my guidance and supervision in partial fulfillment of the requirements for the degree of Master of Technology (Res.) in Metallurgical and Material Engineering and is bonafide record of work.*

To the best of my knowledge, the matter embodied in the thesis has not been submitted to any other University / Institute for the award of any Degree or Diploma.

(Dr.) Sudipta Sen
Associate Professor
Dept. of Metallurgical and Materials Engineering
National Institute of Technology
Rourkela- 769 008

Date:
Place: NIT, Rourkela

ACKNOWLEDGEMENT

With deep regards and profound respect, I avail this opportunity to express my deep sense of gratitude and indebtedness to Dr. Sudipta Sen, Associate Professor, Department of Metallurgical and Materials Engineering for introducing the present research topic and for his inspiring guidance, constructive criticism and valuable suggestion throughout in this research work. It would have not been possible for me to bring out this thesis without his help and constant encouragement.

I am sincerely thankful to Prof. (Dr.) B. B. Verma, Head, Department of Metallurgical and Materials Engineering, for his advice and providing necessary facility for my work.

I would also like to thank Prof. (Dr.) S. C. Mishra, Department of Metallurgical and Materials Engineering, NIT Rourkela, and Prof. (Dr.) P. K. Ray, Department of Mechanical Engineering for helping and for their talented advices.

Special thanks to Mr. Rajesh Pattnaik, Mr. Hembram, of the department for being so supportive and helpful in every possible way. I am also thankful to Ms. Abhipsa Mohapatra for her kind support throughout my research period.

I am highly grateful to all staff members of Department of Metallurgical and Materials Engineering, NIT Rourkela, for their help during the execution of experiments and also thank to my well wishers and friends for their kind support.

I feel pleased and privileged to fulfill my parents' ambition and I am greatly indebted to my family members and parents for bearing the inconvenience during my M.Tech (Res.) course.

Jan, 2013 **Sweta Rani Biswal**

CONTENTS

ABSTRACT

The utility of medium carbon steel is well known now-a- days. It has got so many applications in different industries. The importance of fatigue failure of materials is a very important topic in the field of mechanical behavior of materials since 90% of failures resulted from mechanical causes is due to fatigue. In the present work fatigue of medium carbon steel (EN9 grade) has been studied. Since the mechanical properties are greatly influenced by heat-treatment techniques, the effect of various heat treatment operations (like annealing, normalizing, tempering) on fatigue life has been investigated.

The emphasis has been given on the value of endurance limit. The change in the value of endurance limit of the material concerned as a result of various heat-treatment operations were studied thoroughly. It has been found that the specimens tempered at low temperature (200^0C) exhibits the best results as far as fatigue strength is concerned.

LIST OF FIGURES

LIST OF TABLES

Chapter 1

1. INTRODUCTION

INTRODUCTION

Way back in 1850, it was observed that a material, when subjected to cyclic (or dynamic) loading, would fail at a much lower stress than that required to cause failure in static loading. The failure under dynamic loading was termed “fatigue” by the scientists. Later, it was found that nearly 90% of material failure due to mechanical cause resulted from fatigue. So, the study on fatigue failure became very important and since then enormous work has been done in order to study different aspects of fatigue failure and to develop various methods to prevent this mechanical phenomenon. Different experiments have done different types of work in this regard to determine different features of this type of failure.

In the present work, the dependence of fatigue strength of differently heat-treated steels has been studied. There is practically no doubt about the fact that steel is a very important engineering material and wide range of different mechanical properties can be developed in steel by means of heat-treatment technique. The material selected for the present work is medium carbon steel since its properties are greatly affected by various heat-treatment procedures like annealing, normalizing and most importantly tempering. The material, En9 steel (0.55%C), was subjected to different heat-treatment procedures like annealing, normalizing and tempering. Tempering was performed at different temperatures and for different time intervals. The endurance limit (the stress below which no fatigue failure is possible despite the application of innumerable no. of cycles) has been determined in all cases. The effect of heat-treatment on the mechanical property has been studied. The microstructure of differently heat-treated steels has also been studied and efforts are made to correlate the microstructure with the fatigue or endurance limit.

In this way efforts have been made to study the relation between the microstructure and fatigue strength. Fractographic analysis of different specimens failed due to dynamic loading has also been carried out with the help of scanning electron microscope. Efforts have been made to correlate the different aspects of fractographic study of microstructure and fatigue strength of differently heat-treated medium carbon steels.

Chapter 2

2. LITERATURE REVIEW

LITERATURE REVIEW

2.1. BACKGROUND OF STEEL

In last 20 years, there have been major advances in the field of production of steel. Steel is the most important alloy which is used as a structural material and this work will show some technological advances in steel heat treatment. The micro-structures of most steels are well known for their effects on mechanical properties under different heat treatment conditions. For instance, both martensite (obtained during rapid cooling) and pearlite (obtained during slow cooling) comes from austenite.

Steel is an alloy formed by combining iron and small amount of carbon content (0.2% and 2.1% by weight) depending upon the type. Lacktin[1] explained that carbon is the most appropriate material for iron to make bond in steel; it also solidifies the inherent structures of iron. By experimenting with the different amounts of carbon present in the alloys, many properties like density, hardness and malleability can be adjusted. By increasing the level of carbon in steel, we can make steel more structurally delicate as well as harder at the same time.

Other alloying elements such as manganese, chromium, vanadium, silicon and tungsten are also present in steel. Carbon and these alloying elements act as a hardening agent, preventing dislocations in the iron atom crystal lattice from sliding past one another. Varying the amount of alloying elements also enhance the qualities such as the hardness, ductility, and tensile strength of the resulting steel.

According to the varying alloying elements steel can be classified in two types. These are carbon steel and alloy steel and it also again classified as follows which is shown in Fig 2.1.

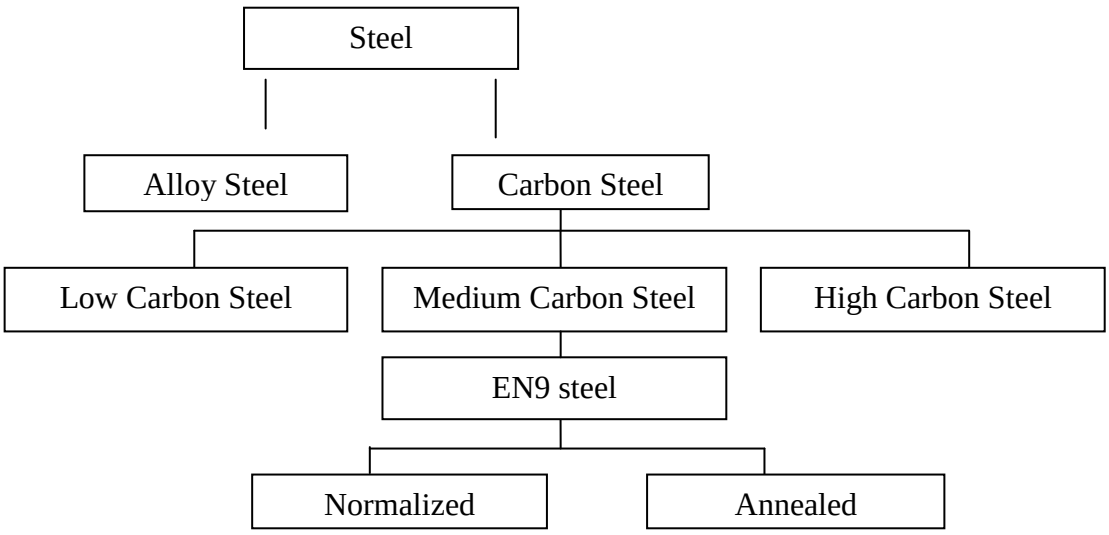

Fig 2.1: **Classification of Steels (Lovatt and Shercliff, 2002)**

2.2. HISTORY OF STEEL

2.2.1. Plain Carbon Steel

Plain carbon steel is essentially an alloy of iron and carbon which also contains manganese and a variety of residual elements. These residual elements are added in a smaller amount. The American Iron and Steel Institute (AISI) has defined a plain carbon steel to be an alloy of iron and carbon which contains specified amounts of Mn below to a maximum amount of 1.65 % wt., less than 0.6 % wt. Si, less than 0.6 % wt. Cu and which does not have any specified minimum content of any other deliberately added alloying element [2]. It is usual for maximum amounts (e.g. 0.05 % wt.) of S and P to be specified. As carbon content rises, the metal becomes harder and stronger but less ductile and more difficult to weld. Higher carbon content lowers steel melting point and its temperature resistance in general [3].

These steels usually are iron with less than 2 percent carbon, plus small amounts of chromium, cobalt, columbium [niobium], molybdenum, nickel, titanium, tungsten, vanadium or zirconium manganese, phosphorus, sulphur, and silicon. The weld ability and other characteristics of these steels are primarily a product of carbon content, although the alloying and residual elements do have a minor influence.

Some other residual elements like manganese, sulphur, phosphorus are also present after refining of plain carbon steel which has some influence on the properties of steel. In plain carbon steel, the residual elements like Mn (1.65% max) and Si (0.6% max) are present [4]. Mainly, carbon steel is an alloy made up of the residual elements which is shown in the table below.

Elements	Maximum weight %
C	1.00
Mn	1.65
P	0.40
Si	0.60
S	0.05

Table 2.1: **Percentage of Weight of Residual Elements in Plain Carbon Steel**

Out of these elements, phosphorus, sulphur, silicon has negative impact. Some other residual elements are also present but that does not have any significant effects on plain carbon steel.

2.2.2. Effect of Residual Elements on Steel

Like already stated above sulphur, phosphorus, silicon are undesirable due to their drawbacks. In fact, here more details of the description of effects of the residual elements like the ductility and toughness hinder due to the presence of phosphorus when the plain carbon steel undergoes heat treatment like quenching and tempering and also it has a tendency to form a compound with iron which is brittle. So, the presence of phosphorus reduces the ductility, where as silicon is not that harmful to steel but it also has some negative impact on its properties like the surface quality reduces.

Like phosphorus, it also reacts with iron to form sulphide which produces red or hot shortness since the low melting eutectic forms in network around the grain, which holds them loosely. So, break up of grain boundaries can easily occur during hot forming. So, it plays a great role to drop the impart toughness and ductility.

From above, we can conclude that these residual elements are normally disadvantageous to steel but still if they present in some amount they able to import some beneficial properties to steel. Both manganese and silicon have ability to improve their toughness and hardness, when used in an appropriate proportion. The reason behind this can be explained as; they can dissolve in austenite and cause a significant decrease in the transformation rate of the austenite phase to pearlite or upper bainite. But, at the same time silicon has a tendency to combine with others which has been already discussed [5].

Material	**Density 10^3 kg/m^3**	**Thermal conductivity $Jm^{-1}K^{-1}s^{-1}$**	**Thermal expansion 10^{-6} K^{-1}**	**Young's Modulus in Mpa**	**Tensile strength in Mpa**	**% elongation**
0.2%c steel	7.86	50	11.7	210	350	30
0.4%c steel	7.85	48	11.3	210	600	20
0.8%c steel	7.84	46	10.8	210	800	8

Table 2.2: **Physical Properties of Plain Carbon Steel**

Carbon increases the strength and hardness but a higher amount of it will lead to the ductility. It promotes de-oxidation of molten steel by forming silicon dioxide. It also increases the castability. Manganese counteracts the ill effects of sulphur present which increases the strength and hardness. It also promotes soundness of steel casting through its deoxidizing action. Phosphorus when dissolved in ferrite, increases the strength and hardness but in larger quantity, it reduces the ductility. Sulphur

reduces the ability to form iron carbide. It lowers toughness but imparts brittleness to chips removed in machining operation [6].

Its strength is primarily a function of its carbon content, which increases with rise of carbon amount. The ductility of plain carbon steels decreases as the carbon content increases. Some advantages and disadvantages of plain carbon steel are:-

Advantages of Plain Carbon Steel -

- Possesses good formability and weldability.
- Good toughness and ductility.
- Hardness and wear resistance is high.

Disadvantages of Plain Carbon Steel -

- The harden-ability is low.
- The physical properties (Loss of strength and embrittlement) are decreased by both high and low temps and subject to corrosion in most environments.

With varying carbon percentage in steel alloy, it can be subdivided into three groups. It has been shown (Lindberg 1977) [7] that, carbon steel with carbon content between 0.3% and 0.8% is termed as medium carbon steel. While those with lower and higher are respectively classified as mild and high carbon steel.

2.2.3 Types of Steel

Low Carbon Steel

It contains less than 0.3% carbon. Usually ferrite and pearlite, and the material are generally used as it comes from the hot forming or cold forming processes. Lacks in hardenability because of carbon content who helps to do this. Low carbon steel bears low tensile strength and higher ductility compared with other carbon steel. The properties variation is tabulated below in Table 2.3.

S.K Akay [8] explained that before the heat treatment, microstructure of the steel materials shown in the Fig.2.2 has ferrite (dark areas) plus pearlite (light areas) microstructure. The pearlite is distributed uniformly but as irregular shaped volumes embedded in the ferrite matrix.

Properties of Low Carbon Steel	Value (Unit)
Young's Modulus, E	207 GPa
Yield Strength	220 – 250 MPa
Tensile Strength	400 – 500 MPa
Elongation	23%

Table 2.3: S**tandard Properties of Low Carbon Steel (Everett, 1994)**

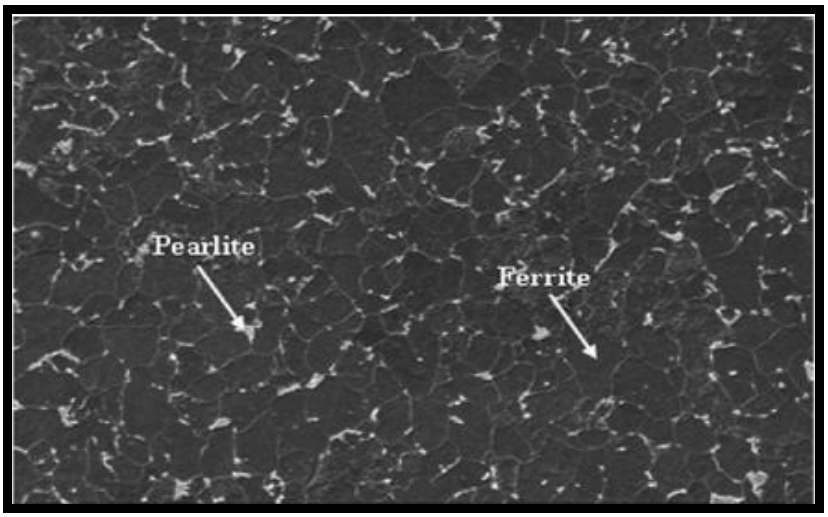

Fig. 2.2: **SEM micrographs of the microstructure of 0.05%wt C steel ferrite(dark) and pearlite(light), optical micrograph x 709 [8]**

Medium Carbon Steel

Medium carbon steel is the most commercial steel. Due to its relatively low price and better mechanical properties such as high strength and toughness, it is acceptable for many engineering applications. This type of steel contains carbon content in between 0.3% - 0.8%. The microstructure of this kind of steel is shown in Fig 2.3 [9].

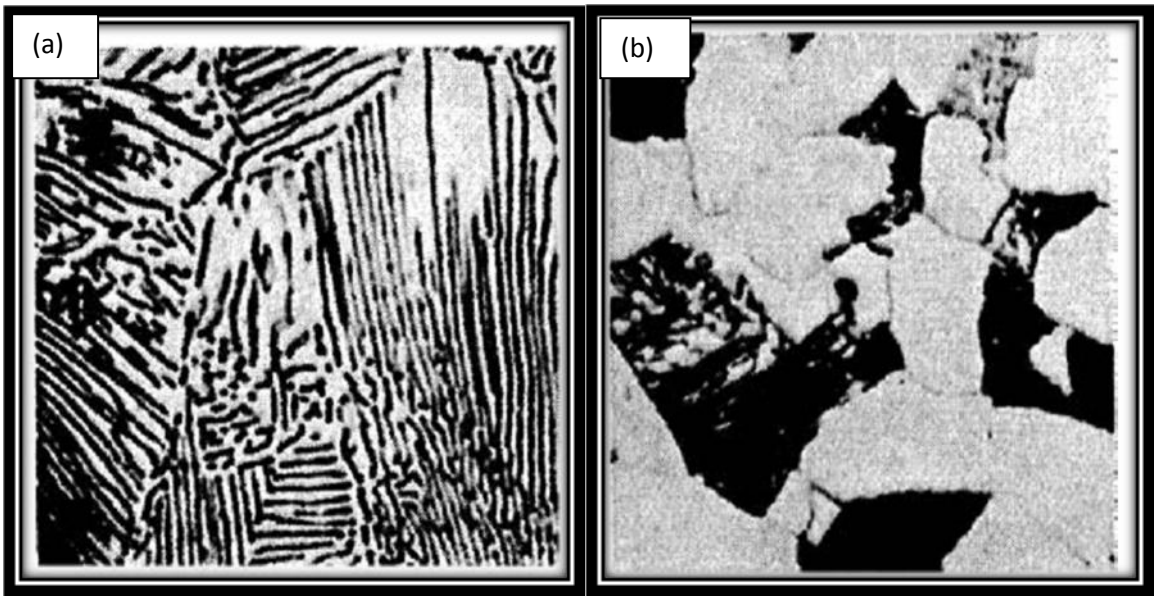

Fig 2.3: **(a) 0.8% wt C steel pearlite (Ricks), Optical micrograph ×1000 and (b) 0.4% wt C steel–ferrite and pearlite (courtesy of Ricks), Optical micrograph ×1100 [9].**

Special Advantages of Medium Carbon Steel -

- Machinability is 60%-70%; therefore cut slightly better than low carbon steels. Both hot and cold rolled steels machine better when annealed. It is less machinable than high carbon steel since that is very hard steel. When welding, there may be some martensite when extreme rapid cooling. So, pre-heat (500 ^{0}F - 600 ^{0}F) and post-heat (1000 ^{0}F - 1200 ^{0}F) will help to remove brittle structure.
- Good toughness and ductility. Enough carbon to be quenched to form martensite and bainite (if the section size is small).
- A good balance of properties can be found. That is optimum carbon level where high toughness and ductility of the low carbon steels is compromised with the strength and hardness of the increased carbon.
- Extremely popular and have numerous applications.
- Fair formability
- Responds to heat treatment but is often used in the natural condition.

Disadvantages of Medium Carbon Steel -

- The harden-ability is low.
- The loss of strength and embrittlement are decreased by both high and low temperatures.
- Subject to corrosion in most environments.

Typical Uses of Medium Carbon Steel -

- 0.3 - 0.4: Lead screws, Gears, Worms, Spindles, Shafts, and Machine parts.
- 0.4 - 0.5: Crankshafts, Gears, Axles, Mandrels, Tool shanks, and Heat-treated machine parts.
- 0.5 - 0.6: Railways rails, Laminated springs, Wire ropes, Wheel spokes and Hammers for pneumatic riveters
- 0.6 - 0.7: Called "low carbon *tool steel*" and is used where a keen edge is not necessary, but where shock strength is wanted. Drop hammers dies, set screws, screwdrivers, and arbors.
- 0.7 - 0.8: Tough & Hard Steel. Anvil faces, Band saws, Hammers, Wrenches, Cable wire, etc.

Medium carbon steel may be heat treated by austenitizing, quenching and then tempering to improve their mechanical properties. Such heat treatment of the steels for the purpose of improvement in mechanical properties have been studied previously by many researchers [5]. Basically, 0.5%-0.6% C having steels are used in practical condition with variable loading condition due to this fatigue failure will arise and to avoid this kind of failure some metallurgical variable should be considered. As the research is based upon this composition, the further study will be explained later in the next chapters.

High Carbon Steel

High carbon steel will contain over 0.8% carbon and less than 2.11% carbon. In Fig 2.4, the microstructure of high carbon steel is shown.

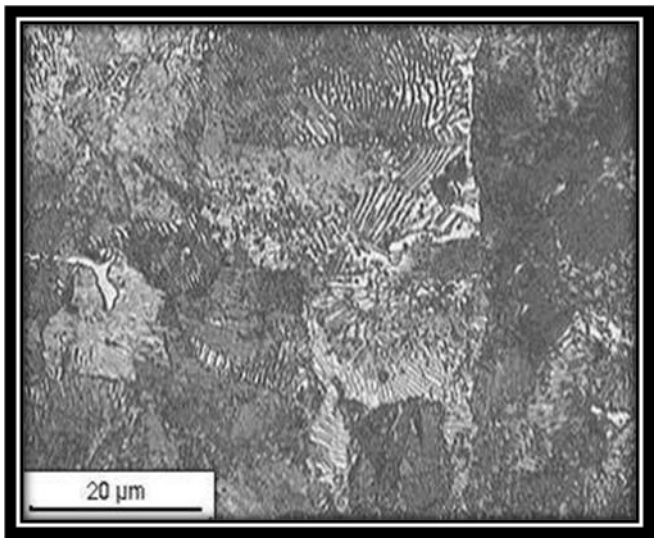

Fig. 2.4: **Microstructure of High Carbon Steel (0.8% Carbon) showing Pearlite.**

Advantages of High Carbon Steel -

- The hardness and wear resistance is high.
- Fair formability.

Disadvantages of High Carbon Steel -

- Toughness, formability and hardenability are quite low.
- Not recommended for welding.
- Usually, joined by brazing with low temperature silver alloy making it possible to repair or fabricate tool-steel parts without affecting their heat treated condition.

An engineer desire these materials because they can be used for so many different things which greatly simplifies the designing process of a project and enables the actual final project to be more versatile at the same time. In an engineer point of view it is necessary to improvise the material's properties in a cheapest manner to use in various fields. That's why they were taken the help of heat treatment processes to enhance the material properties and versatility.

Steel can be heat treated which allows parts to be fabricated in an easily-formable soft state. If enough carbon is present, the alloy can be hardened to increase strength, wear, and impact resistance. Steels are often wrought by cold working methods, which is the shaping of metal through deformation at a low equilibrium or meta- stable temperature. As explained by Smith [10] that high carbon steel content lowers the steel melting point and its temperature resistance in general and bears higher strength which makes the material difficult to weld, whereas low carbon steel has low strength as compared to other steel. So, the focus of our research is based upon the medium carbon steel which is having high strength with better ductility as compared to low steel at different heat treatments.

That's why our objective is to eliminate the confusion in the properties variations of steel and their relations with the microstructures. Then, the study of particular microstructures which are produced and the effects of the alloying elements, as a wide range of properties are available. Mostly, we will concentrate on mechanical properties. Here, EN9 steel has been taken into consideration and for examination and also the effects of heat-treatments on fatigue properties are evaluated. Our purpose is to develop a fundamental understanding. In order to do this, I propose to begin with pure iron, proceed to Fe-C, considering plain carbon steels, put in alloying elements and finally to select particular class of steel for examination.

2.3. HEAT TREATMENT OF STEEL

Heat treatment is the process of controlled heating and cooling of metals to alter their physical and mechanical properties. Heat treatment is an energy intensive process that is carried out in different furnace. Generally, all the heat treatment processes consist of the following three stages: heating of the material, holding the temperature for a time and then cooling, usually to the room temperature. During the heat treatment process, the material usually undergoes phase micro structural and crystallographic changes [11]. The effects of heat treatment are well identified by the variations in mechanical properties and microstructure variations which are shown in Fig 2.5. For instance, the hardness of the AISI 5150 steel could vary from -20 to 60 HRC depending on its heat treatment [12].

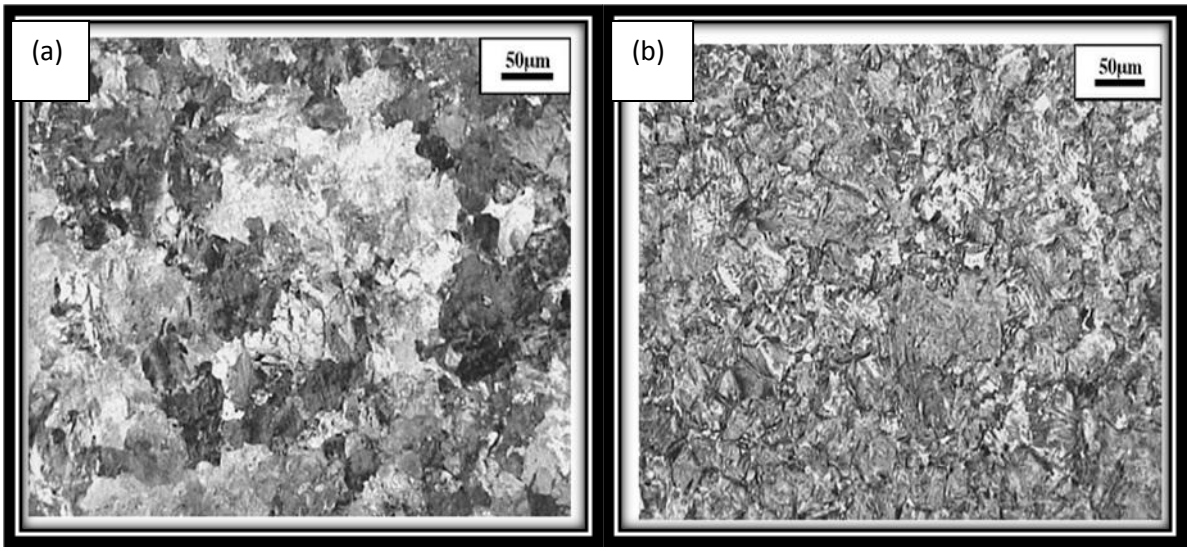

Fig 2.5: **(a) Microstructure of AISI 52100 Steel (Etching: Nital 0.3%)**
(b) Microstructure of the AISI 1020 Steel heat-treated at 750 ^{0}C for 150 min (Etching: Nital 0.3%). [12]

The conditions of heat treatment can modify the microstructure, mechanical and physical properties of steel within a wide range. The basic purpose of heat treating carbon steel is to change mechanical properties of steel usually ductility, hardness, yield strength, tensile strength and impact resistance. The properties like corrosion resistance and thermal conductivity get slightly altered during the heat treatment process.

Several studies have been devoted to describe the fatigue behavior of steel. However, depending on the heat treatment, even if conventional, the microstructure is different, being sometimes ferrito-pearlitic [13-14], or tempered martensitic [15] or even bainitic [16]. Before going for any heat treatment processes in steel alloys, it is important to know about the temperature and compositions

effect on the selection of treating processes. This is well analyzed by the equilibrium diagrams in Fig 2.6 [6].

As we know, iron is an allotropic metal (it can exist in one type of lattice structure depending upon temperature). In Fig 2.5, it is clearly visible that at 2800 ^{0}F when iron first solidifies, it is in body-centered cubic delta (δ) form. On further cooling to a temperature of 2554 ^{0}F, a phase change occurs and the atoms rearrange themselves into the gamma (γ) form, which is FCC and non-magnetic. Again, on cooling up to a temperature of 1666 ^{0}F, another phase change occurs from face centred non-magnetic γ iron to body-centered non-magnetic α iron. Finally, the α iron becomes magnetic without a change in lattice structure at a temperature of 1414 ^{0}F.

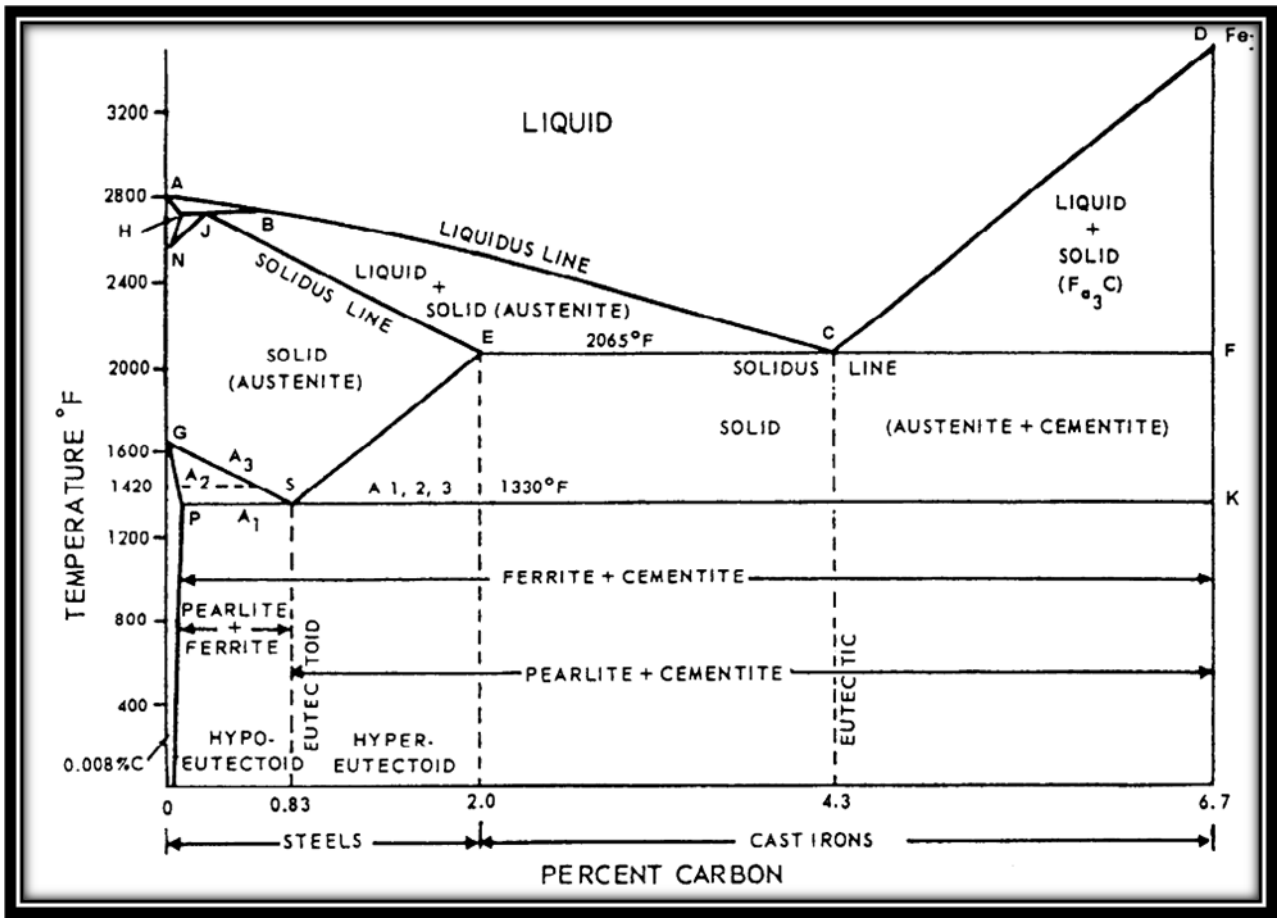

Fig 2.6**: Iron-Carbon Phase Diagram**

The temperature at which the allotropic changes take place in iron is influenced by alloying elements, in which the most important is carbon. The portion of iron-carbon alloy system shown in the figure Fig 2.6. It is that part between pure iron and interstitial compound, iron carbide, containing 6.67% carbon by weight. It is very important to know that this diagram is not a true equilibrium diagram,

since equilibrium implies no change of phase with time. It is a fact that the compound iron carbide will decompose into iron and carbon (graphite). This decomposition will take a very long time at room temperature, and even at 1300 ^{0}F it takes several years to form graphite when iron carbide is in meta-stable phase. Therefore, this diagram technically represents meta-stable conditions which can be considered as representing equilibrium changes, under conditions of relatively slow heating and cooling. The austenite region is known as delta region because of the solid solution. One should recognize the horizontal line at 2720 ^{0}F as being a peritectic reaction.

The composition of carbon steel is given in the Fig. 2.7. It shows the distribution of low, medium and high carbon steel based on percentage. Almost, all the carbon steels contain less than 1.5% carbon.

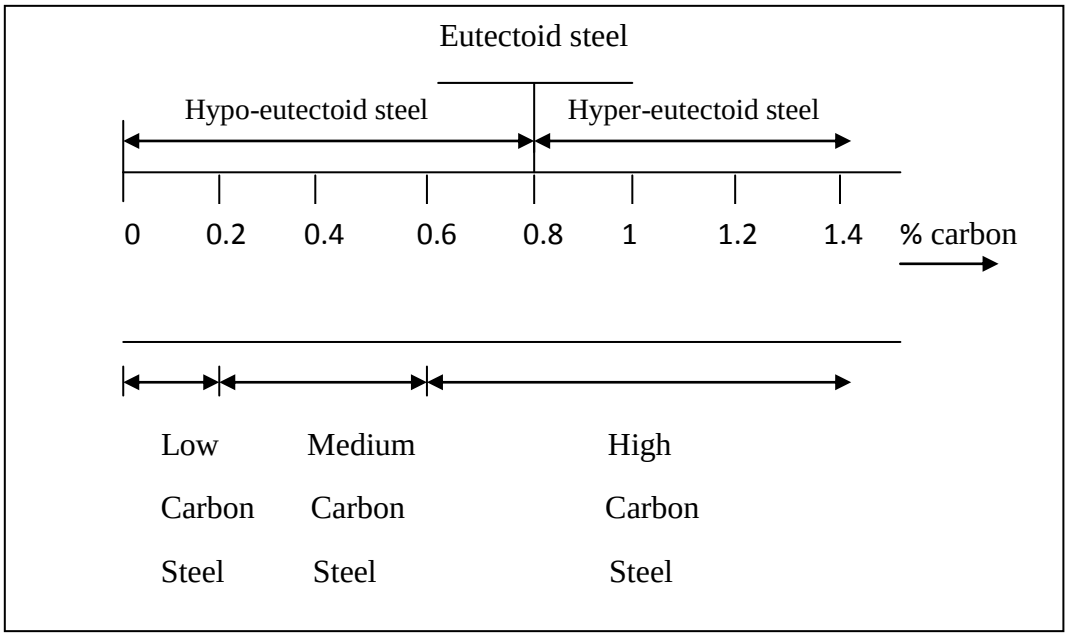

Fig 2.7**: Carbon Steel Composition**

As we have discussed earlier, the properties of a metal or an alloy are directly related to the metallurgical structure of the material. Since, we know that the basic purpose of heat treatment is to change the properties of the materials. For choosing a particular treatment, it is necessary to know the temperature with respect to the composition, which is well explained in Fig 2.8 [17].

In [18], it has been described that plain carbon steel whose principle alloying element is carbon has Ferrite-pearlite structure i.e. low carbon; quenching and tempering if medium to high carbon. Plain carbon steel whose carbon content is 0.45% has structure as fine lamellar pearlite (dark) and ferrite (light) as shown in Fig 2.9 [19].

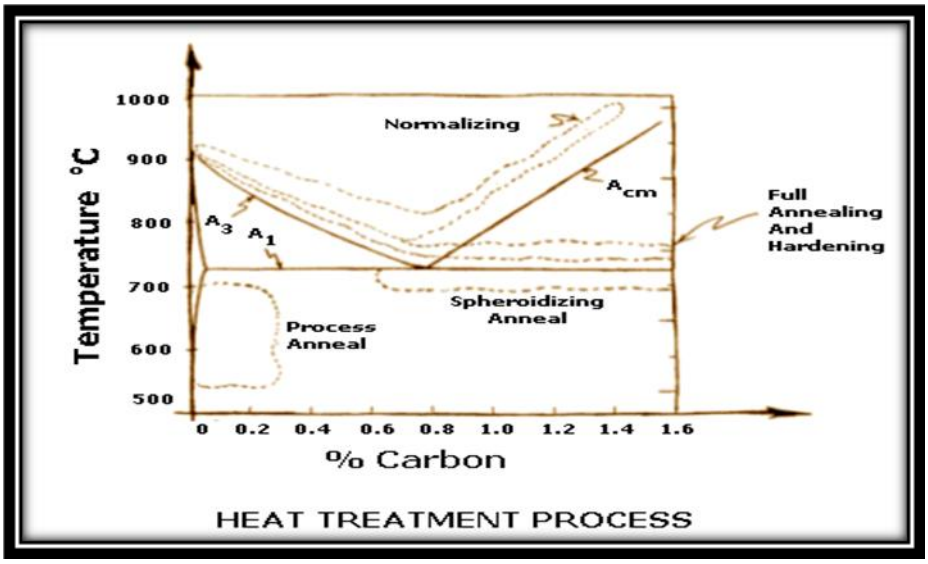

Fig 2.8**: Heat Treatment Process**

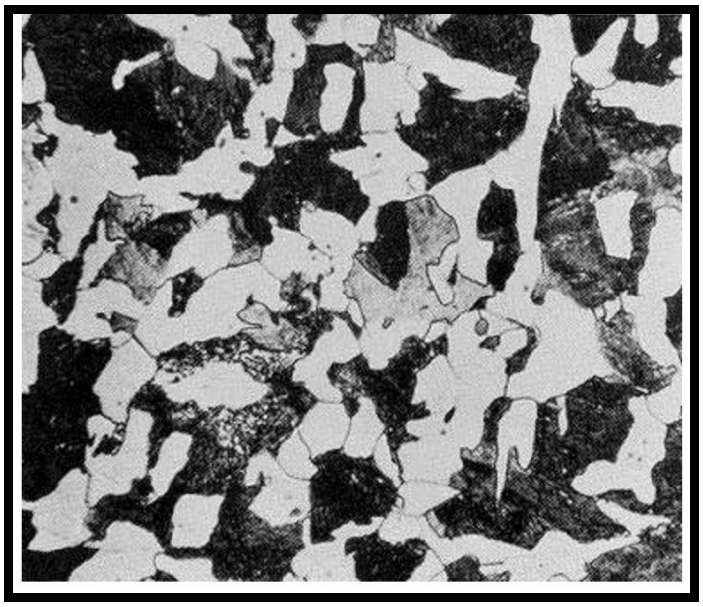

Fig 2.9: **1045 Steel Bar [19]**

The standard strength of steels used in the structural design is prescribed from their yield strength. That's why most engineering calculations for structure are based on yield strength. In [20], heat treatment process on locally produced plain carbon steel, evaluate the effect of heat treatment processes on the mechanical properties such as tensile strength, ductility, toughness and hardness of the rolled steel and determine high strength, high ductility and low yield ratio of the rolled medium carbon steel.

2.3.1. Annealing

Annealing is the type of heat treatment most frequently applied in order to soften iron or steel materials and refines its grains due to ferrite-pearlite microstructure; it's used where elongations and appreciable level of tensile strength are required in engineering materials [21-22].

Spherodizing:- Spherodite forms when carbon steel is heated to approximately 700 for over 30 hours. The purpose is to soften higher carbon steel and allow more formability. This is the softest and most ductile form of steel. Here, cementite is present.

Full Annealing: - Carbon steel is heated to approximately above the upper critical temperature for 1 hour. Here, all the ferrite transforms into austenite. The steel must then cooled in the realm of 38 per hour. This results in a coarse pearlite structure. Full annealed steel is soft and ductile with no internal stress.

Process Annealing: - The steel is heated to a temperature below or close to the lower critical temperature, held at this temperature for some time and then cooled slowly. The purpose is to relive stress in a cold worked carbon steel with less than 0.3% wt C.

Diffusion Annealing: - The process consists of heating the steel by rising the temperature about 20^0C to 40 ^{0}C above Ac_3, is cooled quickly to the temperature of isothermal holding (by transferring the steel to the second furnace), which is below A_1 temperature in the pearlitic region, held there for the required time so that austenite transforms completely. It is also called isothermal annealing. Some typical microstructures are obtained from the above heat treatment processes shown in Fig: 2.10.

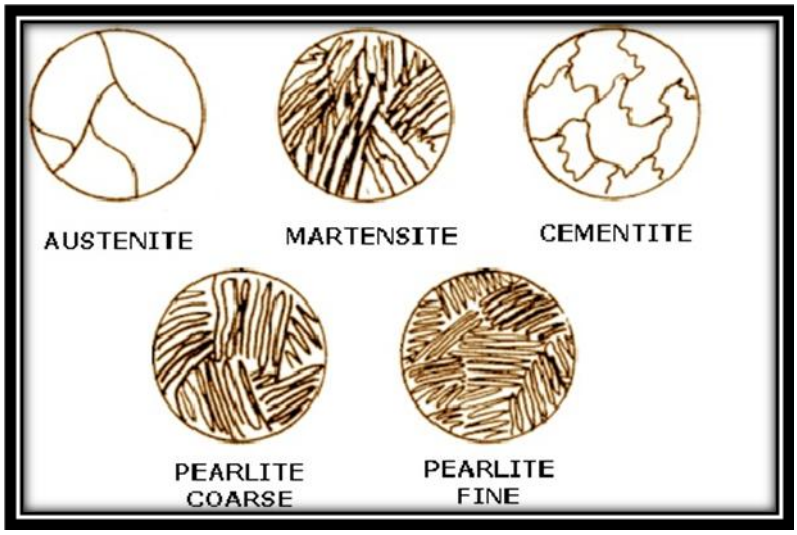

Fig 2.10: **Heat Treated Microstructures**

2.3.2. Normalizing

The process of normalizing consist of heating the metal to a temperature of 30 ^{0}C to 50 ^{0}C above the upper critical temperature for hypo-eutectoid steels and by the same temperature above the lower critical temperature for hyper-eutectoid steel. It is held at this temperature for a considerable time and then quenched in suitable cooling medium. The purpose of normalizing is to refine grain structure, improve machinability and improve tensile strength, to remove strain and to remove dislocation.

This treatment is usually carried out to obtain a mainly pearlite matrix, which results into strength and hardness higher than in as-received condition. It is also used to remove undesirable free carbide present in the as-received sample [23].

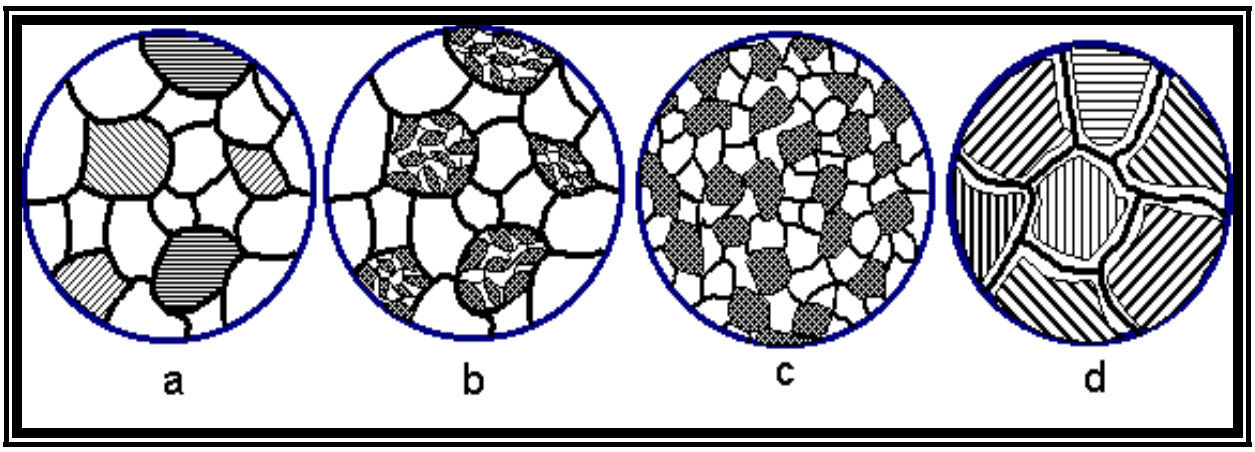

Fig. 2.11: **Microstructure of Plain Carbon Steel before and after Normalizing**

In the above figure, it is clearly visible the mixture of ferrite and pearlite grains, temperature below 723 ^{0}C. Therefore, microstructure not significantly affected. But, Fig.2.11 (b) shows pearlite transformed to austenite, but not sufficient temperature available to exceed 910 ^{0}C, therefore not all ferrite grains are transformed to austenite. On cooling, only the transformed grains will be normalized. Whereas Fig. 2.11(c) shows temperature just exceeds 910 ^{0}C. On cooling, all grains will be normalized and Fig. 2.11(d) shows temperature significantly exceeds 910 ^{0}C permitting grains to grow. On cooling, ferrite will form at the grain boundaries, and a coarse pearlite will form inside the grains. A coarse grain structure is more readily hardened than a finer one; therefore, if the cooling rate between 800 ^{0}C – 1500 ^{0}C is rapid, a hard microstructure will be formed. This is why a brittle fracture is more likely to propagate in this region.

2.3.3. Quenching and Tempering

This process consists of reheating the hardened plain steel which is quenched by water from the soaking temperature to some temperature below the lower critical temperature, followed by any desired rate of cooling for getting a high hardness value [24]. The purpose is to relive internal stress, to reduce brittleness and to make steel tough to resist shock and fatigue. Conventional quenching and tempering heat treatments have long been applied to steels to produce good combinations of strength and toughness from the martensitic structure [25].

More recently, austempering treatments in the bainitic region have been applied to steels. For example, Si which suppresses bainitic carbide formation such that carbon-enriched untransformed austenite is chemically stabilized [26–28]. The resulting microstructure of bainitic ferrite laths intertwined with interlath retained austenite films, rather than the ferrite/carbide combinations usual for pearlitic, bainitic or tempered martensitic structures, has promoted the potential for attractive properties in, for example, formable sheet steels [29-30], and high strength experimental steels [31-33] as well as austempered ductile irons [34-39].

The properties of the heat-treated medium carbon steel from DSC compared favorably well with standard steel products. They have excellent values in terms of tensile strengths and elongation when quenched and tempered in both water and oil. The normalized steel was found to possess good properties in yield strength (508.00 N/mm^2), tensile strength (706 N/mm^2) and impact strength of 43.0 J. The quenched steel materials have their yield points eliminated. The palm oil quenched steel is found to be exhibiting higher level of toughness. It is recommended that these mechanical properties be examined under different tempering temperatures to see their variations [40].

With increasing number of heat treatment cycles the proportion of ferrite and spheroidized cementite increases, the proportion of lamellar pearlite decreases and micro constituents (pearlite and ferrite) become finer [41].

Mechanical properties are enhanced as the materials gone through the heat treatment processes [42]. In this literature, specimens corresponding to all heat treatment temperatures showed higher hardness as compared to the annealed specimens of the same steel.

In general, quenching and tempering results the optimum fatigue properties in heat treated steels although at a hardness level above about Rc 40 bainitic structure produced by austempering results in better fatigue properties than quenched and tempered structure with the same hardness [43].

The poor performance of the quenched and tempered structure indicated by electron micrographs is the result of stress concentration effects of the thin carbide films which are formed during the formation of martensite in tempering and also the fatigue limits increases with decreasing tempering temperature up to a hardness Rc 45 to Rc 55 which is well explained by M.F.Garwood et.al. [44].

Fatigue properties at high hardness level are extremely sensitive to the surface preparation, residual stresses, and inclusions. Only a small amount of non-martensitic transformation products can cause an appreciable reduction in fatigue limit [45]. The influence of small amount of retained austenite on fatigue properties of quenched and tempered steels has not been well established.

Hence, from the above discussion we conclude that steels are normally hardened and tempered to improve their mechanical properties, particularly their strength and wear resistance. In hardening, the steel or its alloy is heated to a temperature high enough to promote the information of austenite, held at that temperature until the desire amount of carbon has been dissolved and then quenched in a particular medium at a suitable rate. Also, in the hardened condition, the steel should have 100% martensite to attain maximum yield strength, but it is very brittle too and thus quenched steel is used for very few engineering applications. By tempering, the properties of quenched steel could be modified to decrease hardness and increase ductility and impact strength gradually. The resulting microstructures are bainite or carbide precipitate in a matrix of ferrite depending on the tempering temperature.

2.4. FATIGUE OF STEEL

Since 1830, it has been recognized that a metal subjected to repetitive or fluctuating stress will fail at a stress much lower than that required to cause fracture on a single application of load. Failures occurring under conditions of dynamic loading are called fatigue failures, presumably because it is generally observed that these failures occur only after a considerable period of service [46]. As technology has been developed, fatigue has become more prevalent in automobiles, aircraft, turbines, etc. subject to repeated loading and vibration. Also, fatigue accounts at least 90 percent of all service failures due to mechanical causes [47]. Many of the research work have been done to study fatigue mechanism, factors affecting fatigue properties and various aspects of fatigue failure since its discovery in 1830. It is not in the scope of the present work to give a detail view of the fatigue study. Here, a brief discussion on the elementary factors, its effects on mechanical and physical properties associated with the heat treatment and the most common techniques used in the study of fatigue have been incorporated.

2.4.1. Fundamentals of Fatigue

Fatigue occurs without obvious warning and it results in a brittle appearing fracture, with no gross deformation at the fracture, where fracture surface is usually normal to the direction of the principal tensile stress. A fatigue failure can usually be recognized from the appearance of the fracture surface, which shows a smooth region, due to the rubbing action as the crack propagated through the section and a rough region, where the member has failed in a ductile manner when the cross section was no longer able to carry the load which is shown in the Fig 2.12. Frequently, the progress of the fracture is indicated by a series of rings, or "beach marks," progressing inward from the point of initiation of failure and also failure usually occurs at a point of stress concentration such as sharp corner or notch or at a metallurgical stress concentration like an intrusion.

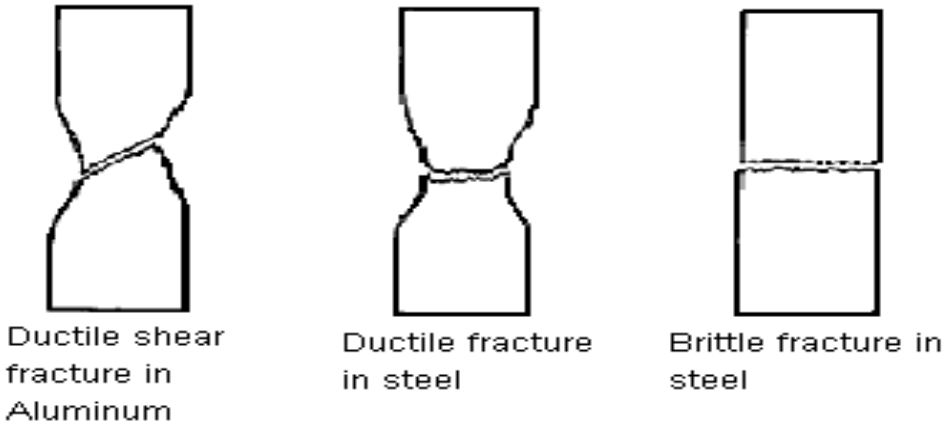

Fig 2.12: **Different type of Fracture Surface in Metal [48]**

Three basic factors are mainly responsible for the fatigue failure. These are as follows:

(1) A maximum tensile stress of sufficiently high value.
(2) Large variation or fluctuation in applied stress.
(3) A sufficiently high cycle for the applied stress.

Some other elements like stress concentration, temperature, metallurgical structure also alter the fatigue conditions [48]. Many components in the field of mechanical engineering are subjected to cyclic loading. That's why fatigue failure is generally considered as the main problem affecting any component under dynamic loading condition [49].

2.4.2. Stress Cycles

Generally fluctuating stresses can cause fatigue failures. Here, some of the fluctuating stress cycles which are shown in Fig 2.13.

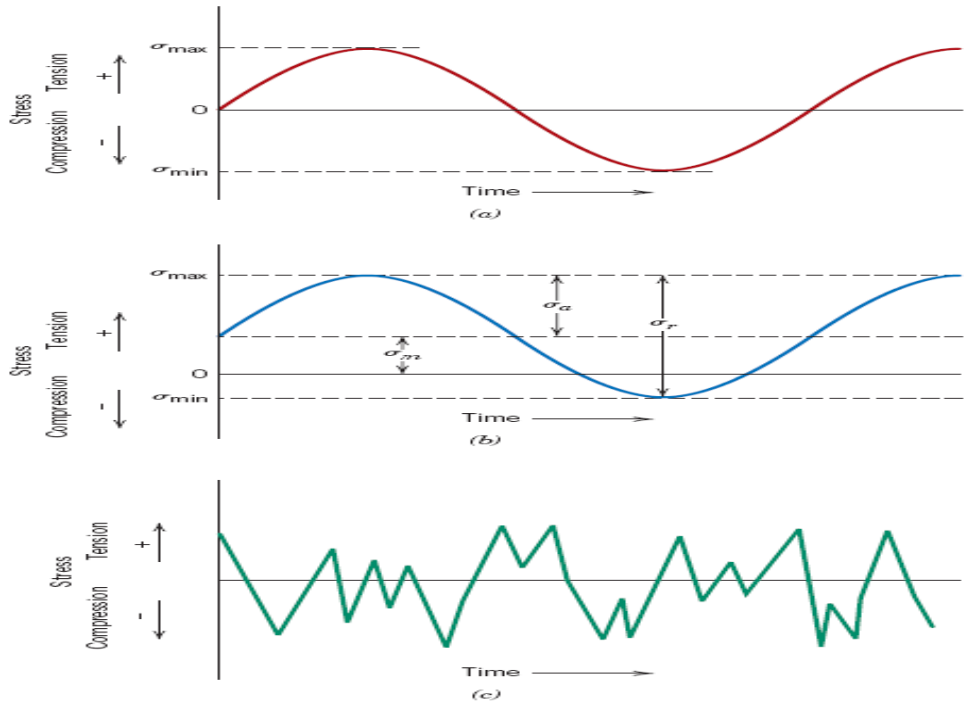

Fig. 2.13: **Stress Cycles (a) Completely Reversed, (b) Repeated Cycles and (c) Random Cycles**

a. Completely reversed cycle of stress of sinusoidal form: In this case, maximum (σ_{max}) and minimum (σ_{min}) stresses are equal in magnitude but opposite in sign. This cycle is obtained in a rotating shaft operating at a constant speed.
b. Repeated stresses cycle: This type of cycle shows that the maximum and minimum cycles are not same.
c. Irregular or random stress cycle: It is a complicated cycle which can be obtained due to periodic unpredictable overloads.

Fluctuating stress cycles can be considered to be made up of two components, a mean or steady stress (σ_m) and an alternating or variable stress (σ_a). The range of the stress or stress amplitude ($\Delta\sigma$) must also be considered. The range of stress is represented as -

$$\Delta\sigma = \sigma_{max} - \sigma_{min}$$

The alternating stress is represented as- $\sigma_a = (\Delta\sigma/2)$

The mean stress is represented as- $\sigma_m = (\sigma_{max} + \sigma_{min})/2$

2.4.3. S-N Curve

Most textbooks assume that most of the materials have a fatigue limit when they are subjected to number of cycles. The common form of presentation of fatigue data is by using the S-N curve, where the total cyclic stress (S) is plotted against the number of cycles to failure (N) in logarithmic scale. A typical S-N curve is shown in Fig 2.14 (a) and (b) [50].

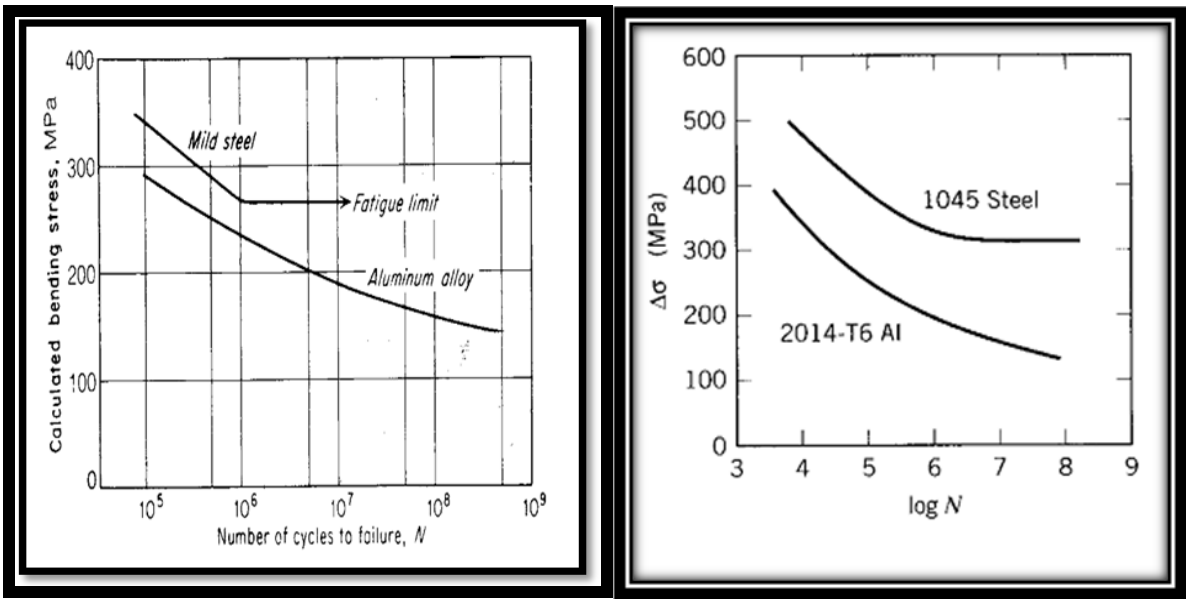

Fig 2.14: **(a) Typical Fatigue Curves for Ferrous and Non-Ferrous**
(b) S − N Curves for Aluminum and Low-Carbon Steel

Most determination of fatigue properties of materials have been made in completely reversed bending where the mean stress is zero i.e. done by rotating beam test machine. For determinations of the S-N curve, the usual procedure is to test the first specimen at a high stress where failure is expected in a fairly short number of cycles, e.g., at about two- thirds the static tensile strength of the material. The test stress is decreased for each succeeding specimen until one or two specimens do not fail in the specified numbers of cycles, which is usually at least 10^7 cycles. This method is used for presenting fatigue in high cycles ($N > 10^5$). In high cycle fatigue, test stress level is relatively low and the deformation is in elastic range.

For a few important engineering materials such as steel and titanium, the S-N curve becomes horizontal at a certain limiting stress. Below this limiting stress, which is called the fatigue limit, or endurance limit, the material presumably can endure an infinite number of cycles without failures. Most nonferrous metals, like aluminium, magnesium, and copper alloys have an S-N curve which

slopes gradually downward with increasing number of cycles. These materials do not have a true fatigue limit because the S- N curve never becomes horizontal.

It will be noted that this S-N curve is concerned chiefly with fatigue failure at high number of cycles ($N>10^5$cycles). Under these conditions, the stress on a gross scale is elastic, but as well as the metal deforms plastically in a highly localized way. For the low cycle fatigue ($N<10^5$cycles), tests are conducted with controlled cycles of elastic plus plastic strain instead of controlled load or stress cycles. The research on conventional fatigue problems can be divided into the following kinds according to the number of cycles of fatigue loading functions: super cyclic fatigue (over 10^7), high cyclic fatigue (from 10^5 to 10^7), and low cyclic fatigue (from 10^3 to 10^5).

2.4.4. Fatigue Mechanism

In the middle of the 19th century, it was first realized that metal will fail at stress much lower than that of the static loading condition when subjected to dynamic loading. At the end of the 19th century, it was accepted by all that the fibrous structure of metals formed due to fatigue transformed into crystalline structure. A fundamental step towards fatigue as a material problem was made in the beginning of the 20th century by Ewing and Humfrey [51] in 1903. They performed rotating bending fatigue tests on annealed Swedish iron and the specimens were examined at intervals during the course of the test. They found that the metal was deformed by slipping on certain planes within crystals when proportional limit was exceeded. But, after some reversal it was found that the appearance of the surface became similar to that of the static stressing. After more few reversals, few dark lines were appeared which were more distinct by the time and showed a tendency to broaden. The process of broadening is continued by the number of reversals and finally cracking occurred. A few reversals after this stage caused fracture of the material.

Different theories of fatigue were put forward after this demonstration that fatigue cracking was associated with slip. Finally, Ewing and Humfrey were come to the conclusion that the repeated slipping occurred on a slip band which resulted in wearing of the material surface and broadening of slip bands and eventually the formation of a crack. The main drawback of this theory was that they did not explain the repeated occurrence of plastic deformation without leading to failure.

In 1923, Gough [52] put forward another explanation of the mechanism of fatigue. He explained that fatigue failure of the ductile materials must be regarded as a consequence of slip. From microscopic measurement of hardness it was clear that the initiation of a fatigue crack did not mean that entire crystal had reached a maximum value of strain hardening on the crystal in general, but in certain local

regions where the limiting lattice strains were exceeded resulting in the rupture of atomic bonds and discontinuities in the lattice.

More information about fatigue as a material phenomenon was going to follow in the 20th century. The development of fatigue problems were reviewed in two historical papers by Peterson [53] in 1950 and Timoshenko [54] in 1954. A handbook published in 1950 was on "Experimental Stress Analysis" by Hete´nyi elaborated that "how does a localized stress can reduce the service of a component." [55].

In mid 90's, some of the researchers were focused on the history regarding fatigue failure [56-60]. Schijve [61] has given main emphasis on physical understanding of the fatigue phenomena for the evaluation of fatigue predictions. For fatigue investigations, main observation was made with the electron microscope around 1960. Fractographic images revealed striations marks with respect to every load cycle [62]. Ductile and brittle striations were well explained in [63].

A study of crack formation in fatigue can be facilitating by interrupting the fatigue test to remove the deformed surface by electro polishing. There will be several slip bands which are more persistent than the rest and which will remain visible when the other slip lines have polished away. Such slip bands have been observed after only 5 percent of the total life of the specimen [64]. These persistent slip bands are embryonic fatigue cracks, since they open into wide cracks on the application of small tensile strains. Once formed fatigue cracks tend to propagate initially along slip planes although they later take a direction normal to the maximum applied tensile stress. Fatigue-crack propagation is ordinarily trans-granular.

An important structural feature which appears to be unique to fatigue deformation is the formation on the surface of ridges and grooves called slip-band extrusions and slip-band intrusions which are shown in Fig.2.15 [65]. Extremely careful metallographic on taper sections thorough the surface of the specimen has shown that fatigue cracks initiate at intrusions and extrusions [66].

W.A.Wood [67], who made many basic contributions to the understanding of the mechanism of fatigue, suggested a mechanism for producing slip-band extrusion and intrusions. He interpreted microscopic observation of slip produced by fatigue as indicating that the slip bands are the result of a systematic buildup of fine slip movement, corresponding to movement of the order of 1nm rather than steps of 100 to 1000nm, which are observed for static slip-bands. Such a mechanism is believed to allow for the accommodation of large total strain hardening. He also explained that slip produced by static deformation would produce a contour at the metal surface, and at the contrast the back-and-

forth fine slip movements of fatigue could build up notches or ridges at the surface as shown in above Fig 2.15. The notch would be a stress raiser with a notch root of atomic dimensions. In such a manner a fatigue crack will initiate. This mechanism for initiation of a fatigue crack is in agreement with the fact that fatigue cracks start at surfaces and that cracks have been found to initiate at slip-band intrusions and extrusions.

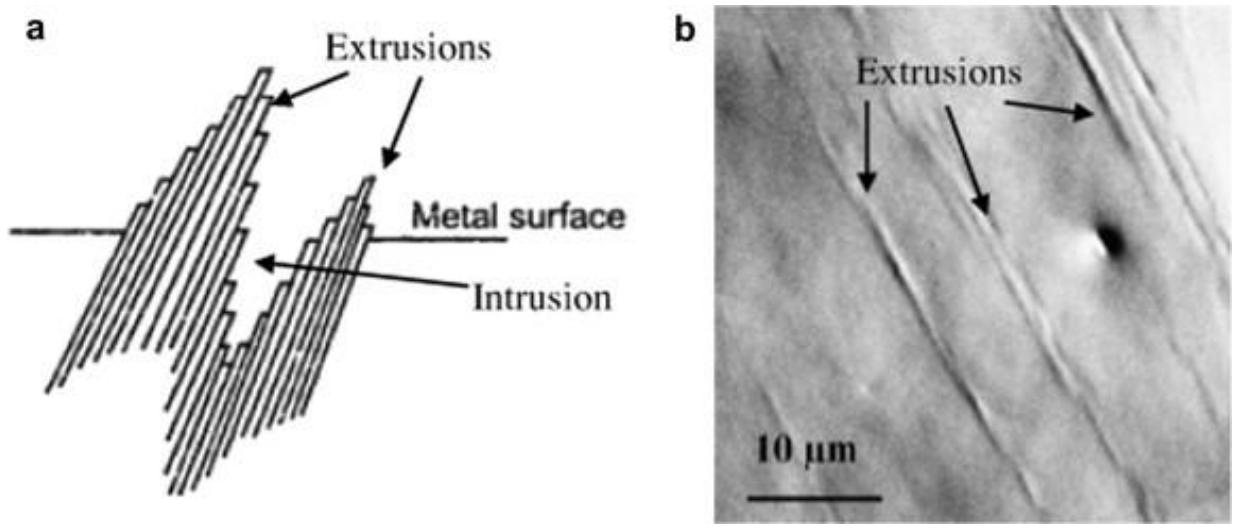

Fig 2.15: **Slip Mechanism [67]**

According to the various investigations during 19th century on fatigue mechanism, we come to a conclusion that metal deforms under cyclic strain by slip on the same atomic plane and in the same crystallographic directions as in unidirectional strain. Whereas, with unidirectional deformation slip is usually widespread throughout all the grains, in fatigue some grains will show slip lines while other grains will give no evidence of slip. Slip lines are generally formed during the first few thousand cycles of stress. Successive cycles produce additional slip bands, but the number of slip bands is not directly proportional to the number of cycles of stresses. In many metals, the increase in visible slip soon reaches saturation value which is observed as distorted regions of heavy slip. Cracks are usually found to occur in the regions of heavy deformation parallel to what was originally a slip band. Sometimes, slip bands have been observed at stresses below the fatigue limit of ferrous materials. Therefore, the occurrence of slip during fatigue does not in itself mean that a crack will form.

2.4.5. Fatigue Process

Some of the study regarding structural changes described that metal is subjected to cyclic stresses undergoes through the fatigue process where this process follows some stages like (1) Crack initiation: includes early development of fatigue damage which can be removed by thermal anneal, (2) Slip-band crack growth- involves the deepening of the initial crack on planes of high shear stress. This frequently is called stage I crack growth, (3) Crack growth on planes of high tensile stress – involves growth of well- defined crack in direction normal to maximum tensile stress. Usually called stage II crack growth and (4) Ultimate ductile failure- occurs when the crack reaches sufficient length so that the remaining cross section cannot support the applied load. However, it is well established that fatigue crack cannot be formed before the 10 percent of total life elapsed. Here, in stage I crack growth comprises the largest segment for low-stress, high-cycle fatigue. If the tensile stress is high, as in the fatigue of sharply notched specimens, stage I crack growth may not be observed at all [68].

Extensive structural studies [69] of dislocation arrangements in persistent slip band have brought much basic understanding to the fatigue fracture process. The stage I crack propagates initially along the persistent slip band in a polycrystalline metal the crack may extend for only of few grain diameters before the crack propagation changes to stage II. The rate of crack propagation in stage I is generally very low, of the order of nm per cycle, compared with crack propagation rate microns per cycle for stage II. The fracture surface of stage I fractures is practically feature less. By marked contrast, the fracture surface of stage II crack propagation frequency show a pattern, a ripple or fatigue fracture striation. Each striation represents the successive position of an advancing crack front that is normal to the greatest tensile stress. Each striation was produced by a single cycle of stress. The presence of this striation unambiguously defines that failure was produced by fatigue [70].

In recent years, many scholars, based on these relational expressions, has began the researches on the mechanism of gap fatigue fracture, parameter calculation, spreading and closing of fatigue cracking [71-74] and the SEM was used to study the fatigue crack initiation and propagation [75-76], which provides a theoretical basis for fatigue safety design of actual structure, so that the breakage of structural components due to fatigue can be avoided thereby. The fatigue of materials possesses both positive and negative functions. The theory of cracking technique is a kind of science by making use of the effect of fatigue. Based on this theory, the generalized fatigue cracking theory consists of two aspects of traditional fatigue safety design and extra-low cyclic [77].

Y. Uematsu et al. described the significant effect of elevated temperature on fatigue strength of ferritic stainless steels. When this material characterized in terms of fatigue ratio, fatigue strength still decreased at elevated temperatures compared with at ambient temperature. At all temperatures studied, cracks were generated at the specimen surface due to cyclic slip deformation, but crack initiation occurred much earlier at elevated temperatures than at ambient temperature. Subsequent small crack growth was considerably faster at elevated temperatures even though difference in elastic modulus was taken into account, indicating the decrease in the intrinsic crack growth resistance. Fractographic analysis revealed some brittle features in fracture surface near the crack initiation site at elevated temperatures [78].

In the article [79], Fatigue behavior and phase transformation in the metastable austenitic steels is well described by taking the AISI 304, 321 and 348, which were investigated in the temperature range from -60 °C to 25 °C. These steels show differences in austenite stability, which lead to significant changes in deformation induced martensite formation and fatigue behavior in total strain controlled low cycle fatigue tests. Dependent on the type of steel and testing temperature, similar values of martensite fraction but different strengths developed.

Japanese researchers [80-86], have discovered the meanwhile well-known phenomenon that high strength steels may fail at very high numbers of cycles due to cracks starting at inclusions. This leads to the question whether steels, in general, do not show a fatigue limit or if this effect is found only in steels, which are heat treated to reach high strength. Carbon steels without hardening treatment are used most frequently for structural applications and therefore this question is of great technical relevance. The fatigue behavior of normalized carbon steels is well documented in the literature [87-90].

Okayasu et al [91] made an examination of the fatigue properties of the two-phase ferrite/martensite low carbon steel; he found that the fatigue strength of steel is found twice as high as that of the as-received steel. Tayanc et al. [92] presented that fatigue strength of steel increased when compared with as-received materials. They have obtained the highest fatigue strength in the annealed steel. Maleque et al. [93] have presented that the as-received specimen has higher fatigue strength or higher endurance to fatigue failure than DPSs but for low cyclic life.

According to the importance of fatigue failure, many researchers had investigated the factors affecting on fatigue and how to enhance the service life of any mechanical component. Motor components, automobile parts, train wheels, tracks, bridges, medical instruments, heavily stressed

power plant components such as engines and rotors have to withstand a number of cycles higher than 10^7. These high numbers of cycles can be a result from high frequency or a long product life. Among the breakages of various mechanical components as mentioned above, 50%-90% of them belong to fatigue breakage. Therefore, for a long time, in order to prevent the components from fatigue breaking, people have been continuously exploring and trying to describe the whole process of fatigue from the viewpoint of some 'controllable factors', so as to achieve the goal of forecasting the fatigue life and avoiding the fracture phenomena.

The best way to show the fatigue failure data is by plotting S-N curve, which is well explained previously. From the viewpoint of engineering applications, the purpose of fatigue research consists of: (1) Predicting the fatigue life of structures, (2) Increasing fatigue life and (3) Simplifying fatigue tests, especially fatigue tests of full-scale structures under a random load spectrum [94].

Starting from the famous relational expression for estimating fatigue life Manson-Coffin Formula [95] presented by Manson and Coffin in early 1960s' and subsequent appearance of Paris's Formula [96] of fatigue spreading rate, many scholars have began the fatigue safety design and research on forecasting fatigue life. Among them, the Neuber's equation [97] and Dowling's formula [98] are the representative achievements to predict the fatigue life.

The fatigue life of an engineering structure principally depends upon that of its critical structure members. The fatigue life of an aircraft structure member can be divided into two phases, the fatigue crack initiation (FCI) life and the fatigue crack propagation (FCP) life, to be experimentally investigated and analyzed [99-108].

In the high cycle fatigue (HCF), it is usual to observe that fatigue strength increases with the increase of tensile strength [109-110]. This trend is well applied in the low and medium strength steels, and however, breaks down in the high strength steels showing a broad band of scattered data [111].

Most available existing research results are all about blanking based on the conditions of rotating and bending fatigue [112-114]. The fracture design for medium carbon steel under extra-low cyclic fatigue in axial loading is also well studied [115].

An overview of the state of research [116], tries to classify metallic materials and influencing factors and explains different failure mechanisms which occur especially in the VHCF-region like subsurface failure. There micro structural in homogeneities play an important role. Two S–N curves describe the fatigue behavior of different material conditions – one for surface fatigue strength in the HCF-region

and one for volume fatigue strength in the VHCF-region. By shifting the both curves to each other according to different factors, the resulting S–N curve can describe the fatigue behavior of different materials or component situations.

The reduction of strength and endurance limit, and enhancement of ductility that happened due to annealing is due to the formation of soft coarse ferrite grains. Quenching followed by tempering produces the hard tempered martensite grains, thus leading to increase strength and endurance limit while ductility is reduced [117].

Fatigue properties in the very high cycle regime of normalized carbon steel with carbon content 0.61% C (Ck60) and 0.15% C (Ck15) have been investigated in this paper by fatigue testing technique at load ratio R = -1 where we come to the conclusion that both steels show a distinct change of slope in the S–N curves at approximately 10^7 cycles. No Ck15 specimen failed above 2.2×10^8 cycles as shown in the Fig 2.16 [A]: (b) [118]; fatigue limit for Ck60 and C15 steel is shown and also fractograph for the same is given in Fig 2.16 [B]. For heat treated normalized Ck60 and Ck15 steel microstructure preferred Fig.2.17.

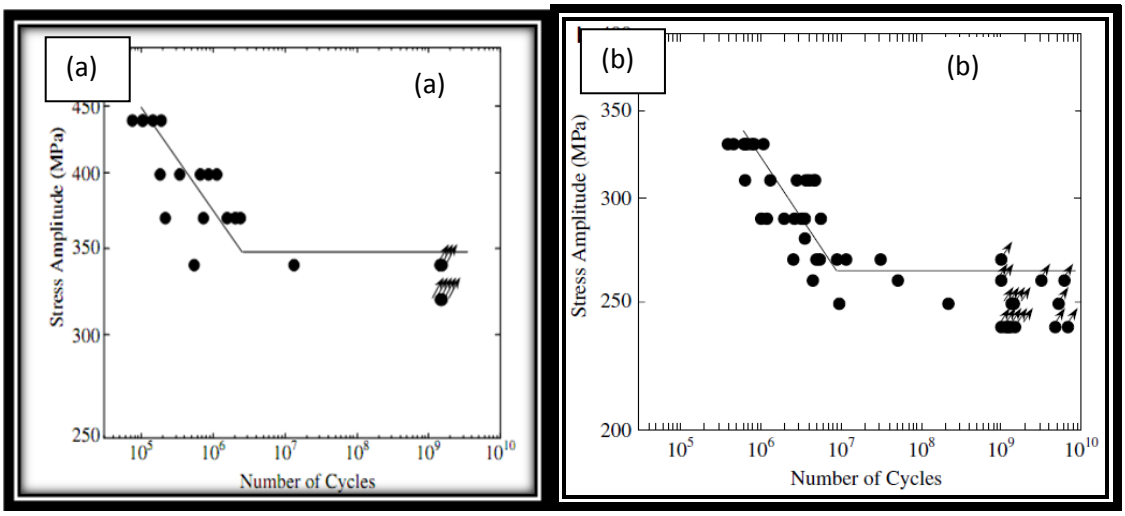

Fig 2.16 [A]: **(a) S–N data for Ck 60 (b) S–N data for Ck 15 [118]**

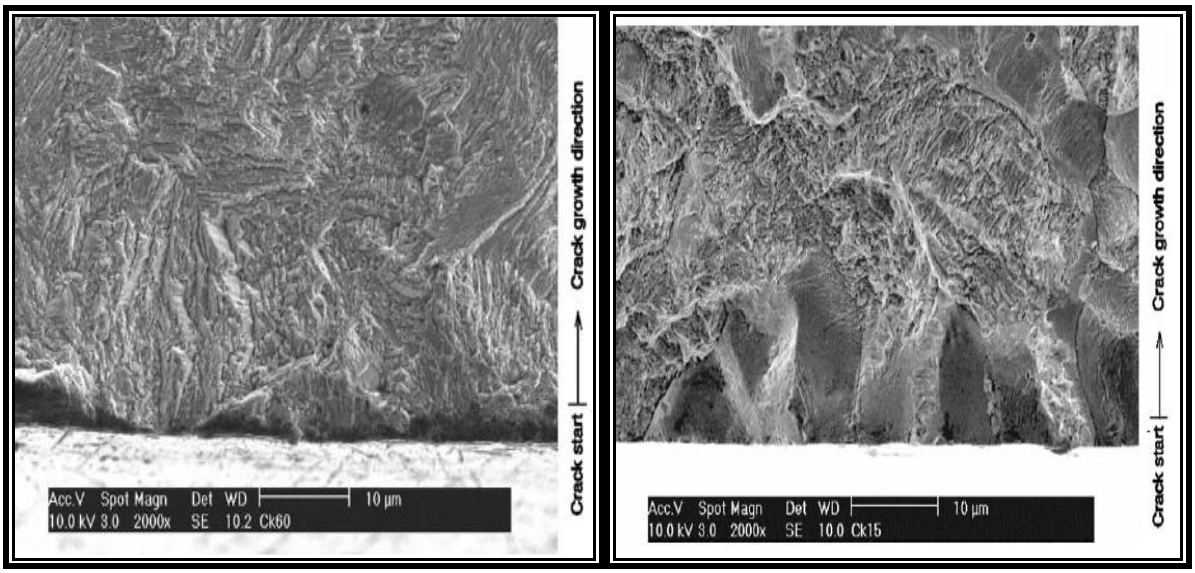

Fig.2.16 [B]: **(a) Crack initiation in Ck60 (b) Crack initiation in Ck15 [118]**

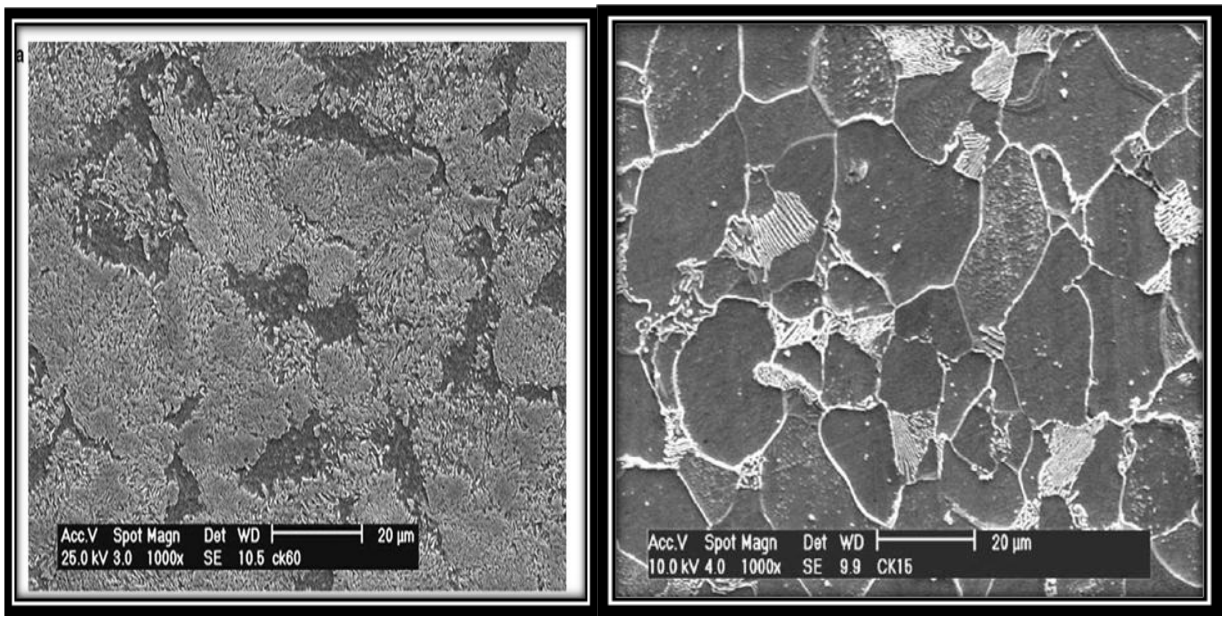

Fig. 2.17: **Microstructure of Ck60 and Ck15: Ferrite and Pearlite Colonies [118]**

It has been reported in the literature [119-121], that the fatigue limit in some steels may be correlated to cracks, which initiate at stresses below the fatigue limit and cannot propagate through grain boundaries or other barriers, like the pearlite colonies. Surfaces of several Ck60 and Ck15 specimens have been investigated carefully under the SEM to find possible non propagating cracks. [118].

According to the previous literature, we can easily correlate the fatigue limit with respect to the different carbon composition by comparing Ck60 and Ck15 steel. In this literature, we can conclude

that, as the carbon % increases there is a distinguish decrement of fatigue limit from Ck60 to Ck15 i.e. 348 MPa to 265 MPa. It clearly implies the carbon % affects on the fatigue behavior.

The literature [122] shows that the strength property increases mainly due to the presence of finer micro constituents (ferrite and pearlite). Thereafter, it decreases marginally with the elimination of lamellar pearlite and the appearance of cementite spheroids in the microstructure. Accordingly, ductility exhibits marginal decrease and increase with increasing number of heat treatment cycles. The fractured surface initially exhibits the regions of wavy lamellar fracture (pearlite regions) along with dimples (ferrite regions). The regions of dimples gradually consume the entire fractured surface and the areas of lamellar fracture are gradually eliminated with increasing number of heat treatment cycles.

A mixed cyclic stress-strain behaviour and much higher cyclic life were observed in steel containing ~50% martensite as compared to that containing ~80% martensite exhibiting complete cyclic softening behavior. Much higher cyclic life of the steel containing ~50% martensite, particularly at low strain amplitude, has been discussed in terms of crack growth retardation phenomena [123]. According to V. Wagner et al. [124], the cyclic deformation behaviour of the railway wheel steels SAE 1050 and SAE 1060, which was investigated in the very high cycle fatigue (VHCF) regime, their Fatigue failures occurred at $N > 10^7$.

The literature [125] summarized that the low-cycle fatigue process in an annealed medium carbon steel (0.46% C steel) was almost 100% dominated by the growth process of a single crack. In an extreme case, micro crack initiation was observed on the surface of a plain specimen during the first stress cycle.

According to the fundamental research, the fatigue limit of pearlitic carbon steel is increased by decreasing the prior austenite grain size and is not directly governed by the mean inter cementite spacing in the pearlite. Gensamer showed that the fatigue limit of eutectoid steel increased with decreasing isothermal-reaction temperature in the same fashion as did the yield strength and the tensile strength. However, G.E. Dieter explained that the structure sensitivity of fatigue properties can compare with tensile properties and also we can observe some variation in fatigue limit of plain eutectoid steel heat treated to coarse pearlite and to spheroidite of the same tensile strength. Parlitic structure can give a significantly lower fatigue limit due to the high notch effects of the carbide lamellae in pearlite. So Like austenite, the formation of martensite structure is increased the hardness so like the tensile strength which also influence the fatigue properties[126]. And in the other hand

The decrease in hardness is due to the disappearance of Martensite phase, Which Lower tempering time yield a finer martensite structure and less number of cementite and therefore higher hardness was obtained. But, as the holding/treatment time increased further, the hardness values were again decreased due to the occurrence of coarse bainite or carbide precipitate in a matrix of ferrite structure which greatly affect the tensile as well as fatigue properties [127-128].

From the above discussions, it is evident that fatigue failure of steel is influenced by a number of factors and microstructure is one of those important factors. Since, heat treatment plays a vital role in developing different microstructure, it is necessary to study the fatigue behavior of differently heat treated steels. This is due to the fact that differently heat treated steels have their applications in different fields. Depending upon the researches carried out previously in 19^{th} and 20^{th} century, our research work focused upon the fatigue behavior of EN9 steel on heat- treated conditions.

Chapter 3

3. EXPERIMENTAL TECHNIQUES

EXPERIMENTAL TECHNIQUES

The experimental techniques for the project work are listed as:

3.1) Specimen Specification

3.2) Heat Treatment

3.3) Study of Mechanical Properties

3.4) Micro-structural and Fracto-graphical Analysis

3.5) Fatigue Life Estimation

3.1. SPECIMEN SPECIFICATION

The first and foremost job for the experiment is the specimen preparation. The specimen size should be compatible to the machine specifications: We got the sample from medium carbon steel trader. The sample that we got was medium carbon steel AISI1055 or EN9 OR Ck55. It is one of the American standard specifications of the medium carbon steel having the pearlitic matrix with relatively equal amount of ferrite and so it has high hardness with moderate ductility and high strength as specified below. So, also we can state that it is particularly a combination of pearlitic and ferritic mixture. Chemical composition of the specimen is given in the Table 3.1.

C	Mn	Si	Mo	S	P	Fe
0.55	0.75	0.20	0.05	0.035	0.02	Balance

Table 3.1: **Chemical Composition as received**

The specimen is prepared according to the Moore testing machine. For this firstly the samples are cut into pieces from the sheets. The dimensional specification is as shown in the Fig 3.1.

As prior to the fabrication, heat treatment should be done because due to heat treatment there are some dimensional changes in the samples. This one is done to maintain the uniformity in the desired samples for further tests.

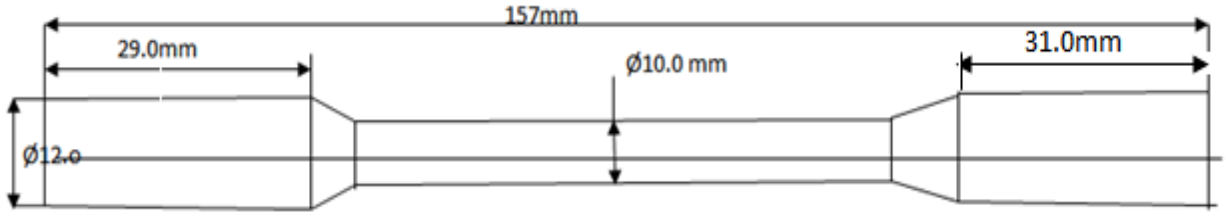

Fig 3.1: **Specimen used for Tensile Test and Fatigue Life Test**

Medium Carbon Steel is primarily heat treated to create matrix microstructures and associated mechanical properties not readily obtained in the as-cast condition. As cast grounded substance microstructures usually consist of ferrite or pearlite or combinations of both, depending on substance size and alloy composition. The principle objective of the project is to carry out the heat treatment of medium carbon steel at different temperatures according to heat treatment process diagram [15] and then to compare the mechanical properties. There are various types of heat treatment processes we had adopted.

3.2.1. Annealing

a) The specimen was heated to a annealed temperature of 800^0C.
b) At 800^0C, the specimen was held for 1 hour.
c) After soaking for 1hour the furnace was switched off so that the specimen temperature will decrease with the same rate as that of the furnace.

The objective of keeping the specimen at 800^0C for 1 hrs is to homogenize the specimen. The temperature 800^0C lies above A3 temperature so that the specimen at that temperature gets sufficient time to get homogenized .The specimen was taken out of the furnace after 1 day when the furnace temperature had already reached the room temperature.

3.2.2. Normalizing

a) Firstly, the specimen was heated to the temperature of 800^0C.
b) There the specimen was kept for 1 hour.
c) After soaking for desired time, the furnace was switched off and the specimen was taken out.
d) Now, the specimen is allowed to cool in the ordinary environment i.e. the Specimen is air cooled to room temperature.

Specimen heated above A3 temperature line and cooled by environmental conditions is called normalizing.

3.2.3. Quenching and Tempering

This is the important experiment carried out with the objective of the experiment being to induce some amount of softness in the material by heating to a moderate temperature range.

a) First, the some of the specimen were heated to 800^0C for 1 hour and then quenched in the water bath maintained at room temp.
b) Among them some of the specimens were heated to 200^0C but for different time period of 1 hour, 1 ½ hours and 2 hours respectively.
c) Now, some more specimens were heated to 400^0C and for the same time periods.
d) The remaining specimens were heated to 600^0C for same time interval of 1 hr., 1 ½ hr. and 2 hr. respectively.

Precautions: Preventing from oxidation the samples are placed inside the furnace in a container having charcoal.

After the specimens got heated to different temperatures for a different time period, they were air cooled. The heat treatment of tempering at different temp for different time periods develops variety of properties within them.

3.3. STUDY OF MECHANICAL PROPERTIES

As the main objective of the project is to compare the mechanical properties variation of heat treated steel specimens, now the specimens were subjected to hardness testing and tensile testing.

All the variations of these properties due to above these two tests are elaborated in next chapter.

3.3.1. Hardness Testing

The heat treated specimens hardness was measured by means of Rockwell hardness tester. The processes should be taken as listed as below:

a) First, the brale indenter was inserted in the machine; the load is adjusted to150 kg.
b) The minor load of a 10 kg was first applied to seat of the specimen.
c) Now the major load applied and the depth of indentation is automatically recorded on a dial gauge in terms of arbitrary hardness numbers. The dial gauge of 100 divisions in which each division corresponds to a penetration of 0.002 mm. The dial is reversed so that high hardness which results in small penetration, gives results of high hardness number. The hardness value obtained from this experiment was converted into a scale by using the standard converter chart. As all the specimens had undergone upon major load testing so scale measured to calculate the hardness value will be taken in R_C scale.

3.3.2. Ultimate Tensile Strength Testing

The heat treated specimens were treated in UTS Machine as in Fig.3.2 for obtaining the mechanical properties: the percentage of elongation, ultimate tensile strength, yields strength. For tensile test of the desired specimens INSTRON 8502 is used which has cross head speed 1mm/min which is also known as servo hydraulic testing machine.

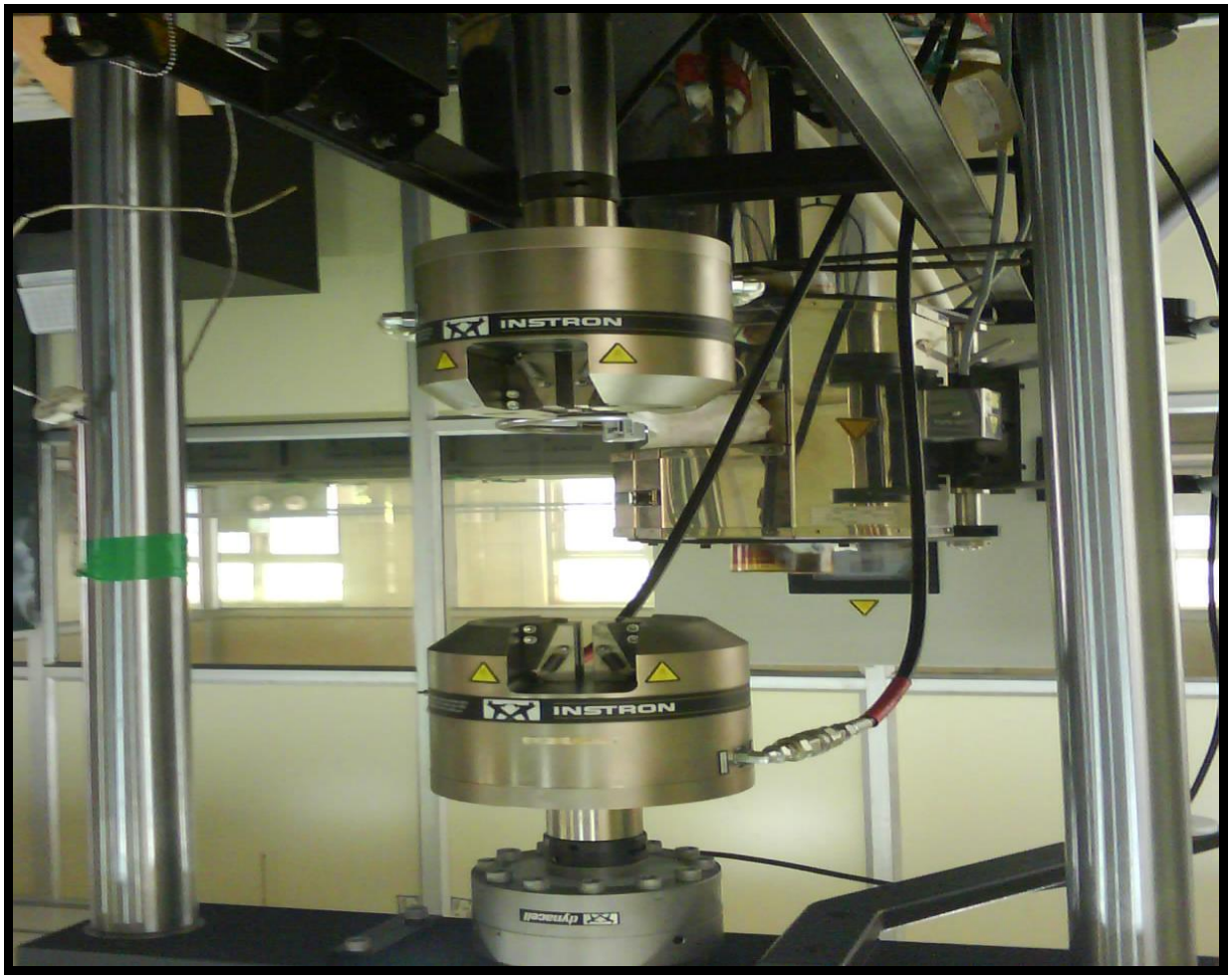

Fig 3.2: **INSTRON-8502 Servo-Hydraulic Testing Machine**

The procedures for obtaining these values can be listed as follows -

a) At first the cross section area of the specimen was measured by means of an electronic slide caliper and then the gauge length was calculated.
b) Now the distance between the jaws of the UTS was fixed to the gauge length of the specimen
c) The specimen was gripped by the jaws of the holder.
d) The maximum load was set at 150 KN.
e) The specimen was loaded till it fails

f) The corresponding Load vs. Displacement diagrams were plotted by using the software. From the data obtained, the % elongation, yield strength and ultimate tensile strength were calculated by using the following formula -

% Elongation = (change in gauge length of specimen/initial gauge length of the specimen.) *100

% Reduction of Area = (change in gauge diameter/original gauge diameter of the specimen)*100

Yield Strength = load at 0.2% offset yield/ initial cross section area

Ultimate Tensile Strength = maximum load/ initial cross section area

3.4. MICROSTRUCTURAL AND FRACTOGRAPHICAL ANALYSIS

After the completion of all these testing processes, the specimens were subjected to micro structural and fractographical study. This study consists of two different processes:

(a) Scanning Electron Microscopy Study (Fig 3.3. (a))
(b) Optical Microscopy Study (Fig 3.3. (b))

For these study the specimen were cut by 10 mm and thoroughly polished by different grade papers and also by fine polishing machines for microstructure study.

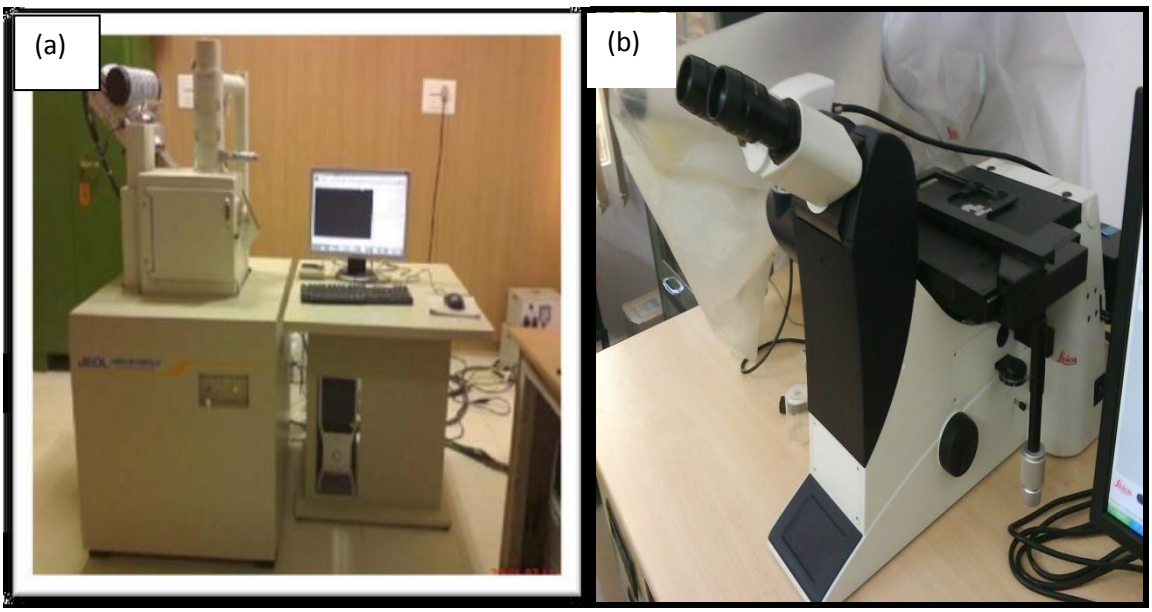

Fig 3.3: **(a) Scanning Electron Microscope (SEM) and (b) Optical Microscope**

3.5. FATIGUE LIFE ESTIMATION

According to research point of view, this test is the vital among all. These tests were carried out under Moore testing machine which is also known as Rotating beam fatigue testing machine. The schematic diagram of Moore testing machine is shown in Fig 3.4.

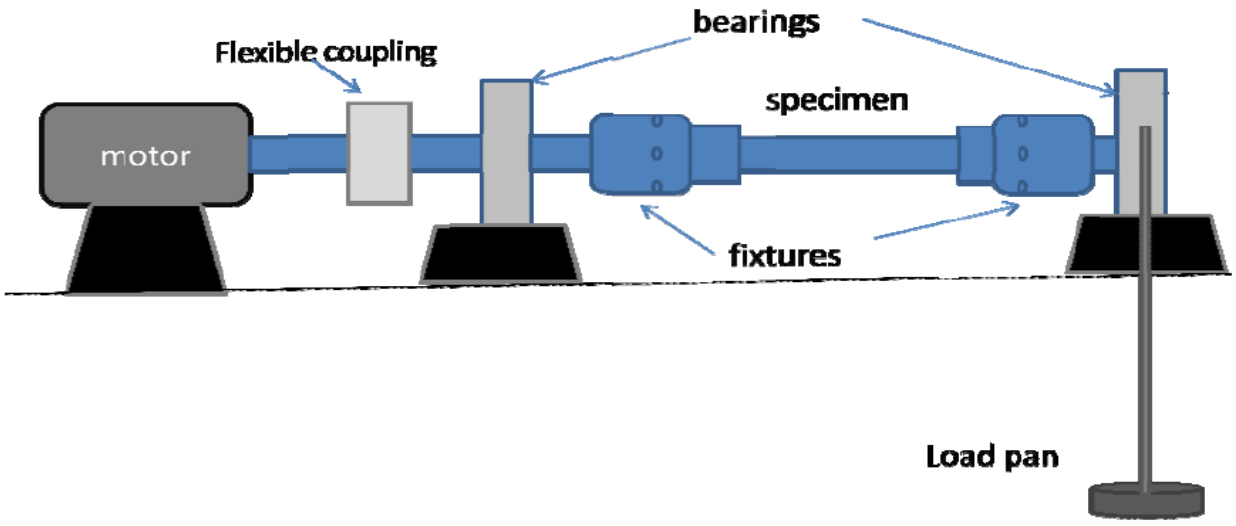

Fig 3.4: **Moore Fatigue Testing Machine**

Procedure:

A Rotating Bending Machine (RBM) is generally used to test the fatigue properties at zero mean stress. A standard specimen is clamped in two three point bearing at the ends. One end point is fixed and other one is loaded at free end point as shown in Fig.3.4. According to this, the region of rotating beam between built-in ends is subjected to pure bending with a constant load at its free end. While under the influence of this constant load, the specimen is rotated by drive spindles around the longitudinal axis; any point on the specimen is thus subjected to completely reversed steer pattern as shown in Fig.3.5. This is also helpful to study crack initiation phenomenon from the surface. In the present investigation, a set of specimen of specified length were subjected to the machine at frequency of 100Hz (stress ratio, R= -1).

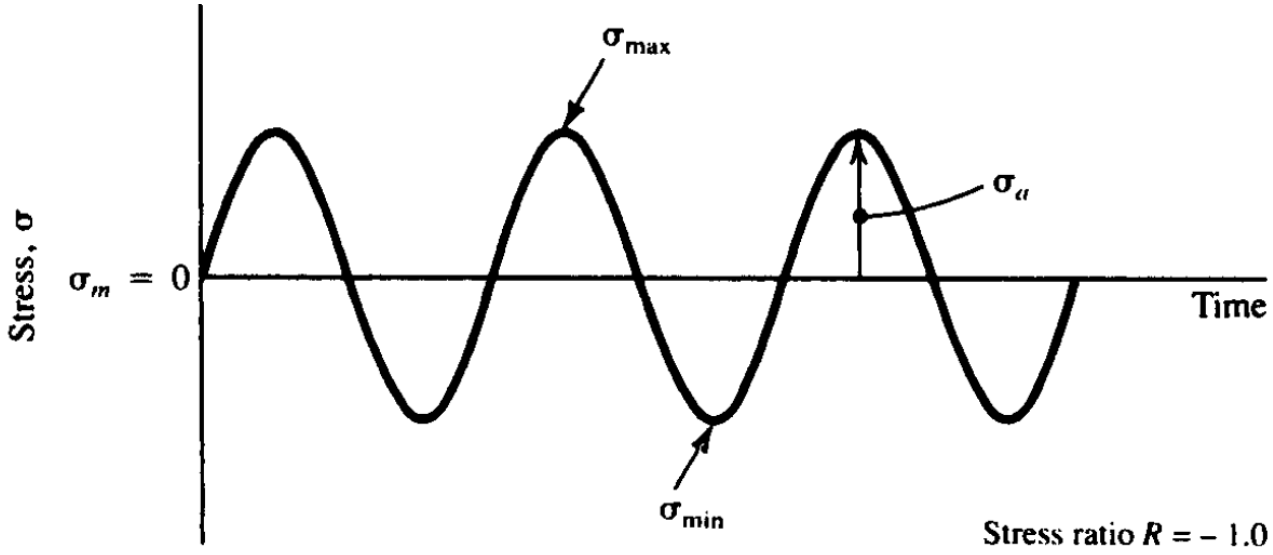

Fig 3.5: **Completely Reversed Cycle**

Working Principle:

Design of the machine is based on the rotating beam principle. The specimen is a simple beam symmetrically loaded at two points. When rotated one half revolution, the stresses in the fibers originally below the neutral axis are reversed from tension to compression and vice versa. Upon completing the revolution, the stresses are again reversed so that during one revolution the test specimen passes through a complete cycle of flexural stress (tension and compression).

For calculation of application of load for unnotched specimens according to this testing machine reversed bending formula is applicable. Formula taken over here is:

$$\mathbf{M / I = \sigma / Y}$$

Where, M = W × g × L,

M= Moment of inertia in N-m,

g = Acceleration due to gravity in m/sec^2 = 10 m/sec^2,

W = Weight or load in kg,

L = Total length up to the application of load = 210mm,

σ = Yield stress in MPa,

I = d4/64 in mm4,

Y = d/2 in mm.

d = gauge diameter in mm. = 10mm.

Chapter 4

4. Results and Discussions

RESULTS AND DISCUSSIONS

4.1. INTRODUCTION

EN9 steel (composition has been shown in Table 3.1) was used for the present work. The mechanical properties like Y.S., U.T.S. and % of elongation (ductility) was determined for differently heat-treated steels. Efforts have also made to establish structure–property relationship. This was possible because microstructure of steel is greatly influenced by heat-treatment. Last, but not the least fatigue property analysis with respect to the heat treatments and estimation of fatigue life and fatigue limit for all the heat-treatments.

4.2. MICROSTRUCTURAL RESULTS AND ANALYSIS

The microstructure of investigated EN9 normalized steel reveals equiaxed grains where the grain boundaries are not clearly visible. Typical optical micrographs of normalized steel are illustrated in Fig 4.1 where microstructure comprises of ferrite (light areas) and pearlite (dark areas) [19] and a typical SEM micrograph which is taken in various magnifications is also shown in Fig 4.2. The SEM microstructure of normalized specimen comprises of ferrite (dark areas) and pearlite (light areas) and it also free from carbides [23] as shown in Fig 4.2 is same as that of previously discussed [8].

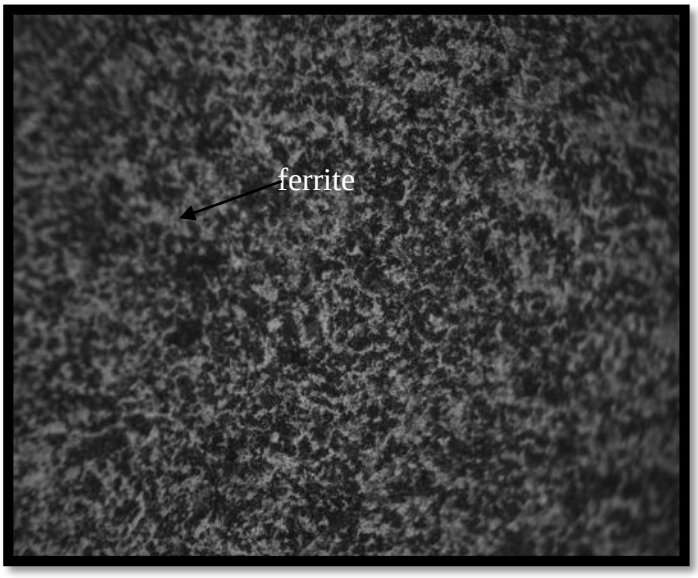

Fig 4.1: **Optical Micrograph of Normalized Steel**

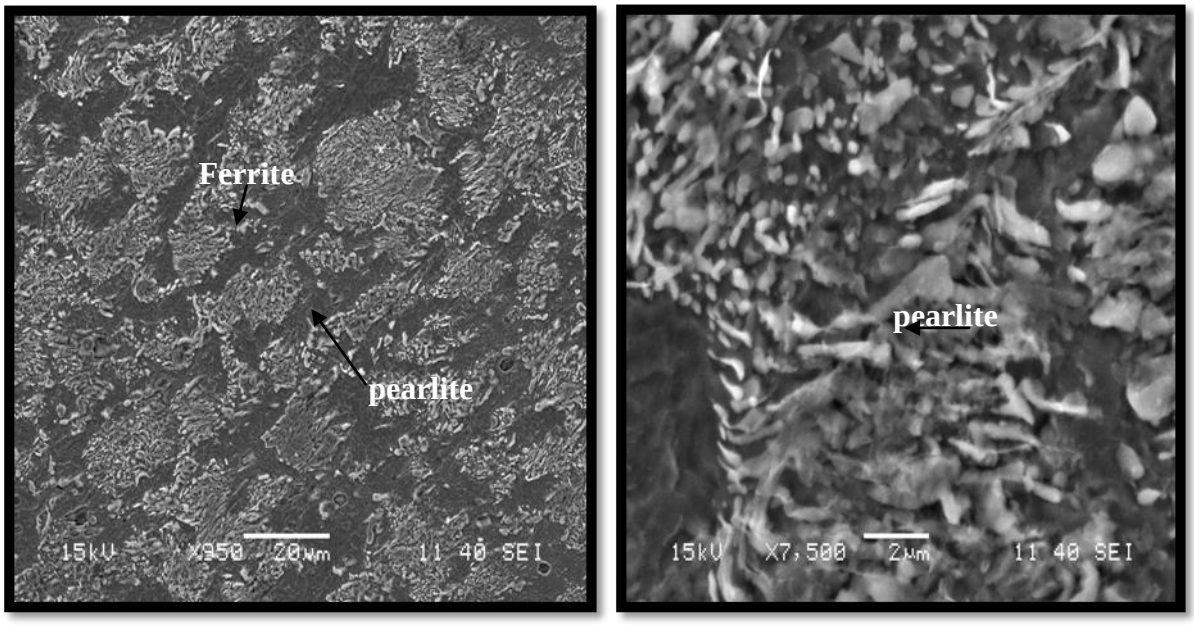

Fig 4.2: **(a) Normalized Sample at 1000X, (b) Normalized Sample at 7500X**

The optical fractograph Fig 4.3 shows the structural changes due to annealing heat-treatment. The microstructure of annealed samples comprises of both ferrite and pearlite [21-22] in equal proportion as like normalized ones, and the grain boundaries are also not well defined. As shown in figure 4.4 a t the 1000X and at 7500X magnification, it is clearly predicted that the grain boundaries are coarser than that of the normalized one.

Fig 4.3**: Optical Micrograph of Annealed Steel**

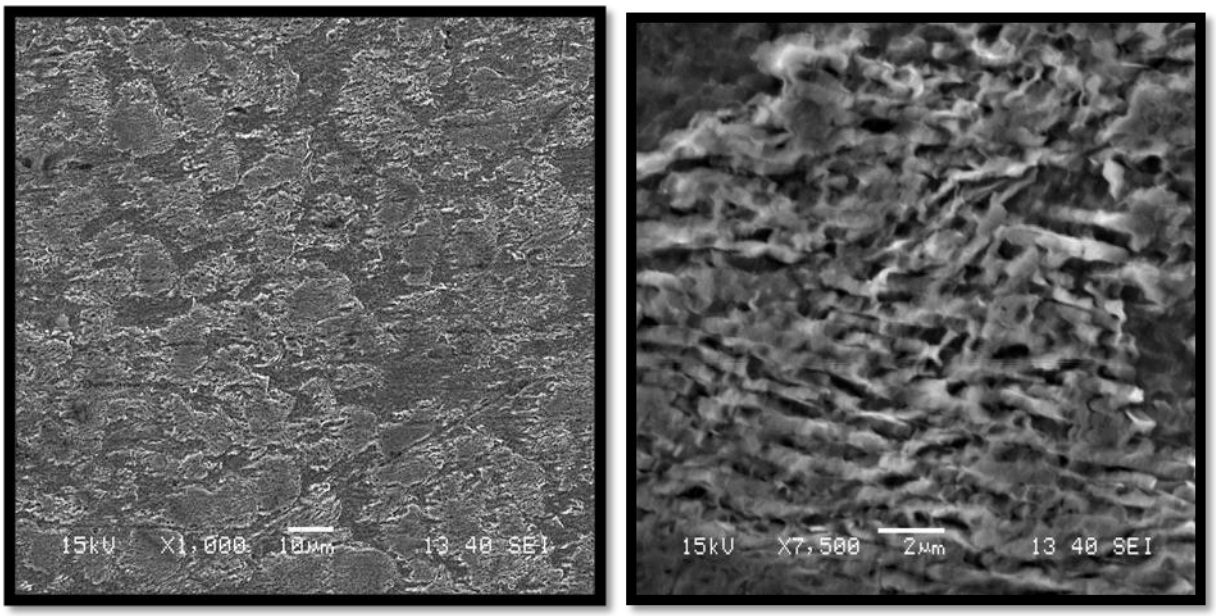

Fig 4.4: **(a) Annealed Sample at 1000X, (b) Annealed Sample at 7500X**

Some other optical micrograps are also illustrated in Fig 4.5, Fig 4.6 and Fig 4.7, which gives a cleared view about the microstructural changes at different tempering temperatures. Here, we can see the formation of spherodized carbide [43] increases as the tempering temperature increases.

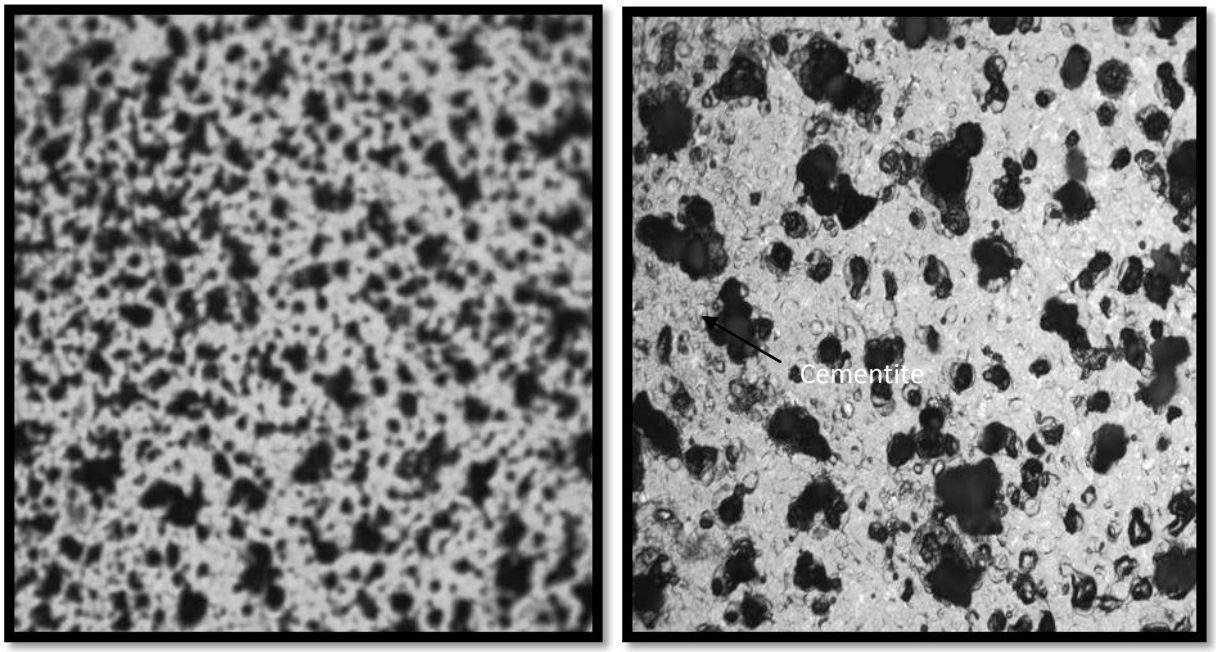

Fig 4.5: **(a) Tempered at 200^0C in 10X, (b) Tempered at 200^0C in 20X**

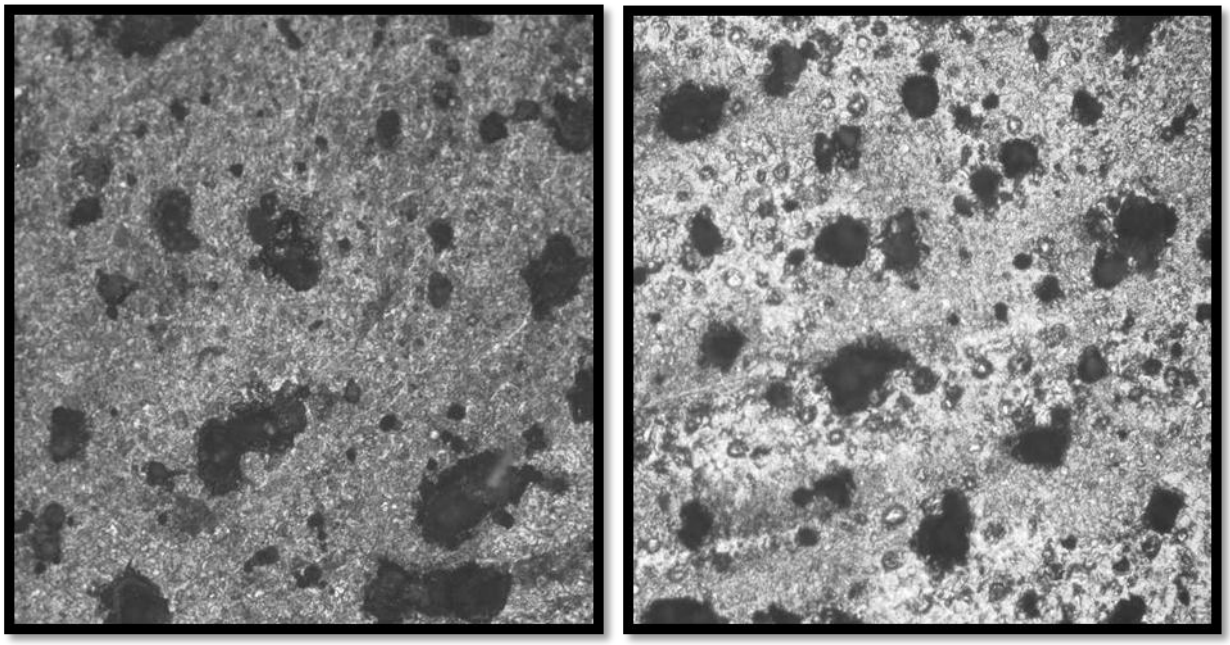

Fig 4.6: **(a) Tempered at 400^0C in 10X, (b) Tempered at 400^0C in 20X**

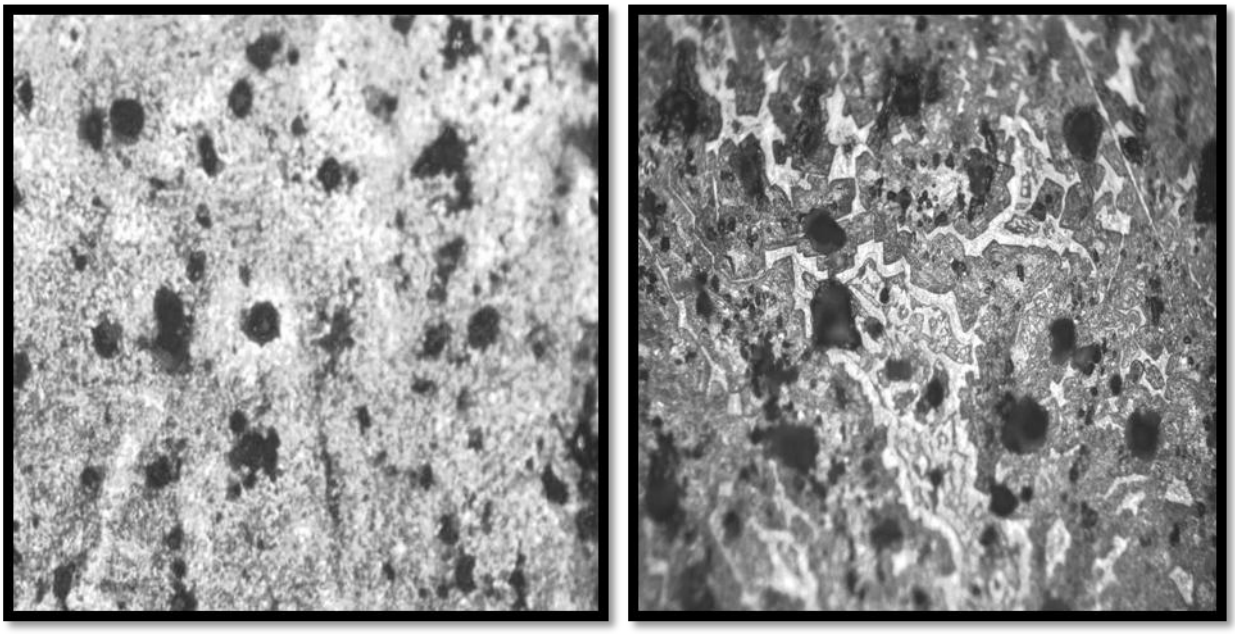

Fig 4.7: **(a) Tempered at 600^0C in 10X, (b) Tempered at 600^0C in 20X**

From the above Fig 4.5, Fig 4.6 and Fig 4.7, we can differentiate the micro-structural changes. All the optical micrographs are taken in magnification 10X to 20X range. Here, we can see the formation of ferrite decreases from 600^0C to 200^0C. In case of low temperature tempering (200^0C) tempered martensite are formed due to rapid cooling and cementite formation gradually decreases. In case of intermediate tempering (400^0C) both the tempered martensite and globular cementites are formed.

But, in 600^0C more ferrite and more globular cementite are formed which may induce some softness than that of the low temperature tempering [43].

According to the researchers heat-treatments are done to improve or to alter the mechanical and physical properties and the micro-structural changes due to heat treatment plays the vital role for this. As the micro-structural changes have relation with the mechanical properties, it is important to make a keen observation on the various tensile tests which are done on these heat-treated samples.

4.3. MECHANICAL PROPERTIES RESULTS AND ANALYSIS

Tensile test done under INSTRON 8502 as described in the Chapter 3 and the hardness tests are done in Rockwell hardness tester gives various results for both heat treated and as received (non-treated) samples. The results from the tensile tests and hardness tests show the mechanical properties variation at every heat-treatment conditions. Variation of tempering temperature and tempering time also alters the mechanical properties. The effect of heat treatment on mechanical properties is well analyzed and predicted below.

4.3.1. Hardness Measurement

Rockwell hardness tester gives the hardness values for as received and also for heat treated specimens. Hardness values for these samples tabulated below in Table 4.1. According to the tabulated results some of the comparison graphs are drawn which are shown in the Fig 4.8 and Fig 4.9, whereas Fig 4.8 shows the comparison of hardness at all treating conditions and Fig 4.9 shows the comparison between the different tempering temperature at different time length.

Specimen Specification	Time in Hours(hr.)	Hardness in RC
As received	nil	35
Normalized at 800^0C	1 hr.	64.5
Annealed at 800^0C	1 hr.	52
Tempered at 200^0C	1 hr.	62
	1 ½ hrs.	59

	2 hrs.	56
Tempered at 400^0C	1 hr.	58
	1 ½ hr.	55
	2 hr.	53
Tempered at 600^0C	1 hr.	55
	1 ½ hr.	52
	2 hr.	50

Table 4.1: **Variation of Hardness for Heat Treated Specimen**

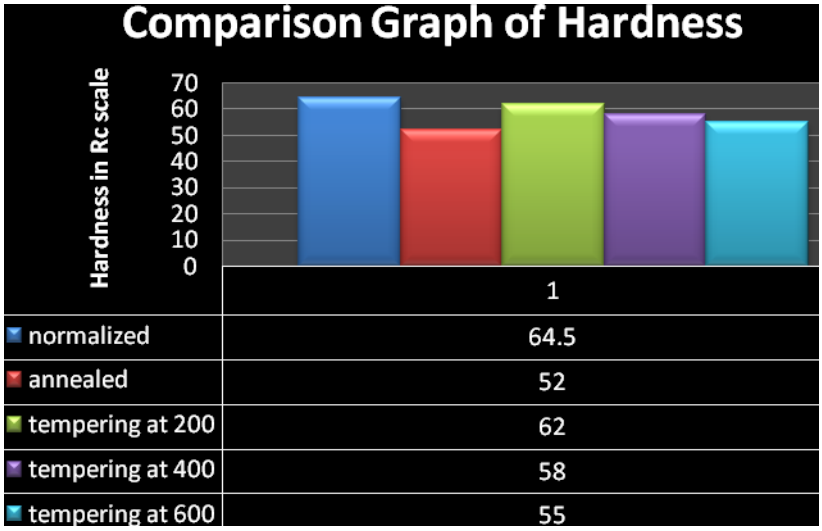

Fig 4.8: **Comparison Graph of Hardness for all Heat-Treatment**

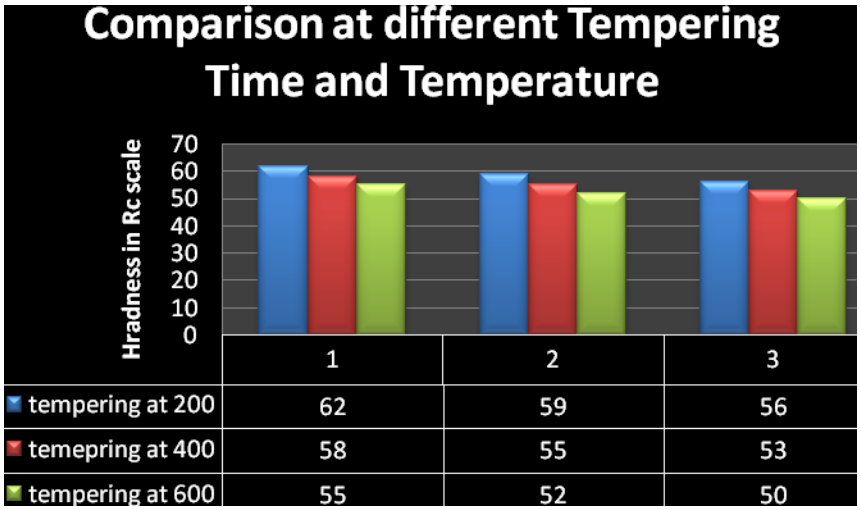

Fig 4.9: **Comparison Graph of Hardness for Tempered Specimens**

*1, *2, *3 – Tempered for 1 hr, 1 ½ hrs, and 2 hrs respectively

Hardness test results show the variation w.r.to both time and temperature. Some variations are also shown due to the different treating conditions. These are the interpret results which can make difference in heat-treatment types and it also help us to understand the mechanism behind the property alteration. Mechanical properties are enhanced as the materials gone through the heat treatment processes [41]. In this literature, specimens corresponding to all heat-treatment temperatures showed higher hardness as compared to the annealed specimens of the same steel. From the above plotted results, we also find that the annealed specimens are softer than that of the other heat-treatments. Also, it is clearly visible that air cooling (normalized) samples, where the grains are finer has higher hardness value (64.5 Rc) as compared to the furnace cooling (annealed) samples having hardness value (52 Rc). Here, we can conclude that the cooling rate affects the hardness properties of the material. As the normalized samples had higher cooling rate than that of the annealed one, the hardness is more for normalized samples. The result of stress concentration effects of the thin carbide films which are formed during the formation of martensite in tempering at lower temperature gives hardness Rc 56 to Rc 62 which is more than that of the other tempered conditions [43].

The variation of tempering time w.r.to constant temperature and vice versa also shows good results. Fig. 4.9 shows that hardness decreases as the tempering temperature increases. This is due to the transformation of martensite to tempered martensite. The hardness of martensite is due to the tetragonal structure of the martensite where carbon occupies tetrahedral voids. This structure results from the diffusion less transformation which occurs by shear mechanism. So, when martensite is tempered, diffusion of C from the tetrahedral sites of the BCT structure takes place and thus the tetragonality of martensite gets reduced. Alternatively, the structure of martensite becomes less strained after holding it at a higher temperature but less than the lower critical temperature because of carbon diffusion. Thus, the hardness of tempered martensite is lesser than quenched martensite [126]. The decrease in hardness from 1 hr. to 2 hr. time period is due to the disappearance of Martensite phase. Lower tempering time yield a finer martensite structure and less number of cementite and therefore higher hardness was obtained. But, as the holding/treatment time increased further, the hardness values were again decreased due to the occurrence of coarse bainite or carbide precipitate in a matrix of ferrite structure [127-128]. From all the discussions based upon the experimental results shows that tempering at 200 ^{0}C at 1 hour gives the best results for hardness (Rc 62) at different tempering temperature for various time lengths. Rc 64.5 for normalized treatment due to the finer microstructure is highest among all treatments.

4.3.2. Tensile Test Results and Analysis

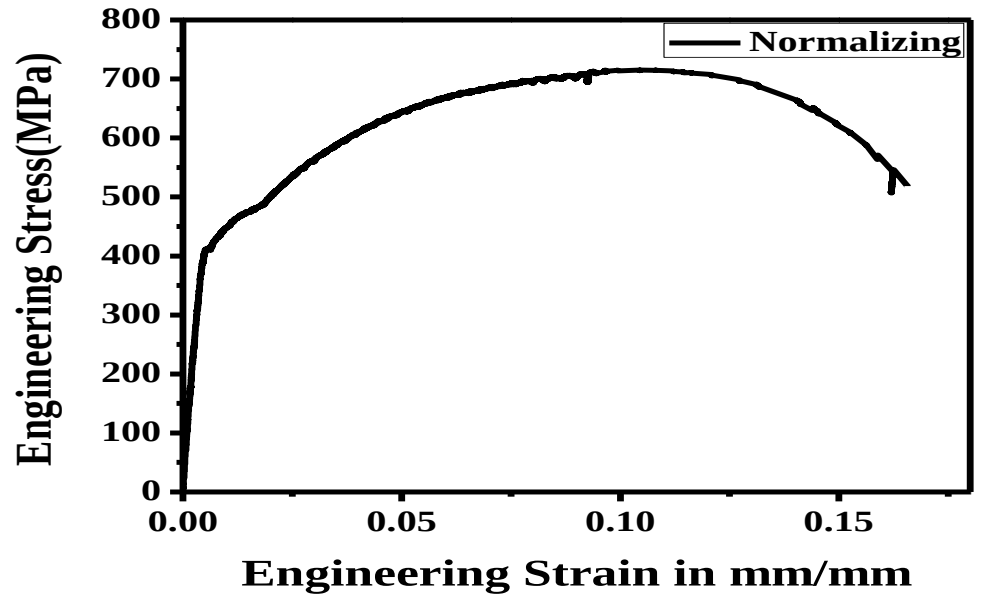

Fig 4.10: **Engineering Stress vs. Engineering Strain Curve for Normalizing**

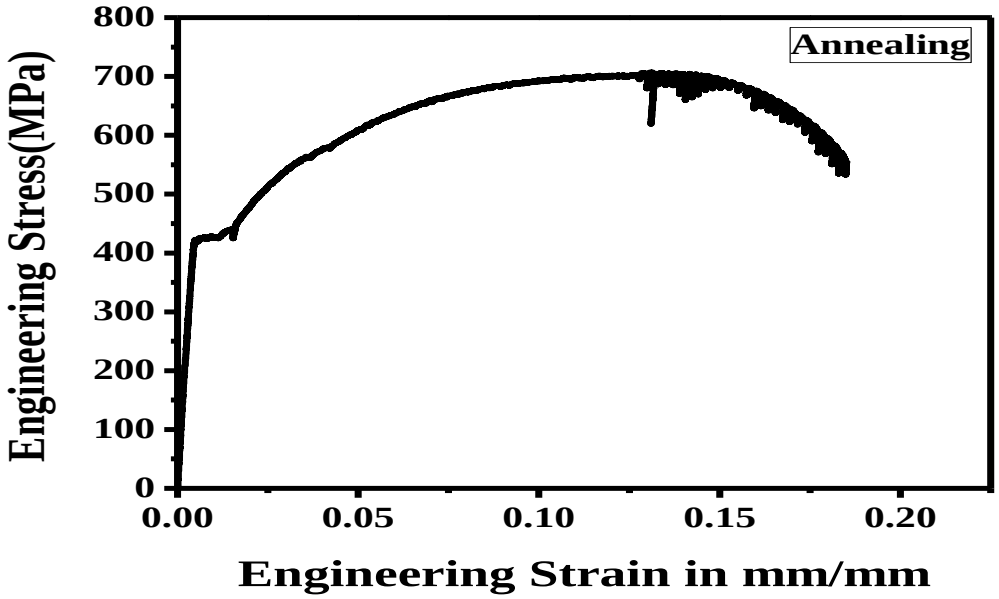

Fig 4.11: **Engineering Stress vs. Engineering Strain Curve for Annealing**

Some of the tensile test data are plotted with the help of INSTRON 8502. The test data are plotted against engineering stress vs. engineering strain. The variation of U.T.S., yield stress and % of elongation for all the heat treating conditions which are shown by these plotted graphs. From Fig 4.10 to Fig 4.20, we can get the stress vs. strain curve of all heat-treatments.

From above Fig.4.10 and Fig.4.11, we can see that some significant changes obtained due to changes in heat treatment type. Here, the results show that yield stress and ultimate tensile stress is more for normalized as compared to annealed treatment. This enhancement is occurred may be due to the fact that the cooling process influences by the cooling rate used for these treatments. Normalizing cooling rate compared to annealing is faster, because in normalizing cooling process is done by air cooling and in annealing this is done by furnace cooling. Due to this, more refine grains are obtained as compared to the annealed one which induces more strength and less ductility in the material [23]. Other tempering heat treatments are also plotted by engineering stress vs. engineering strain figures as shown in below figures.

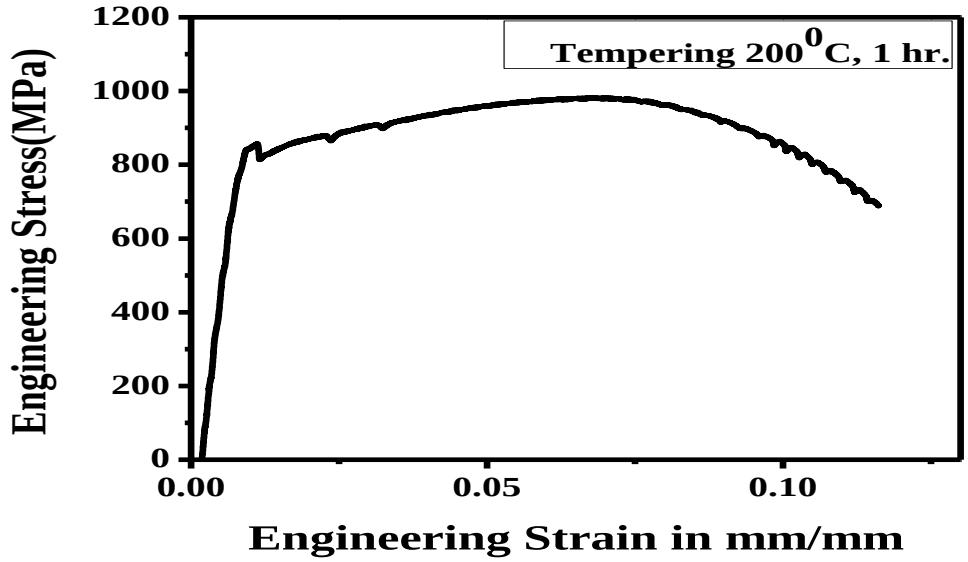

Fig 4.12: **Engineering Stress vs. Engineering Strain Curve for Tempering at 200 ^{0}C, 1 hour**

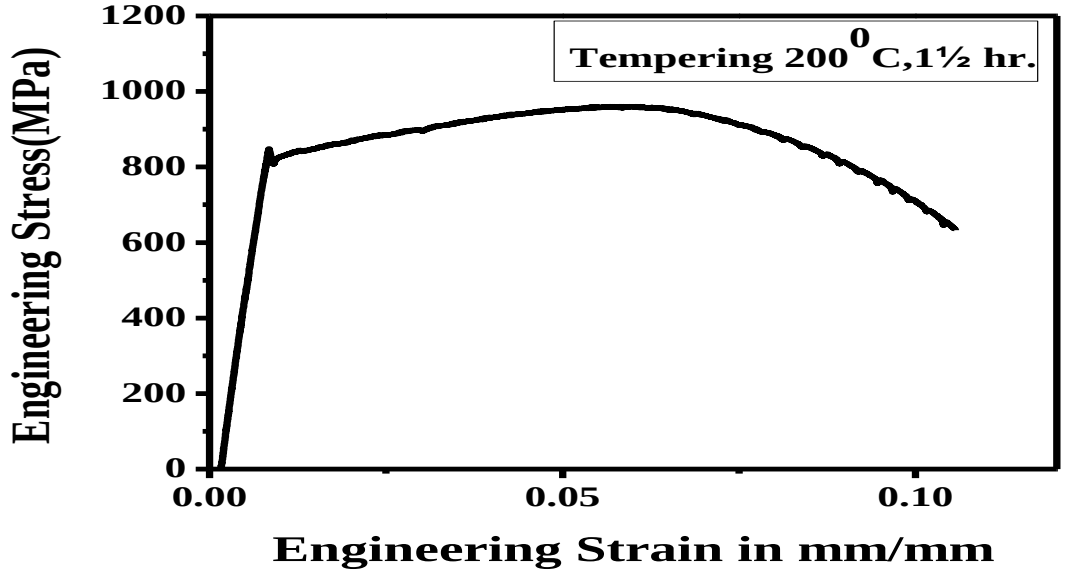

Fig 4.13: **Engineering Stress vs. Engineering Strain Curve for Tempering 200^{0}C, 1½ hours**

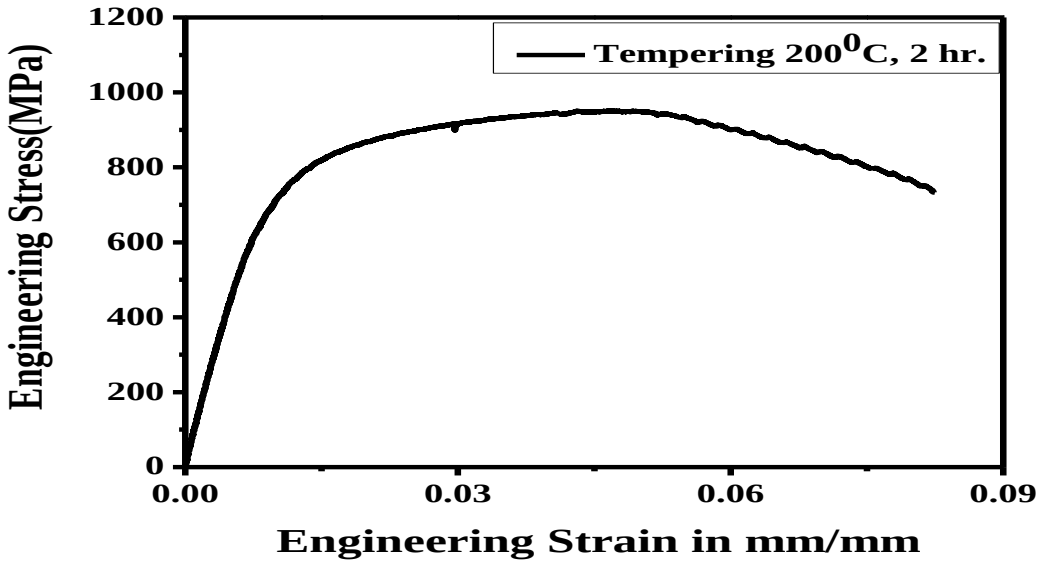

Fig 4.14: **Engineering Stress vs. Engineering Strain Curve for tempering 200^{0}C, 2 hours**

From the Fig 4.12, Fig 4.13 and Fig 4.14, it is distinctly visible that UTS and YS are increased as the tempering time decreases. The UTS at 200 ^{0}C, 1 hour is 978 MPa which is slightly more than that of the 1½ hours and 2 hours, there is increased in YS value which is well identified by seeing the Fig 4.12, Fig 4.13 and fig 4.14. Compared to the normalizing and annealing treatments tempering has higher value due to the more refined grains, as the specimens were subjected to austenizing, quenching and then tempering [25]. There are also some other changes, we can see for this treatments which are well explained in upcoming chapters. Another mechanical property variation which should be in consideration is ductility. During the tensile test, materials are elongated and then broken due to tensile stress. As a result of this, some dimensional changes are made which are well described by ductility measurements. According to the tensile test of tempering 200 ^{0}C for higher time we get a result of 18 mm/mm % of elongation and for lower time i.e. 11 mm/mm. Here, we have seen some slight decrease in ductility as the temperature decreases with slightly sacrificing stress. But having less ductility as compared to the normalizing and annealing. From this we can conclude that when strength induced in the materials, it makes the material more hard which gives the result of less ductility in the material.

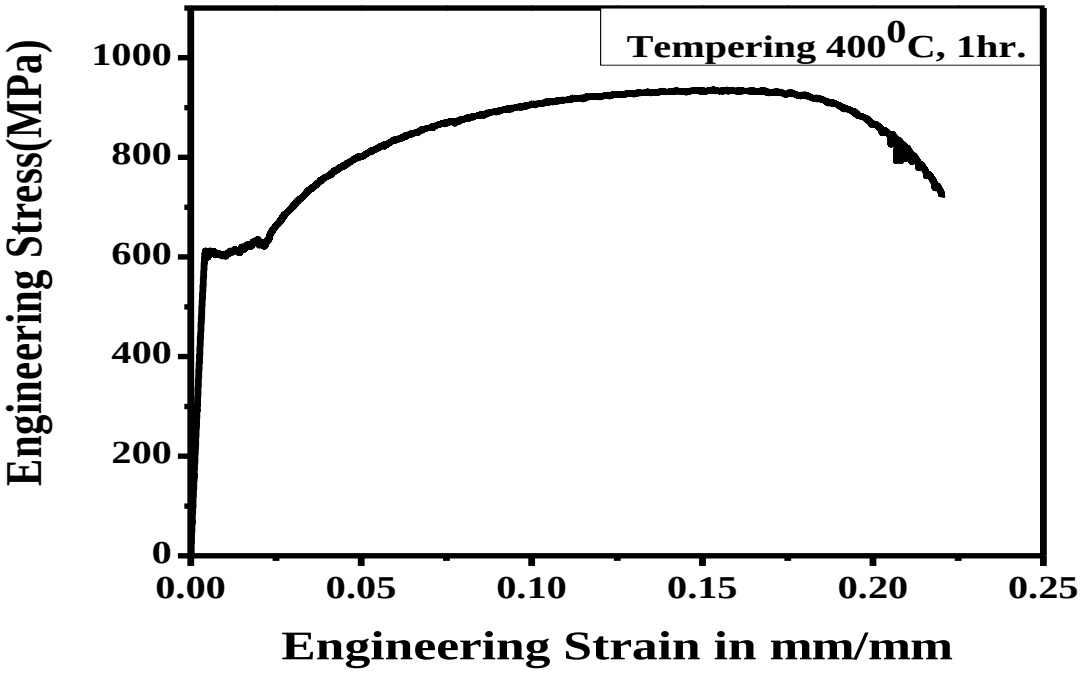

Fig 4.15: **Engineering Stress vs. Engineering Strain Curve for Tempering 400 ^{0}C, 1 hour**

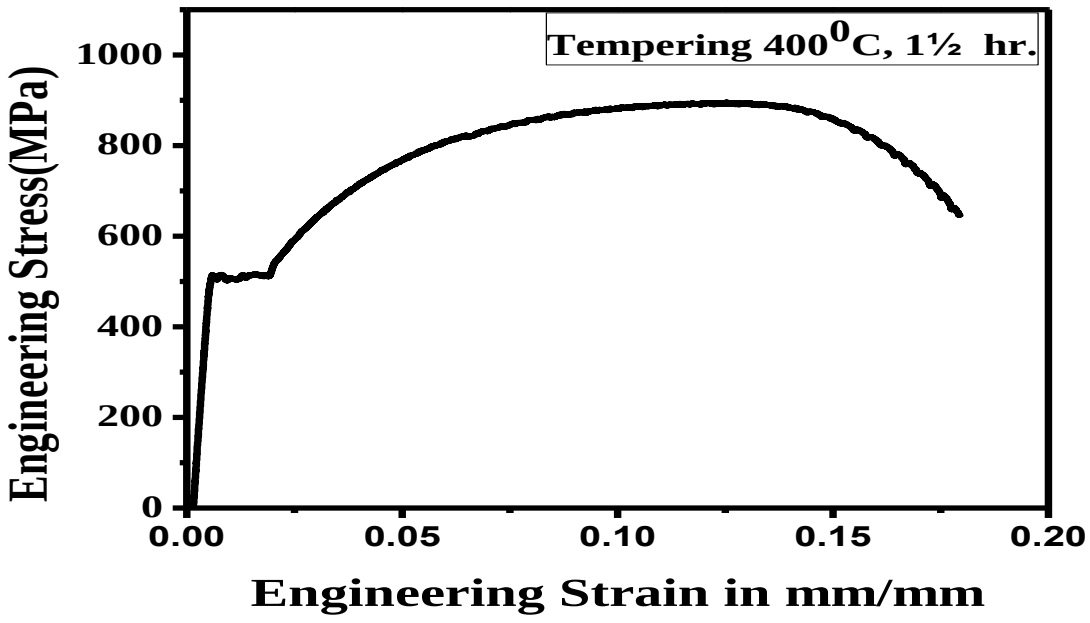

Fig 4.16: **Engineering Stress vs. Engineering Strain Curve for Tempering 400 ^{0}C, 1 ½ hours**

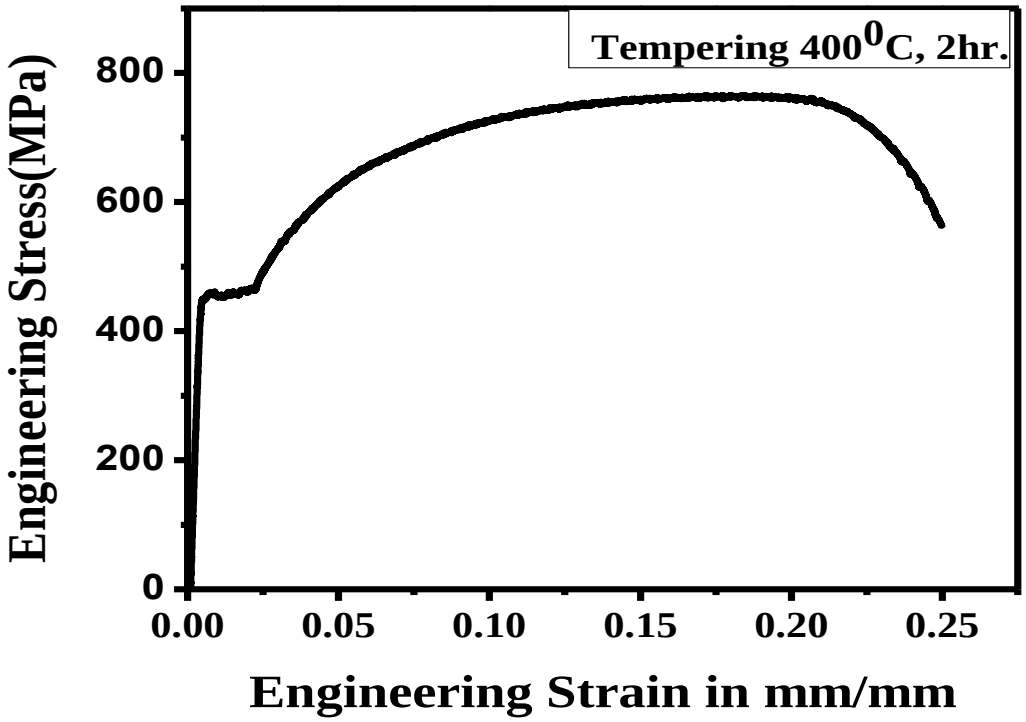

Fig 4.17: **Engineering Stress vs. Engineering Strain Curve for Tempering 400 ^{0}C, 2 hours**

We have also seen the same kind of variations at 400 ^{0}C tempering as in 200 ^{0}C tempering temperature w.r.to time which are shown in Fig 4.15, Fig 4.16 and Fig 4.17. At 400 ^{0}C tempering we also get better results for UTS and YS than the normalizing and annealing. Ductility is induced as time increased for the same. But as compared to the 200 ^{0}C tempering elongation is more which directly indicates that material is soft as compared to the 200 ^{0}C tempered materials. We get highest % of elongation at 400 ^{0}C, 2 hours. i.e. 24 mm/mm at 762 MPa and less % of elongation at 400 ^{0}C, 1 hour. i.e. 22.5 mm/mm UTS and YS maximum values are 934 MPa and 619 MPa respectively for 400 ^{0}C, 1 hour whereas for 400 ^{0}C, 2 hour, we get the lowest one i.e. 762 MPa, and 465 MPa respectively. Here, we can conclude that the material is softer than the 200 ^{0}C tempering because of its more ductility and less strength. But comparing with normalized and annealed it has more strength and more ductility.

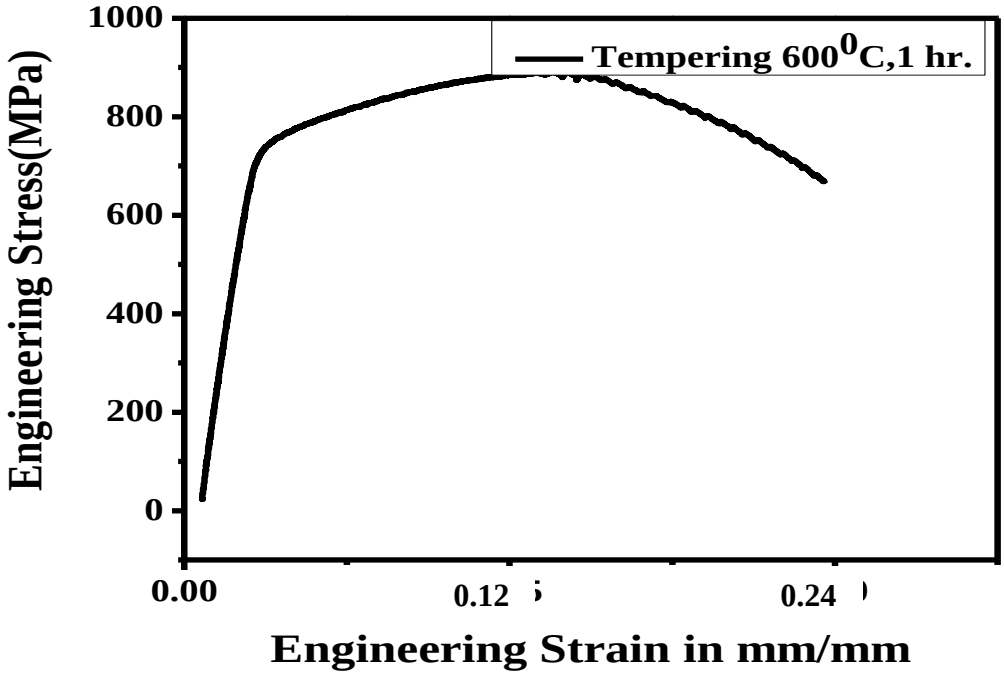

Fig 4.18: **Engineering Stress vs. Engineering Strain Curve for Tempering 600 ^{0}C, 1 hour**

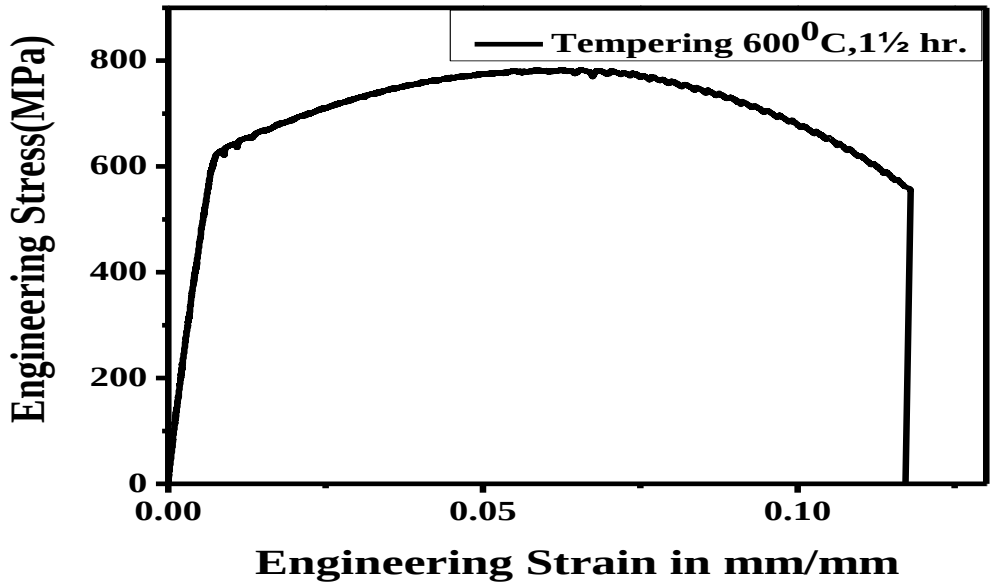

Fig 4.19: **Engineering Stress vs. Engineering Strain Curve for Tempering 600 ^{0}C, 1½ hours**

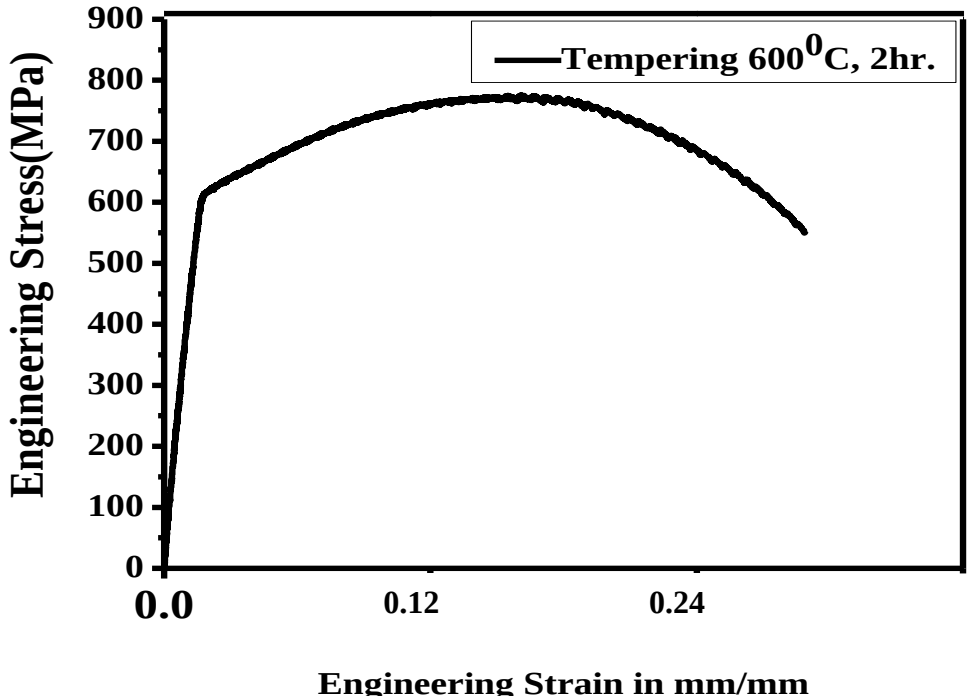

Fig 4.20: **Engineering Stress vs. Engineering Strain Curve for Tempering 600^{0}C, 2 hours**

Fig 4.18, Fig 4.19 and Fig 4.20 show that variation of engineering stress w.r.t strain as a result of tensile test for tempering 600 ^{0}C at varying time periods, where we will get the UTS, YS and % of elongation, according to time the variation of these properties are same as that of 400 ^{0}C and 200 ^{0}C. At 600 ^{0}C for 2 Hours, UTS and YS are minimum 772 MPa and 618 MPa respectively as compared to 1½ hours and 1hour but % of elongation is more as compared to them. In case of 600 ^{0}C for 1 hour, UTS and YS are maximum 891 MPa and 741 MPa respectively, whereas % of elongation is 24 mm/mm less than that of 600^{0}C (2 hours) and also there is decreased in strength when compared to the low temperature tempering 400 ^{0}C and 200 ^{0}C.

All the above graphs show the variation of mechanical properties for different heat treatments. From the above plotted tensile test graphs, we get the values of various mechanical properties like U.T.S., yield stress and % of elongation. All these data are shown in the Table 4.2.

Specimen Specification	**Time in Hr.**	**Yield Stress (YS) in MPa**	**Ultimate Tensile Stress in MPa**	**% of Elongation**	**Maximum Load in KN**
Specimen as received		397.61	583.16	21.60	45.795
Normalizing at 800^0C	1hr.	433.627	716.08	17	56.24
Annealing at 800^0C	1hr.	425	707	18.5	55.57
Quenched from 800^0C and Tempered at 200^0C	1hr.	819	978	11	76.802
	1½ hr.	812	969.789	12	76.157
	2hr.	728	951.69	18	74.736
Quenched from 800^0C and Tempered at 400^0C	1hr.	619	934	22.5	73.347
	1½ hr.	507	894	23	70.205
	2hr.	465	762	24	59.839
Quenched from 800^0C and Tempered at 600^0C	1hr.	741.12	891	24	69.970
	1½ hr	623.43	783	25	61.488
	2hr	618.51	783	26	60.625

Table 4.2: **Tensile Properties Variation in different Heat Treatment Conditions**

(A)

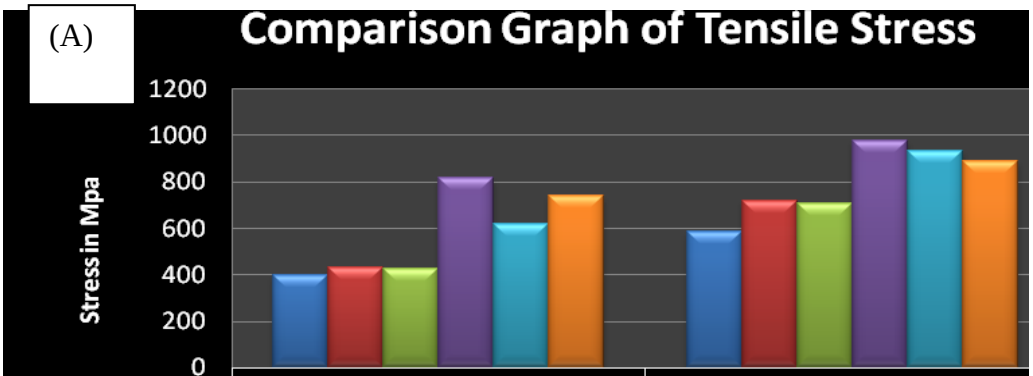

	1	2
as received	397.61	583.16
normalized	433.627	716.08
annealed	425	707
tempering at 200	819	978
tempering at 400	619	934
tempering at 600	741.12	891

(B)

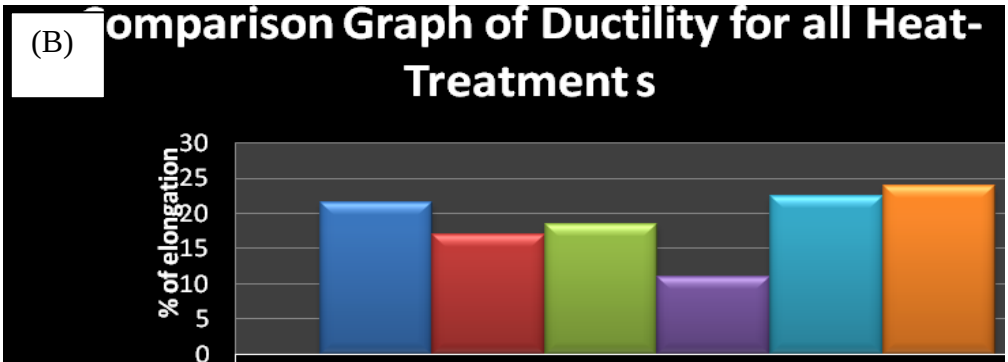

	% of elongation
as received	21.6
normalized	17
annealed	18.5
tempering at 200	11
tempering at 400	22.5
tempering at 600	24

Fig 4.21: **(A) & (B) Comparison Graphs of Tensile Properties**

(A)

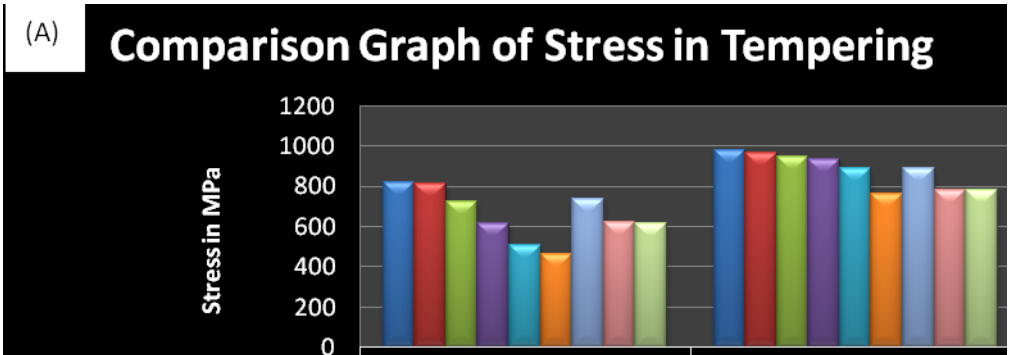

	1	2
Tempered at 200 (1hr.)	819	978
Tempered at 200 (1.5 hr.)	812	969.789
Tempered at 200 (2 hr.)	728	951.69
Tempered at 400 (1 hr.)	619	934
Tempered at 400 (1.5 hr.)	507	894
Tempered at 400 (2 hr.)	465	762
tempered at 600 (1 hr.)	741.12	891
Tempered at 600 (1.5 hr.)	623.43	783
Tempered at 600 (2 hr.)	618.51	783

(B)

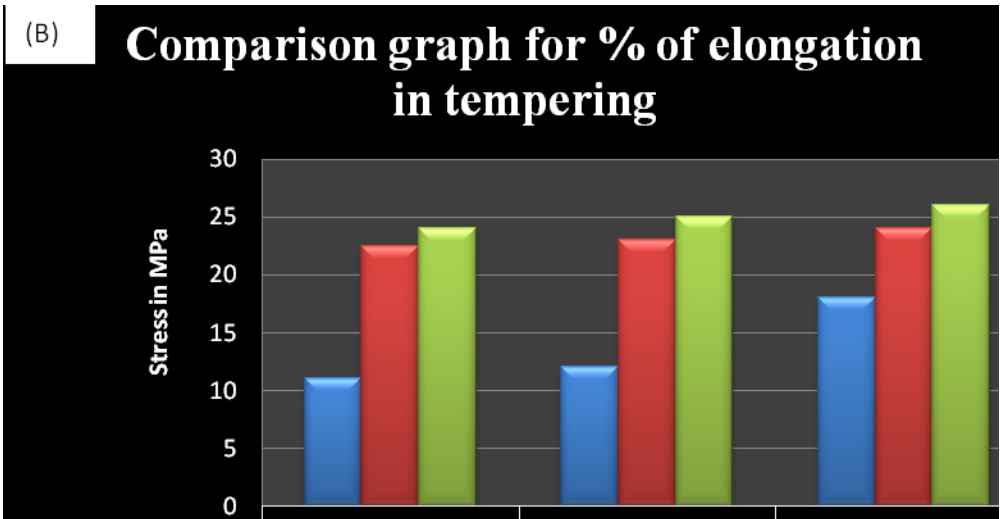

	1	2	3
Tempered at 200	11	12	18
Tempered at 400	22.5	23	24
Tempered at 600	24	25	26

Fig 4.22 [A] & [B]: **Comparison Graphs of Tensile properties w.r.t Tempering Time**

*1 – Y.S, *2 – U.T.S

From the above results, following observations and inferences were made. It was seen that the various tensile properties followed a particular sequence with respect to microstructure:

1. All the mechanical properties are enhanced as the materials gone through the heat treatment processes [42].
2. Microstructure photographs taken by SEM and metallurgical inspections indicated that the surfaces of tempered samples are martensitic at low temperature [31-33].
3. We have also marked that the UTS and YS values for the normalized specimen is more than that of the annealed one due to the fact that the normalized micro structures are more finer as compared to annealed ones which is clearly visible in Fig 4.1 (a) and Fig 4.2 (a) [21-23].
4. At a high tempering temperature, more softness (ductility) induced in the tempered specimens as from the Fig 4.18, Fig 4.19 and Fig 4.20 indicated may be because of more carbide are formed as the tempering temp increases and also more ferrite are present which are the main reasons to induce ductility inside the material as the ferrite has softer microstructure than others.
5. More is the tempering time (keeping the tempering temperature constant), more is the ductility induced in the specimen because of the formation of carbide and ferrite increased but the disappearance of tempered martensite takes place.
6. This clearly implies that the UTS and also to some extent the yield strength decreases with increase in tempering time where as the ductility (% of elongation) increases by the formation of more ferrite as the tempered temperature increases the strength.
7. For a given tempering time, an increase in the tempering temperature decreases the UTS value and the yield strength of the specimen due to the ferrite formation where as on the other hand it increases the % elongation and hence the ductility.
8. One distinguishable change occurred from 400 ^{0}C to 600 ^{0}C; here we had seen that YS is more at 600 ^{0}C than 400 ^{0}C, which contradict the normal fundamentals but UTS follows the general trend. This may be occurred due to the formation of more carbide from 400^{0}C to 600 ^{0}C or may be due to some microstructural changes or may be due to other factors.

4.4. POST TENSILE TEST FRACTOGRAPHICAL RESULTS AND ANALYSIS

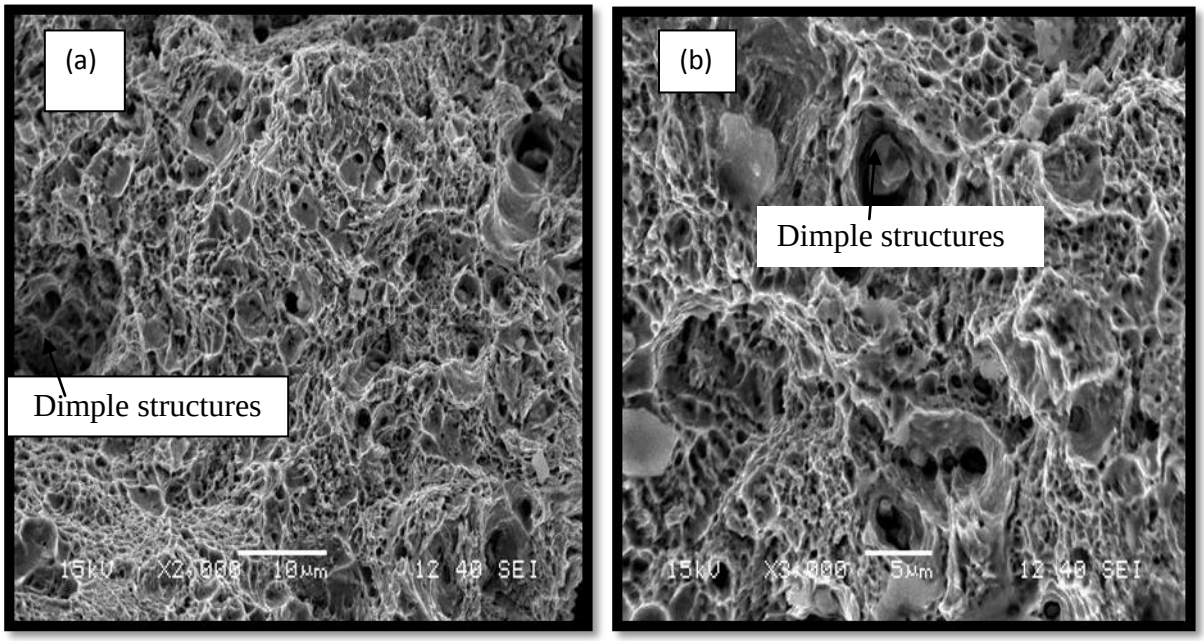

Fig 4.23: **(a) Normalized Tensile Test Fractograph at 2000X,**

(b) Normalized Tensile Test Fractograph at 3000X

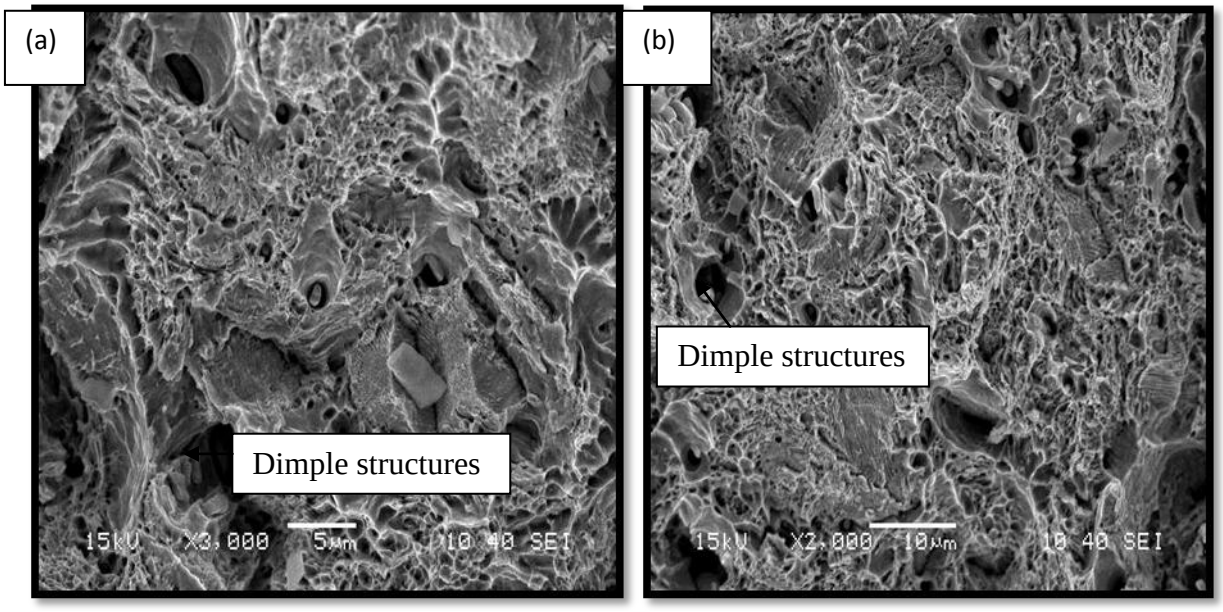

Fig 4.24: **(a) Annealed Tensile Test Fractograph at 2000X,**

(b) Annealed Tensile Test Fractograph at 3000X

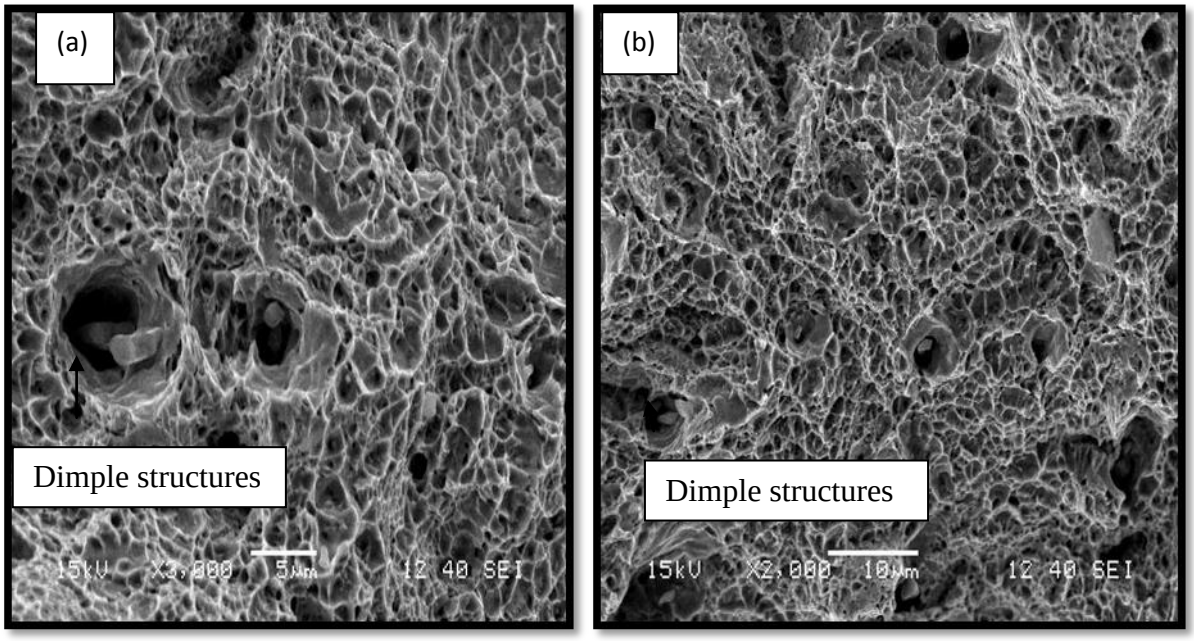

Fig 4.25: **(a) Tempered at 200^{0}C, Tensile Test Fractograph at 3000X,**

(b) Tempered at 200^{0}C, Tensile Test Fractograph at 2000X

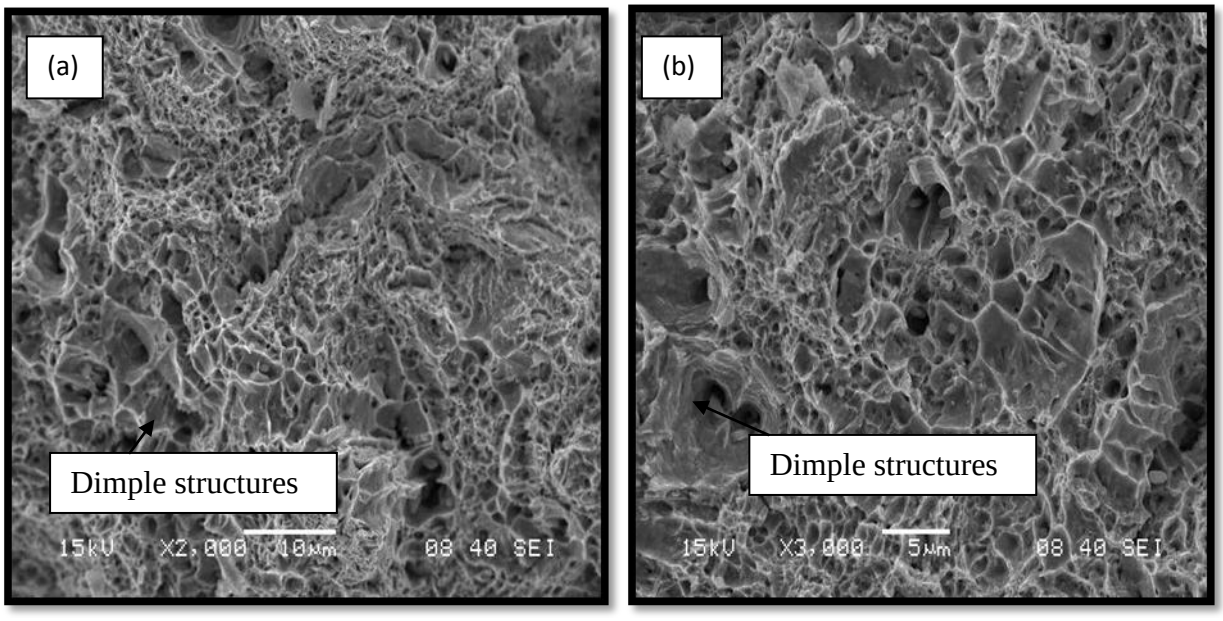

Fig 4.26: **(a) Tempered at 400^{0}C, Tensile Test Fractograph at 3000X**

(b) Tempered at 400^{0}C, Tensile Test Fractograph at 2000X

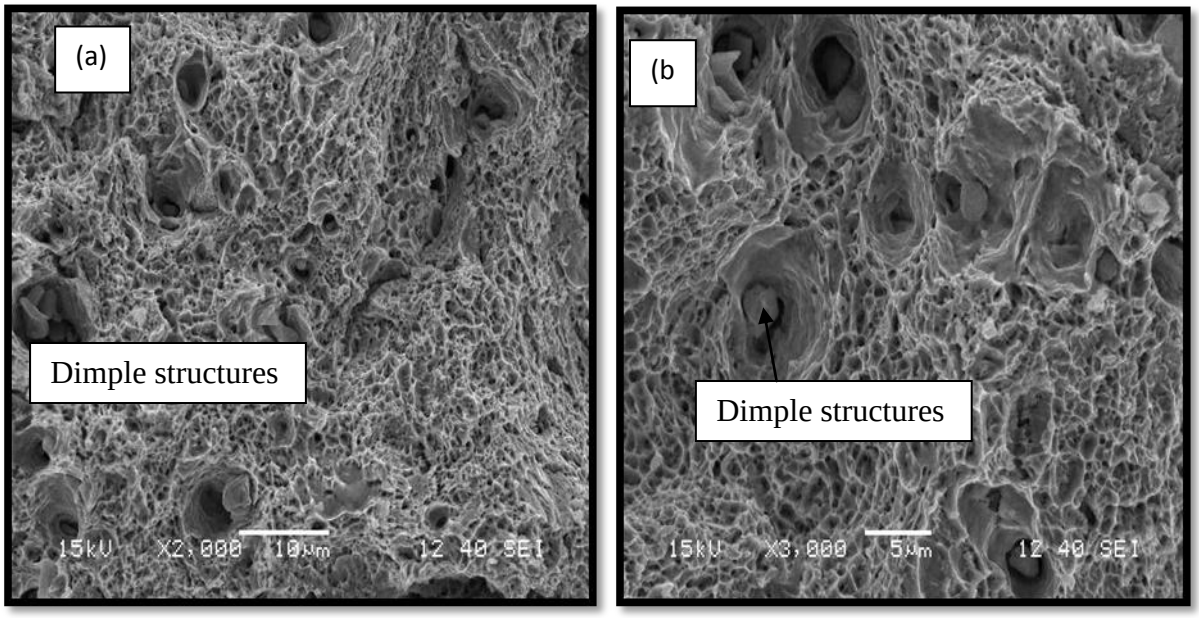

Fig 4.27: **(a) Tempered at 600 ^{0}C, Tensile Test Fractograph at 2000X**

(b) Tempered at 600 ^{0}C, Tensile Test Fractograph at 3000X

The morphology of the fracture specimens are analyzed by Scanning Electron Microscopy (SEM). Fig 4.23 - Fig 4.27 shows the fracture surface of the different samples. As steel shows a fully dimpled fracture, the fracture pattern of both annealed samples are same as in as medium carbon steel with greater numbers of dimples as shown in Fig 4.23 and Fig 4.24. So, the fracture surfaces confirms with the induced ductility in both the annealed and normalized samples. The fracture pattern of tempered samples at low temperatures show a mixed mode of fracture because of the untransformed martensite presents at that temperature, but as the tempering temperature increases the major fracture pattern is ductile in nature. So, this confirms to the increase in ductility i.e. the elongation percentage. There is decrease in strength and hardness when tempering temperature is increased from 200 °C to 400 °C. But, the strength and hardness values remain constant with further increase in tempering temperature to 600 °C. This is due to the occurrence of strain-hardening phenomena [25].

4.5. FATIGUE LIFE ESTIMATION RESULTS AND ANALYSIS

Moore testing machine gives the desired results which shows the variation of life cycles w.r.to stress where load applied is calculated using by the formula which is elaborated in chapter 3.5. Here, all the dimensional values are considered according to the dimension of the specimen which is described in chapter 3.1. From these life cycles, different heat treatments are estimated and tabulated below and graphical presentations are also made.

Serial no.	Stress in (MPa)	No. of cycles to failure, N	Value of Log N
1	433 (YS)	1.6×10^5	5.2
2	411 (0.95 YS)	3.2×10^5	5.5
3	390 (0.90 YS)	6.3×10^5	5.8
4	368 (0.85 YS)	1.2×10^6	6.1
5	346 (0.80 YS)	2.5×10^6	6.4
6	346 (0.80 YS)	5.0×10^6	6.7
7	346 (0.80 YS)	1.0×10^7	7.0
8	346 (0.80 YS)	2.0×10^7	7.3
9	346 (0.80 YS)	4.5×10^7	7.7
10	346 (0.80 YS)	9×10^7	8.0

Table 4.3: **Life Estimation for Normalizing**

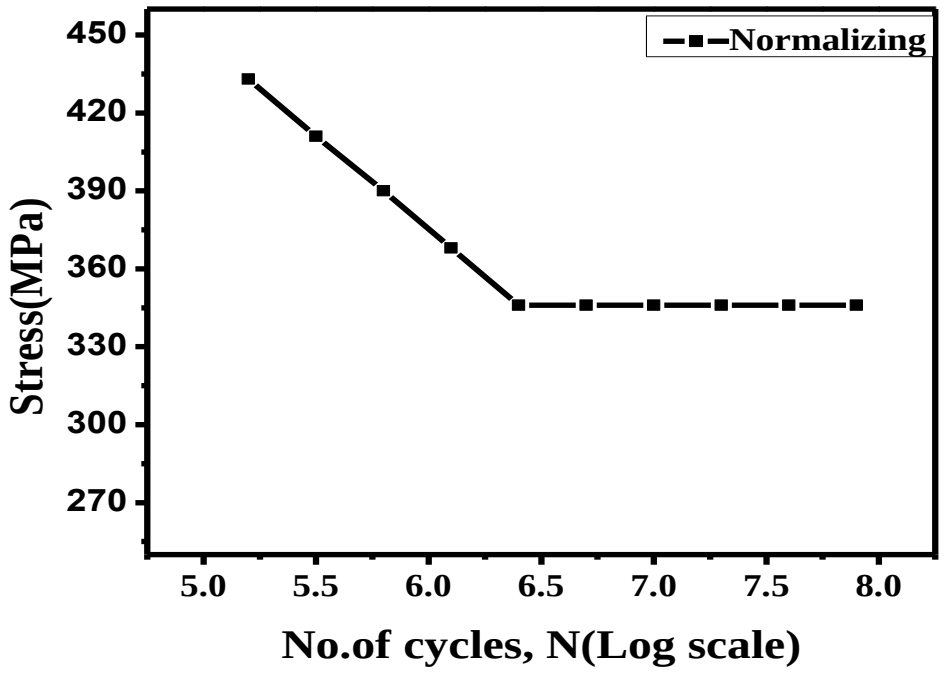

Fig 4.28: **S-N Curve for Normalizing**

Serial no.	Stress in (MPa)	No. of cycles to failure, N	Value of Log N
1	425 (Y.S.)	3.2×10^{5}	5.5
2	403 (0.95 Y.S.)	6.3×10^{5}	5.8
3	382 (0.9 Y.S.)	1.2×10^{6}	6.1
4	361(0.85 Y.S.)	2.5×10^{6}	6.4
5	340 (0.80 Y.S.)	5.0×10^{6}	6.7
6	318 (0.75 YS)	1.0×10^{7}	7.0
7	318 (0.75 YS)	1.9×10^{7}	7.3
8	318 (0.75 YS)	3.9×10^{7}	7.6
9	318 (0.75 YS)	7.9×10^{7}	7.9
10	318 (0.75 YS)	1.5×10^{8}	8.2

Table 4.4: **Life Estimation for Annealing**

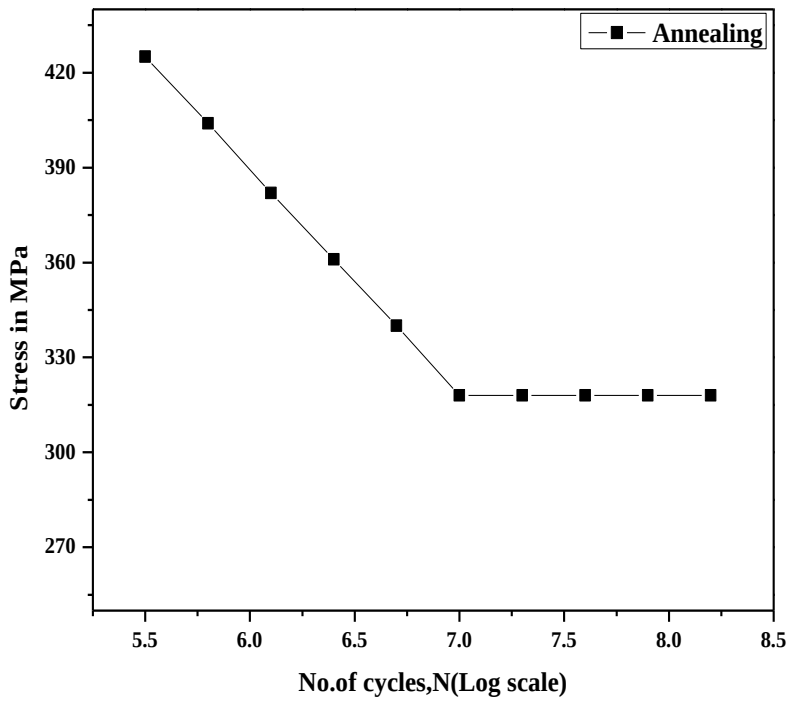

Fig 4.29: **S-N Curve for Annealing**

Serial no.	Stress in (MPa)	No. of cycles to failure, N	Value of Log N
1	819 (Y.S.)	4.9×10^{4}	4.9
2	778 (0.95 Y.S.)	1.26×10^{5}	5.1
3	737 (0.90 Y.S.)	1.9×10^{5}	5.3
4	696 (0.85 Y.S.)	3.16×10^{5}	5.5
5	655 (0.80Y.S.)	5.01×10^{5}	5.7
6	614 (0.75Y.S.)	7.94×10^{5}	5.9
7	573 (0.70Y.S.)	1.26×10^{6}	6.1
8	573 (0.70Y.S.)	1.99×10^{6}	6.3
9	573 (0.70Y.S.)	3.1×10^{6}	6.5
10	573 (0.70Y.S.)	5.01×10^{6}	6.7

Table 4.5: **Life Estimation for Tempering at 200^{0}C, 1 hr**

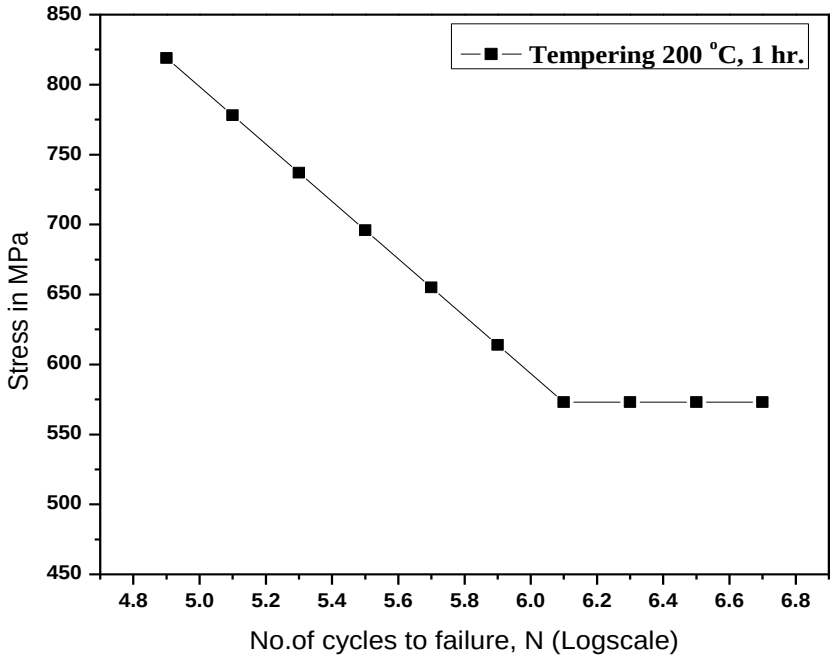

Fig 4.30: **S-N Curve for Tempering at 200 ^{0}C, 1hr**

Serial no.	Stress in (MPa)	No. of cycles to failure , N	Value of Log N
1	812 (Y.S.)	1.26×10^5	5.1
2	771 (0.95 Y.S.)	1.9×10^5	5.3
3	730 (0.90 Y.S.)	3.16×10^5	5.5
4	690(0.85 Y.S.)	5.01×10^5	5.7
5	649(0.80 Y.S.)	7.94×10^5	5.9
6	609 (0.75 Y.S.)	1.26×10^6	6.1
7	568 (0.70Y.S.)	1.99×10^6	6.3
8	527 (0.65 Y.S.)	3.1×10^6	6.5
9	527 (0.65 Y.S.)	5.01×10^6	6.7
10	527 (0.65 Y.S.)	7.9×10^6	6.9

Table 4.6: **Life Estimation for Tempering at 200^{0}C, 1½hr**

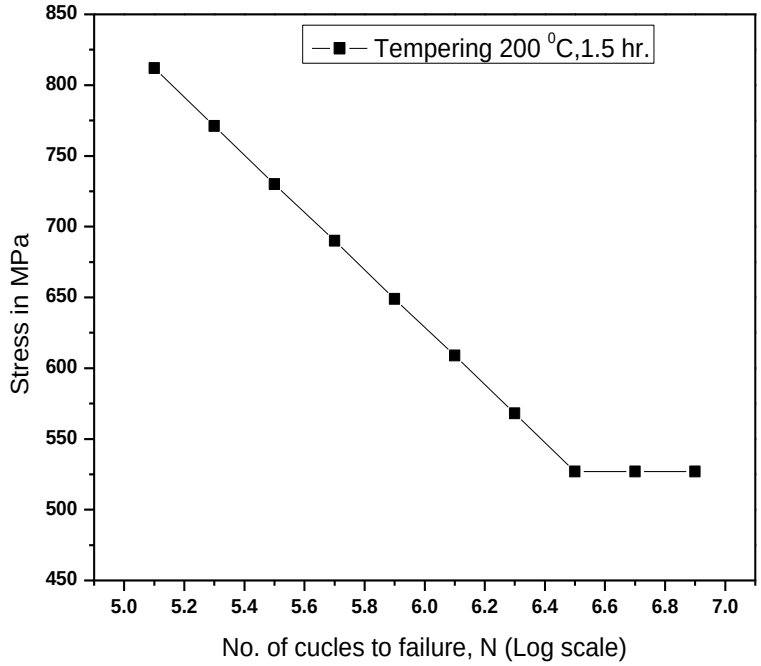

Fig 4.31: **S-N Curve for Tempering at 200 ^{0}C, 1½hr**

Serial no.	Stress in (MPa)	No. of cycles to failure, N	Value of Log N
1	728 (Y.S.)	1.9×10^5	5.3
2	691 (0.95 Y.S.)	3.16×10^5	5.5
3	655 (0.90 Y.S.)	5.01×10^5	5.7
4	619 (0.85 Y.S.)	7.94×10^5	5.9
5	582 (0.80 Y.S.)	1.26×10^6	6.1
6	546 (0.75 Y.S.)	1.99×10^6	6.3
7	510 (0.70 Y.S.)	3.1×10^6	6.5
8	473 (0.65 Y.S.)	5.01×10^6	6.7
9	473 (0.65 Y.S.)	7.9×10^6	6.9
10	473 (0.65 Y.S.)	1.2×10^7	7.1

Table 4.7: **Life Estimation for Tempering at 200 ^{0}C, 2 hr**

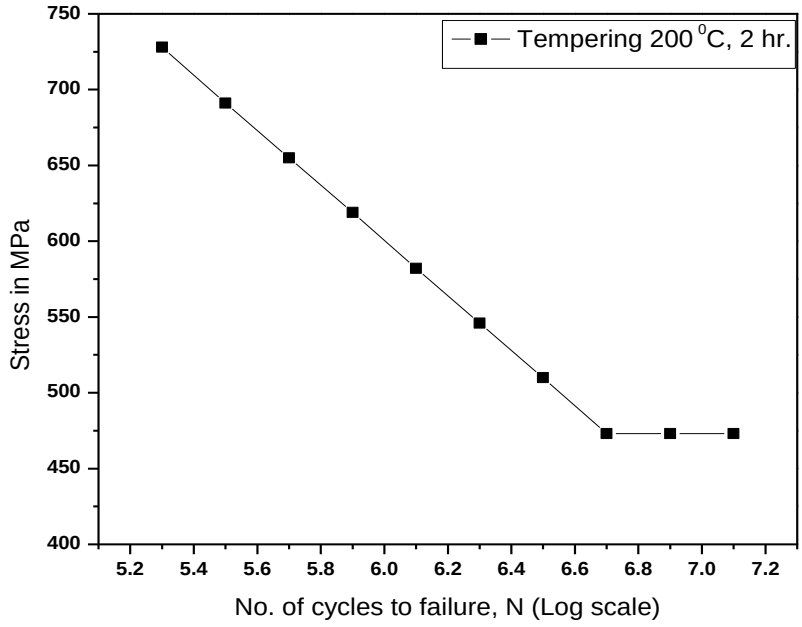

Fig 4.32: **S-N Curve for Tempering at 200^{0}C, 2 hr**

Serial no.	Stress in (MPa)	No. of cycles to failure, N	Value of Log N
1	619 (Y.S.)	2.51×10^5	5.4
2	588 (0.95 Y.S.)	3.98×10^5	5.6
3	557 (0.90 Y.S.)	6.3×10^5	5.8
4	557 (0.90 Y.S.)	1×10^6	6.0
5	557 (0.90 Y.S.)	1.58×10^6	6.2
6	557 (0.90 Y.S.)	2.51×10^6	6.4
7	557 (0.90 Y.S.)	3.98×10^6	6.6
8	557 (0.90 Y.S.)	6.3×10^6	6.8
9	557 (0.90 Y.S.)	1×10^7	7.0
10	557 (0.90 Y.S.)	1.58×10^7	7.2

Table 4.8: **Life Estimation for Tempering at 400 ^{0}C, 1 hr**

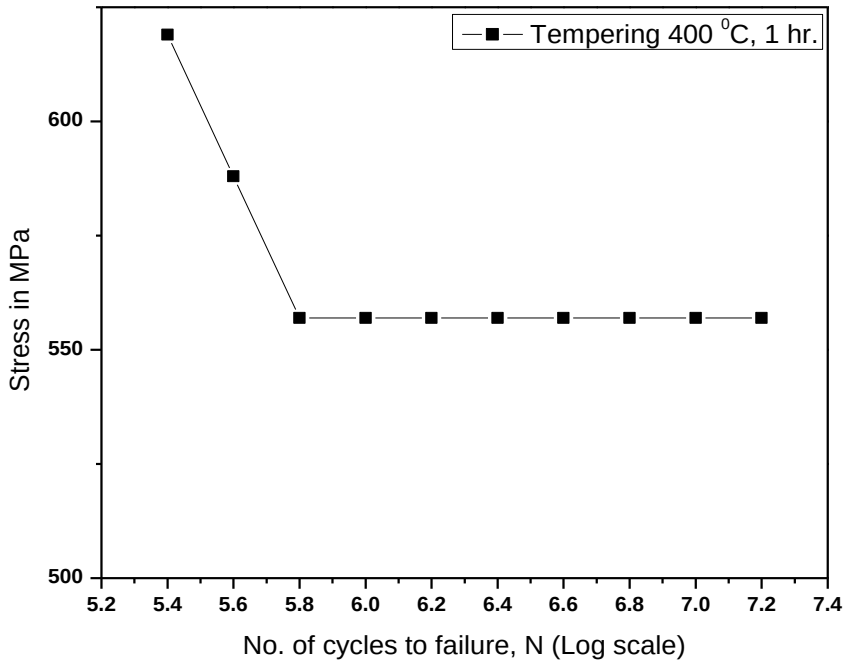

Fig 4.33: **S-N Curve for Tempering at 400 ^{0}C, 1 hr**

Serial no.	Stress in (MPa)	No. of cycles to failure, N	Value of Log N
1	507 (Y.S.)	3.16×10^5	5.5
2	481 (0.95 Y.S.)	5.01×10^5	5.7
3	456 (0.90 Y.S.)	7.94×10^5	5.9
4	430 (0.85 Y.S.)	1.26×10^6	6.1
5	430 (0.85 Y.S.)	1.99×10^6	6.3
6	430 (0.85 Y.S.)	3.1×10^6	6.5
7	430 (0.85 Y.S.)	5.01×10^6	6.7
8	430 (0.85 Y.S.)	7.9×10^6	6.9
9	430 (0.85 Y.S.)	1.2×10^7	7.1
10	430 (0.85 Y.S.)	1.5×10^7	7.2

Table 4.9: **Life Estimation for Tempering at 400 ^{0}C, 1½ hr.**

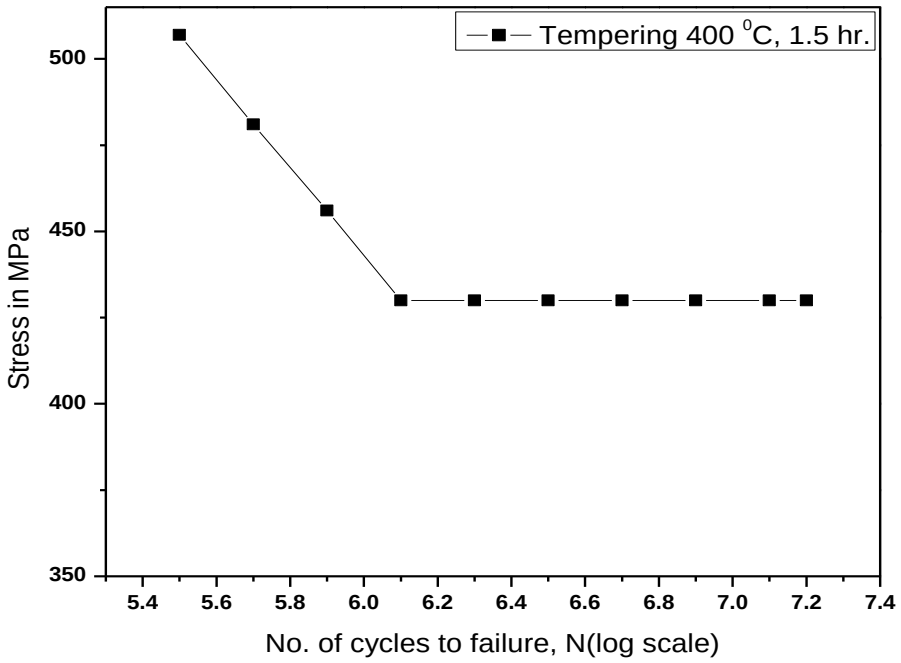

Fig 4.34: **S-N Curve for Tempering at 400^{0}C, 1½ hr**

Serial no.	Stress in (MPa)	No. of cycles to failure, N	Value of Log N
1	465 (Y.S.)	3.98×10^5	5.6
2	441 (0.95 Y.S.)	6.3×10^5	5.8
3	418 (0.90 Y.S.)	1×10^6	6.0
4	395 (0.85 Y.S.)	1.6×10^6	6.2
5	395 (0.85 Y.S.)	2.5×10^6	6.4
6	395 (0.85 Y.S.)	3.98×10^6	6.6
7	395 (0.85 Y.S.)	6.3×10^6	6.8
8	395 (0.85 Y.S.)	1×10^7	7.0
9	395 (0.85 Y.S.)	1.58×10^7	7.2
10	395 (0.85 Y.S.)	2.51×10^5	7.4

Table 4.10: **Life Estimation for Tempering at 400 ^{0}C, 2 hr**

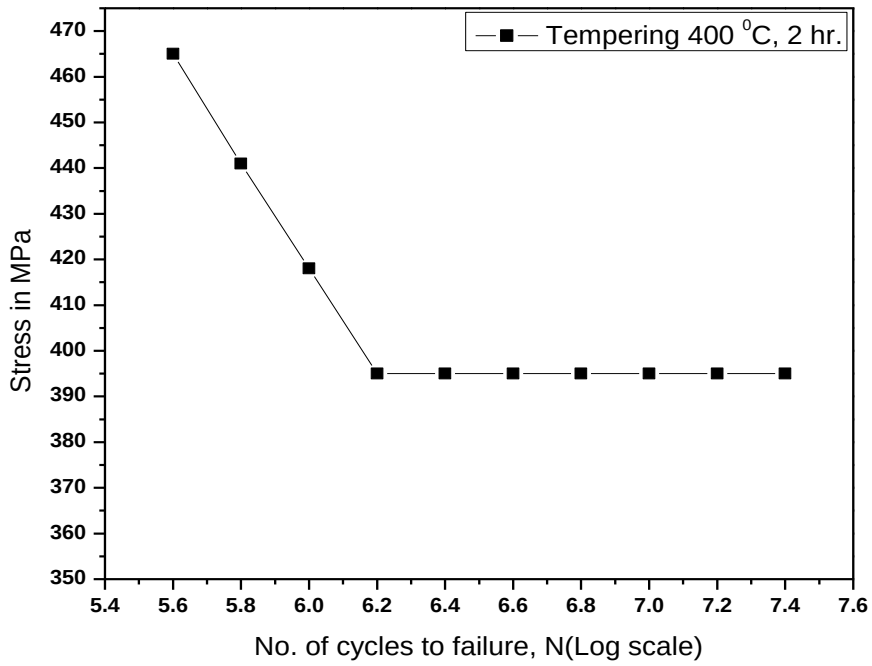

Fig 4.35: **S-N Curve for Tempering at 400 ^{0}C, 2 hr.**

Serial no.	Stress inMPa	No. of cycles to failure, N	Value of Log N
1	741 (Y.S.)	1.25×10^5	5.1
2	704 (0.95 Y.S.)	1.9×10^5	5.3
3	667 (0.90 Y.S.)	3.16×10^5	5.5
4	629 (0.85 Y.S.)	5.01×10^5	5.7
5	592 (0.80 Y.S.)	7.94×10^5	5.9
6	555 (0.75 Y.S.)	1.26×10^6	6.1
7	518 (0.70 Y.S.)	1.99×10^6	6.3
8	518 (0.70 Y.S.)	3.1×10^6	6.5
9	518 (0.70 Y.S.)	5.01×10^6	6.7
10	518 (0.70 Y.S.)	7.9×10^6	6.9

Table 4.11: **Life Estimation for Tempering at 600 ^{0}C, 1 hr**

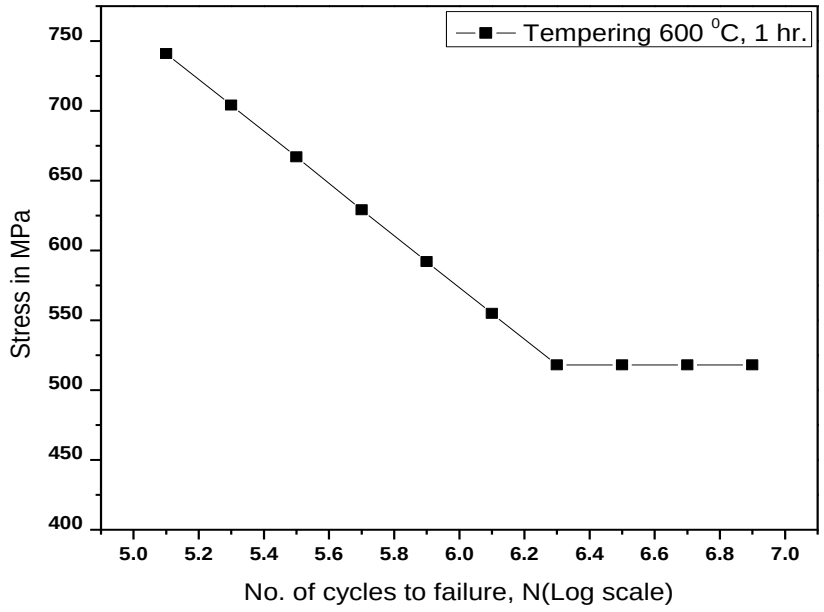

Fig 4.36: **S-N Curve for Tempering at 600 ^{0}C, 1 hr.**

Serial no.	Stress in (MPa)	No. of cycles to failure, N	Value of Log N
1	623 (Y.S.)	1.25×10^5	5.3
2	592 (0.95 Y.S.)	1.9×10^5	5.5
3	561 (0.90 Y.S.)	3.16×10^5	5.7
4	529 (0.85 Y.S.)	5.01×10^5	5.9
5	498 (0.80 Y.S.)	1.25×10^6	6.1
6	467 (0.75 Y.S.)	1.99×10^6	6.3
7	436 (0.70 Y.S.)	3.16×10^6	6.5
8	405 (0.65 Y.S.)	5.01×10^6	6.7
9	405 (0.65 Y.S.)	7.94×10^6	6.9
10	405 (0.65 Y.S.)	1.25×10^7	7.1

Table 4.12: **Life Estimation for Tempering at 600^{0}C, 1½ hr**

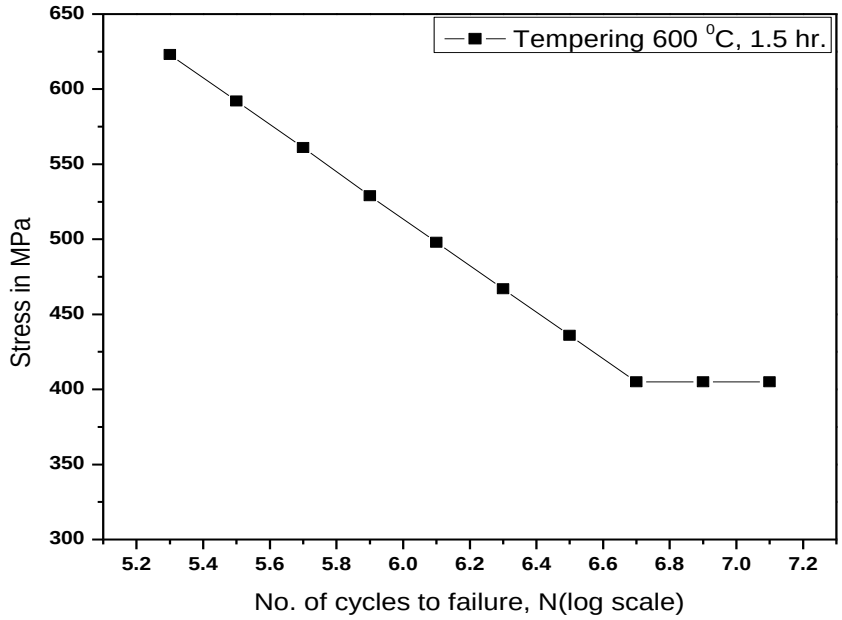

Fig 4.37: **S-N Curve for Tempering at 600 ^{0}C, 1½ hr**

Serial no.	Stress in (MPa)	No. of cycles to failure, N	Value of Log N
1	618 (Y.S.)	3.98×10^5	5.6
2	587 (0.95 Y.S.)	5.01×10^5	5.7
3	556 (0.90 Y.S.)	6.3×10^5	5.8
4	525 (0.85 Y.S.)	7.94×10^5	5.9
5	494 (0.80 Y.S.)	1×10^6	6.0
6	465 (0.75 Y.S.)	1.26×10^6	6.1
7	434 (0.70 Y.S.)	1.58×10^6	6.2
8	400 (0.65 Y.S.)	1.99×10^6	6.3
9	400(0.65 Y.S.)	2.5×10^6	6.4
10	400 (0.65 Y.S.)	3.1×10^6	6.5

Table 4.13: **Life Estimation for Tempering at 600 ^{0}C, 2 hr**

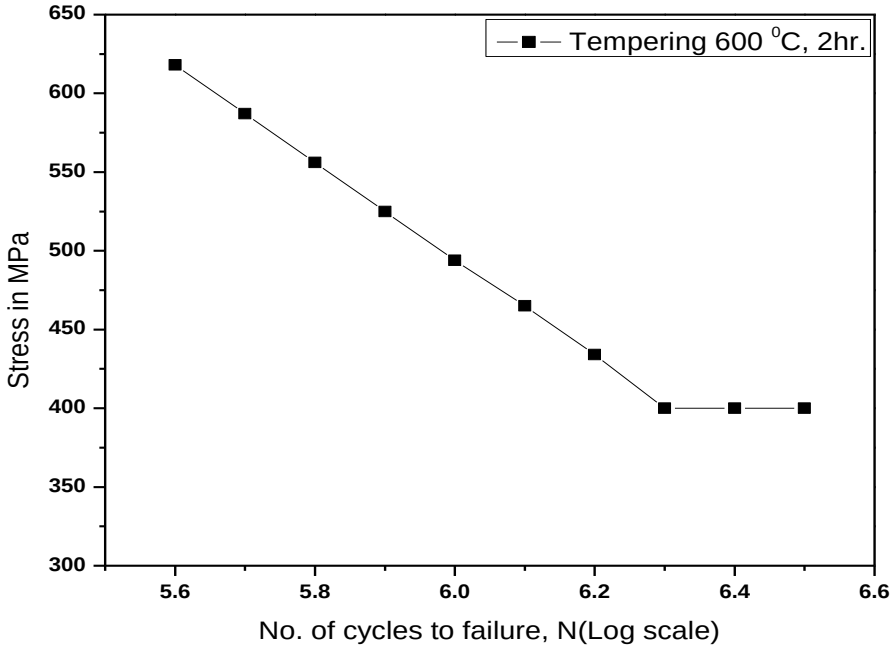

Fig 4.38: **S-N Curve for Tempering at 600 ^{0}C, 2 hr**

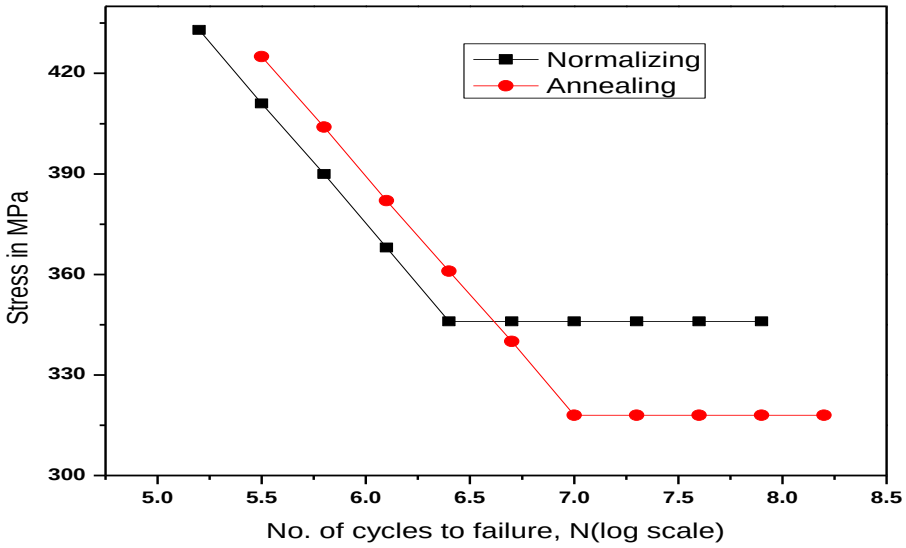

Fig 4.39: **Comparison of S-N Curves between Normalizing and Annealing**

S-N curve presented in Fig 4.39 is used to compare between normalizing and annealing treatment effect; which shows that the endurance limit for normalized steel is higher than that of annealed one. As normalized materials have higher yield stress as compared to annealed one, the endurance limit is also higher than that of annealed one. Here for normalized treatment, fatigue limit comes around 346 MPa for stress level at 2.5×10^6 cycles. But for annealed one, it came 318 MPa at 10^7 no. of cycles.

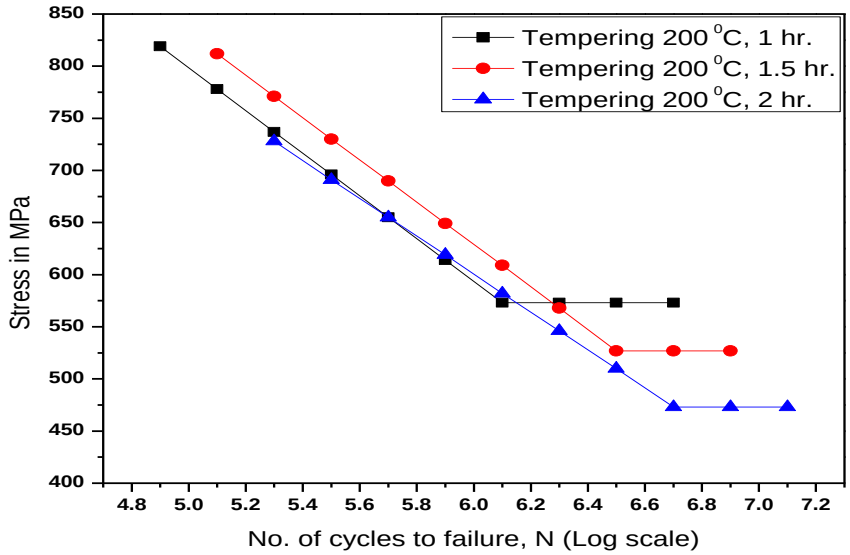

Fig 4.40: **Comparison of S-N Curves of Tempering at 200 ^{0}C at various Time Periods**

In Fig. 4.40, the variation of S-N curve will be analyzed for tempering at 200 ^{0}C. The graphical representation well describes the variation of fatigue limit w.r.to time, where with varying time period from 1 hour to 2 hours, the fatigue limits decreases. As shown in Fig 4.40, the fatigue limit for 200 ^{0}C in 1 hr. is 573 MPa, at 10^5 no. of cycles to failure. The lowest fatigue limit of 473 MPa shown here is for 200 ^{0}C in 2hr. which is more than that of the normalized and annealed ones as shown in Fig 4.39, but for the same the no of cycles to failure is more in case of annealed one. Another important change shown here is that the variation from 1 hr to 2 hr is significant. Here from 1 hr to 2 hr fatigue limit changes drastically from 573 MPa to 473 MPa. Fatigue limit comes for 2 hr tempering is at 5.0×10^6 no. of cycles to failure.

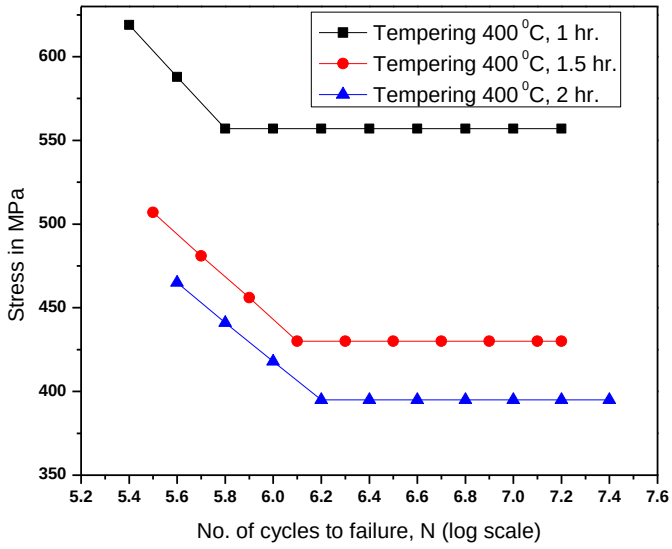

Fig 4.41: **Comparison of S-N Curves of Tempering at 400 ^{0}C at various Time Periods**

From the above Fig. 4.41, we come to the conclusion that the variation of fatigue limit and also the respective cycles are significantly visible for 400 ^{0}C. Fatigue limit of 400 ^{0}C, 1hr is much higher than that of the 1 ½ hr and 2 hr. For 400 ^{0}C 1hr., fatigue limit comes around 557 MPa at 6.0×10^5 no. of cycles. But for 1 ½ hr, it will come around 430 MPa which is less than that of the 1hr tempering at 400 ^{0}C but from 1 ½ hr, when time period changed to 2 hr. there are slight decrement in fatigue limit from 430 MPa to 395 MPa. At 2 hr tempering time for the same temperature the fatigue limit comes at 1.6×10^6 no. of cycles slightly more than that of the 1hr. tempering.

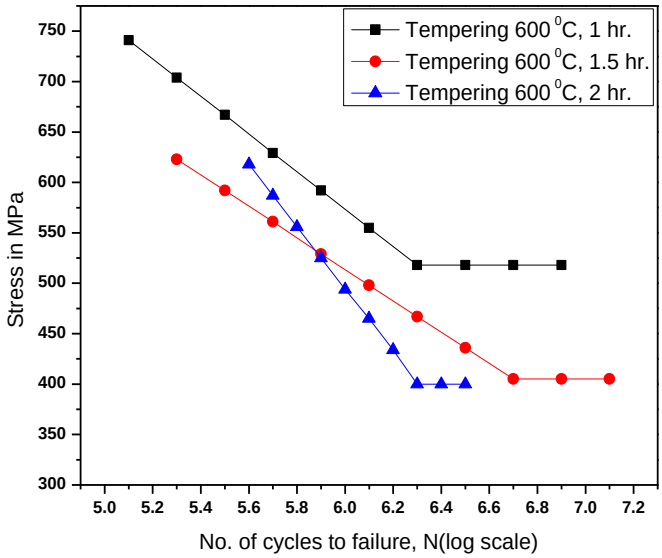

Fig 4.42: **Comparison of S-N Curves of Tempering at 600 ^{0}C at various Time Periods**

For the high temperature tempering the fatigue limits are varied differently as compared to the lower ones which are graphically presented in Fig.4.42. Here, 600 ^{0}C tempering treated specimens are subjected to various time periods from 1 hr. to 2hr. variation of fatigue limit is different as that of 200 ^{0}C and 400 ^{0}C tempering treatments. Highest fatigue limit comes at 1hr tempering treatment for the same temperature i.e. 518 MPa at 2×10^6 no. of cycles. After 1 hr of tempering if we go for higher time periods there is significant decrease in fatigue limit from 518 MPa to 405 MPa which is approximately equal to the fatigue limit value for 2 hr tempering at 600 ^{0}C. The fatigue limit for the time period 1 ½ hr to 2 hr is approximately same. In Fig 4.43 [A], [B] & [C] we can see the variation of fatigue limit w.r.to tempered time and temperature. Here we can see the remarkable variation in fatigue limit from 200 ^{0}C to 600 ^{0}C which follows the normal trend. It is because of variation in tensile stress value from 200 ^{0}C due to the formation of carbide. Here we can see that the variation of fatigue limit depends upon the tensile stress. That's why we get the highest fatigue limit at 200 ^{0}C at 573 MPa for 1.26×10^6 no. of cycles to failure. Some of the fatigue comparison results are also shown in Fig. 4.44 [A] & [B].

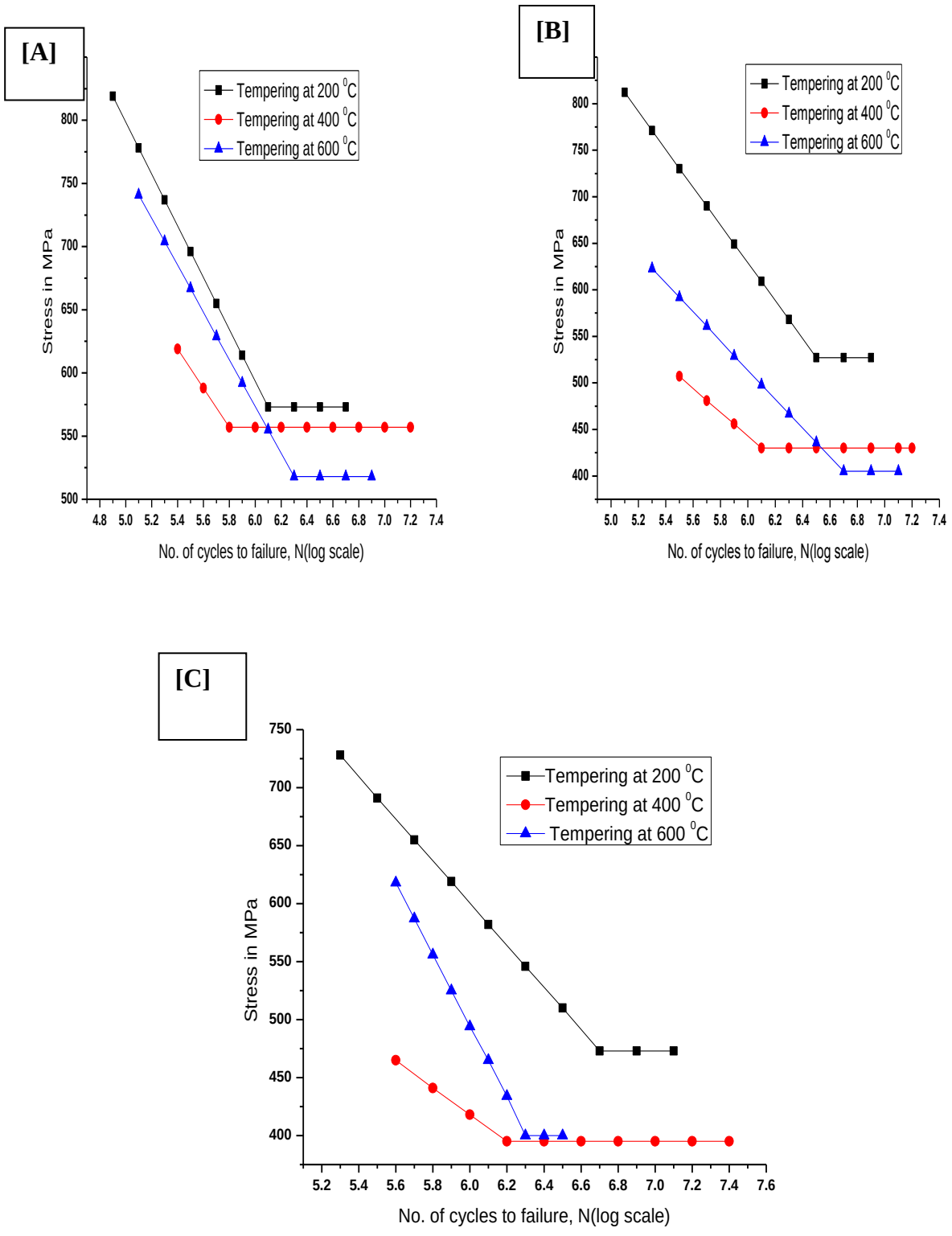

Fig 4.43 [A], [B] & [C]: **Comparison of S-N Curves at various Time Periods w.r.t Temperature**

[A]

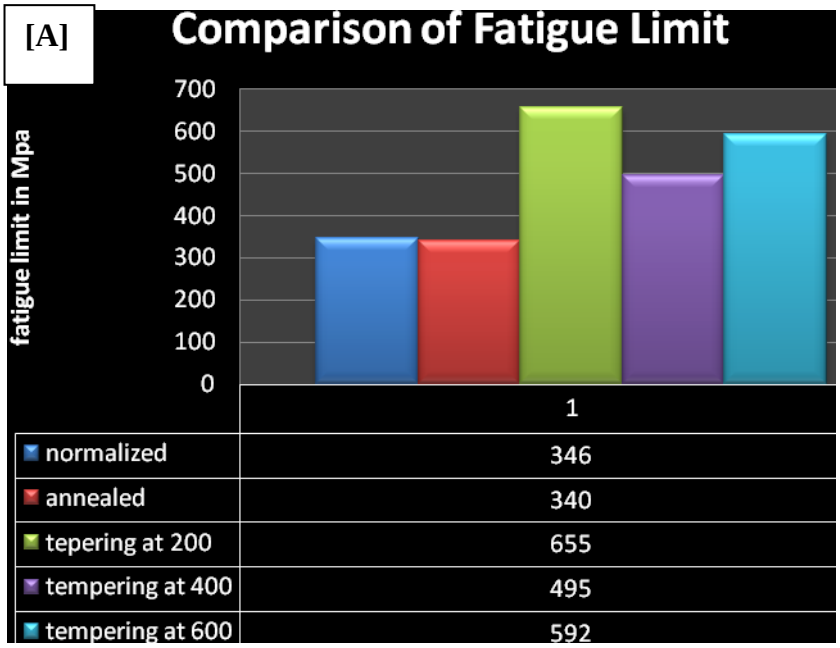

[B]

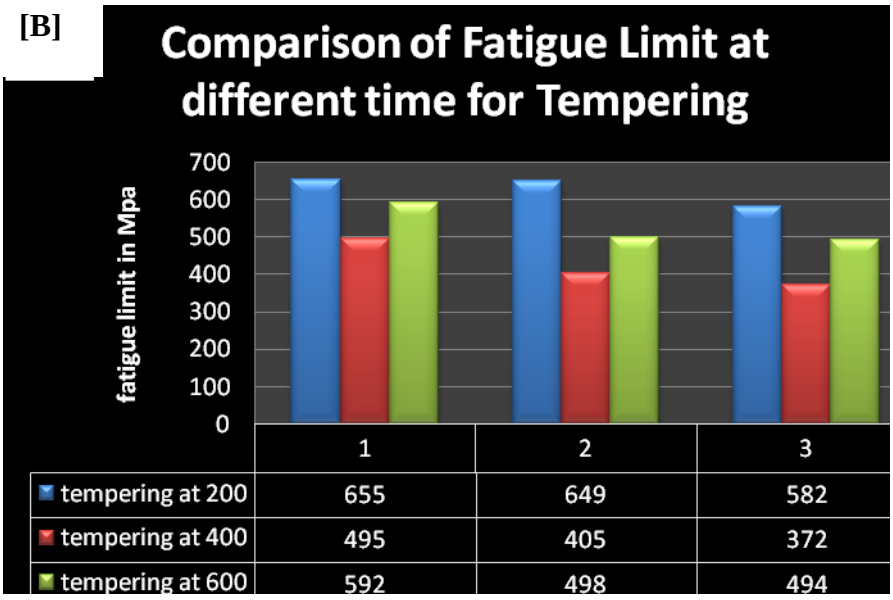

Fig. 4.44 [A] & [B]: **Comparison Graph for Fatigue Limit**

4.6. FRACTOGRAPHS AFTER FATIGUE FAILURE

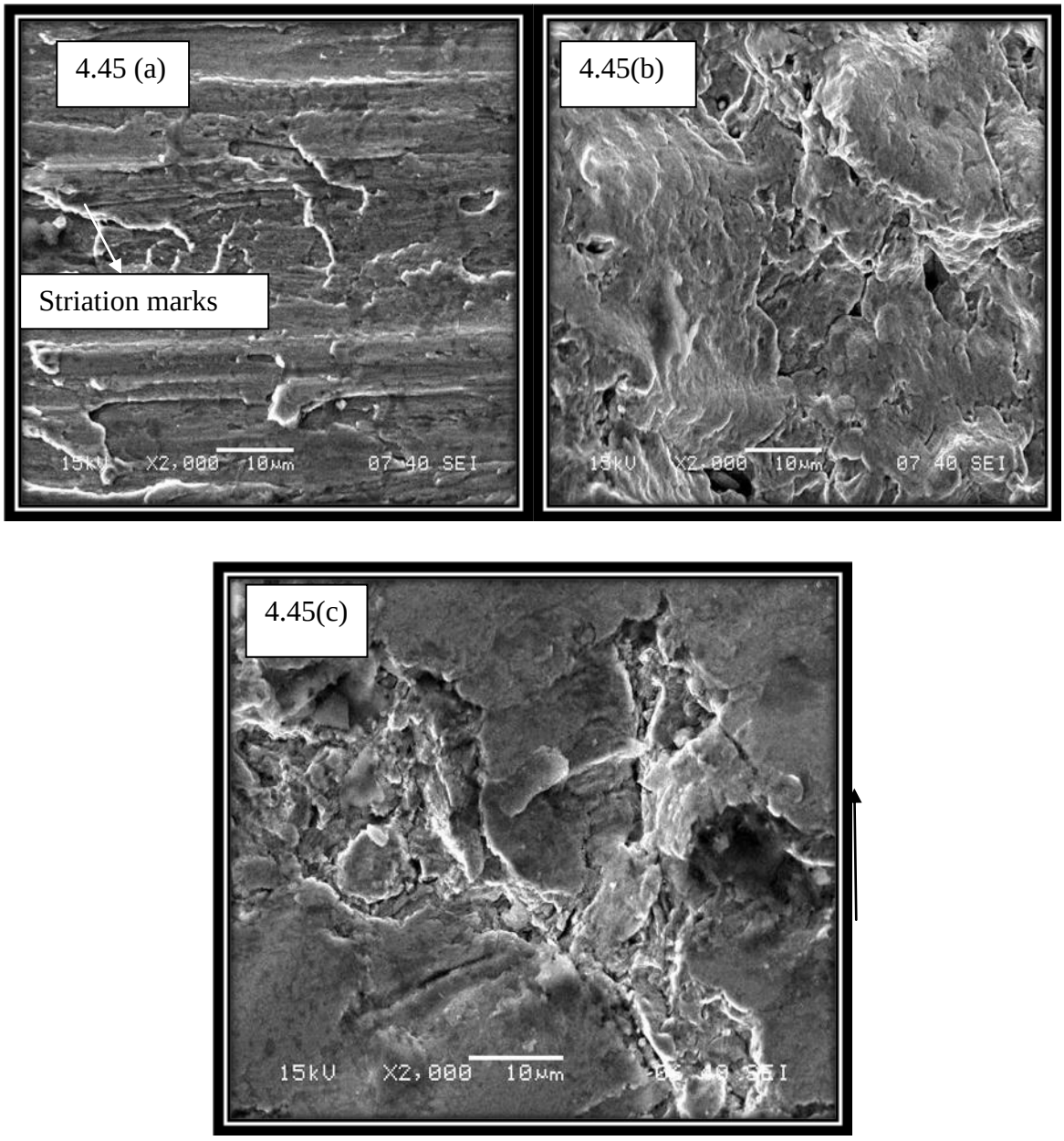

Fig 4.45: **(a), (b) and (c) Fractographs for S-N Curves**

Fracture surfaces of the latest failures of Ck55/EN9 with scanning electron microscope (SEM) are shown in Fig 4.45. The initial crack (~10 µm) forms fracture surface features which are inclined by 45^0 to the principal stress. Saw-tooth-like initial fracture surface is observed, which is better visible in Fig 4.45 (a) fractograph due to the larger ferritic grains presence in the heat treated material. Crack initiation may be considered as stage I, whereas the successive fracture surface is perpendicular to the principal stress (stage II crack growth) is shown in Fig 4.45 (b). The crack initiate at the surface of this material and no interior crack initiation at inclusions, for example was found in Fig 4.44(c). Surfaces of several specimens have been investigated carefully under the SEM to find possible non-

propagating cracks. Studies of fracture surfaces cannot support the assumption that the observed endurance limit is correlated to a non-propagating condition of cracks. From the tensile test fractographs, it is well observed that some dimple like structures are present which describe the material's nature as it is ductile. Some dimple structures are obtained in the post tensile fractographs with nested loops.

Life Estimation by Moore's Fatigue Testing Machine based upon the YS of the specimen gives the results for the samples obtained by various heat treatment processes. Application of various loads as calculated and tabulated in these above tables gives different fatigue limits for different heat treated samples. From these results we come to the following conclusions:

Endurance limit increases with increases in tensile strength. It has been highest 573 MPa for low temperature (200 ^{0}C) tempering. As tensile strength decreases with tempering time, endurance limit also decreases; we can see the changes from Fig 4.40, Fig 4.41 and Fig. 4.42. Endurance limit of normalized steel is higher than that of annealed ones but at a particular stress level (above the endurance limit 346 MPa) cycles required to cause fatigue failure is less for normalized steel. As far as tempered specimens are concerned it has been seen that at a particular temperature the endurance limit decreases with the increase tempering time, highest for 200 ^{0}C at 1 hr. i.e. 573 MPa and lowest for 200 ^{0}C at 2 hr. i.e. 473 MPa. For the other two tempering temperature also the variation of endurance limit will same as that of 200 ^{0}C. For the low temperature tempering the effect of time becomes prominent after 1½ hours and high temperature (600 ^{0}C) the effect is more pronounced for lesser time (1hr.). It has also been found after 1½ hours the effect of time becomes practically insignificant (the endurance limit remains constant). At the intermediate temperature (400 ^{0}C) the effect of time is more significant. There is a sharp fall in the values of endurance limit from 1½ hours to 2 hours of tempering. From above discussions it can be concluded that the micro structural changes as already discussed earlier have a greater impact on fatigue properties. Because, it can be visualized that grain shape/size/structure defers with temperature and heat treatment time. At normalized condition, finer grains (ferrite and pearlite) found as compared to annealed one. In case of tempering, carbide formation takes place and also some ferrite structures are formed which induces both strength and ductility which helps to alter the fatigue properties.

Chapter 5

5. Conclusions and Scope for the Future Work

CONCLUSION & SCOPE FOR FUTURE WORK

5.1. CONCLUSIONS

From this study, it may be concluded that the increase of fatigue strength is directly proportional to increase in tensile strength. The best results are obtained for the specimen tempered at comparatively low temperature (200 ^{0}C). These specimens have also shown the highest endurance limit. This is perhaps due to the fact that these specimen posses vary high strength with significant ductility. So, as far as fatigue strength is concerned, the low temperature tempering may be regarded as the best possible heat treatment operation. Some of the important inference made from this research is as follows:

- All the material of EN9 category failed at high cycle regime.
- Among the heat treatment techniques, tempering has got the most significant effect on fatigue life. The changes caused by normalizing are mainly due to the increase in tensile strength in comparison with annealing.
- Tempering treatment improves fatigue behavior and also other mechanical properties.
- Both tempering time and temperature influences fatigue properties. Best results are obtained for low temperature tempering i.e. for the samples tempered at 200 ^{0}C. It is found that lower the tempering temperature for minimum treatment time, shows better results than treating for longer time. For example, tempering at 200 ^{0}C for 1hr gives the highest UTS and YS values as 978 MPa and 819 MPa and also shows the highest endurance limit at 573 MPa for 5×10^6 cycles.
- It can also be concluded that the material having higher UTS bear higher endurance limits as compared to materials with other treatments.

5.2. SCOPE FOR THE FUTURE WORK

From the results obtained in this work, it may be stated that suitable heat treatments can be performed. In order to improve fatigue resistance since fatigue limit is influenced by heat treatment procedure, it has been found that low temperature tempering gives the highest value of fatigue limit. Further research work may be carried out in this regards and also TEM analysis can be done to know the real mechanism behind the properties variations.

REFERENCES

1. Lakhtin Y.M., Engineering Physical Metallurgy and Heat Treatment. Mir Publ., 1977.
2. Oberg, E., Machinery's Handbook, 25th ed., Industrial Press Inc., 1996.
3. Smith, W.F. and Hashemi, J., Foundations of Materials Science and Engineering, 4th ed., McGraw's - Hill Book, 2006.
4. Oberg, E., Machinery's Handbook, 25th ed., Industrial press Inc., 1996.
5. Avner, S.H., Physical Metallurgy McGraw Hills, 2nd ed., 2008.
6. Singh V., for standard publisher's distributors, Delhi, 2008, pp.417.
7. Lindberg. R.A., Processes and Materials of Manufacture, 2nd ed., Allyn and Bacon, Boston, MD, USA, 1977.
8. Akay S.K., Yazici M., Bayram A., Avinc A., journal of materials processing technology, vol.209, 2009, pp.3358-3365.
9. Bhadeshia H.K.D.H. and Honeycombe R.W.K., steels microstructure and properties, Burlington, USA, Elsevier ltd.
10. Smith, W.F. and Hashemi, J., foundation of materials science and engineering, 4th ed., McGraw's- hill Book, pp 28-36.
11. Honeycombe R.W.K. and Bhadeshia H.K.D.H., Steels, 2nd ed., Butterworth-Heinemann Publishing Ltd. Oxford, U.K. 2000.
12. Rajan T.V; Sharma C.P. and Sharma, A., Heat Treatment Principles and Techniques. Prentice Hall of India Private Limited, New Delhi, 1989.
13. Krauss G., Steels: Heat Treatment and Processing Principles, ASM International, OH, USA, 1989.
14. Jahazi M. and Egbali B., The influence of hot rolling parameters on the microstructure and mechanical properties of anultra-high strength steel. J Mat Pro Tech., vol.103, 2000, pp.276-9.
15. Korda A., Miyashita Y., Mutoh Y. and Sadasue T., Fatigue crack growth behavior in ferritic-pearlitic steels with networked and distributed pearlite structures. Int J Fat., vol.29, 2007, pp. 1140-8.
16. Song P.S., Shieh Y.L., Fracture lifetime of hydrogen-charged AISI 4130 alloy steel under intermittent sustained overloads, Eng Frac. Mech., vol.71, 2004, pp.1577-84.
17. http://www.efunda.com and M. Silverman, personal communication, February 15th, 2007.
18. Dowling N.E., Mechanical behavior of materials, Prentice-hall, 1999.

19. Metals handbook 9th ed., American society for metals, vol.9, 1985.
20. Mamoru O., Yukito T; Hitoshi K. and Yuji F., Development of New Steel Plates for building structural use, Nippon Steel Technical Report, vol.44, 1990. pp.8-15.
21. Kempester M.H.A., Materials for engineers, 3rd ed., Hooder and Stonghton., 1984.
22. Raymond A. and Higgins B., Properties of Engineering Materials. Hooder and Stonghton.
23. Dell K.A., Metallurgy Theory and Practical Textbook, American Technical Society, Chicago, vol.10989, pp. 351-353.
24. Kempster M.H.A., Material for Engineers. Hodder and Stoughton, London, England, 1976, pp.74-75.
25. Krauss G., Repas P.E.(Eds.), Fundamentals of Aging and Tempering in bainitic and Martensitic Steel Products, ISS-AIME, Warrendale, PA, USA,1992.
26. Hehemann R.F., Phase Transformations, ASM, Metals Park. OH, USA, 1970, pp.397–432.
27. Bhadeshia H.K.D.H. and Edmonds D.V., Metall. Trans., vol.10A. 1979.
28. Bhadeshia H.K.D.H., Bainite in Steels. Institute of Materials, Minerals and Mining, London, UK, 1992.
29. Cooman B.C. De (Ed.), TRIP-Aided High Strength Ferrous Alloys. International Conference Proceedings, Technologisch Institute VZW, 2002.
30. Speer J.G. (Ed.), Advanced High-Strength Sheet Steels for Automotive Applications. International Conference Proceedings, AIST, Warrendale, PA, USA, 2004.
31. Bhadeshia H.K.D.H. and Edmonds D.V., Met. Sci. J. vol.17, 1983, pp.411–425.
32. Miihkinen V.T.T. and Edmonds D.V., Mater. Sci. Technol., vol.3, 1987, pp.422–449.
33. Caballero F.G., Bhadeshia H.K.D.H., Mawella K.J.A., Jones D.G. and Brown P., Mater. Sci. Technol., vol.17, 2001, pp.512–522.
34. Dubensky W.J. and Rundman K.B., AFS Trans., vol.64, 1985, pp.389–394.
35. Franetovic V., Shea M.M. and Ryntz E.F., Mater. Sci. Eng., vol.96. 1987, pp.231–245.
36. Darwish N., Elliott R., Mater. Sci. Technol. 9. 1993. pp.572–602.
37. Sidjanin L., Smallman R.E. and Boutorabi S.M., Mater. Sci., vol.10, 1994, pp.711–720.
38. Aranzabel J., Gutierrez I., and Urcola J.J., Mater. Sci. Technol., vol.10, 1994, pp.728–737.
39. Honarbakhsh-Raouf A., and Edmonds D.V., Electron Microscopy, ICEM 14, vol. II, Mater. Sci., 1998, pp.173–174.
40. Ndaliman M. B., An Assessment of Mechanical Properties of Medium Carbon Steel under Different Quenching Media, J.T., vol.10(2), 2006, pp.100-104.

41. Saha A., Mondal D. K., and Maity J., Effect of cyclic heat treatment on microstructure and mechanical properties of 0.6wt% carbon steel. Materials Science and Engineering, vol.527, 2010, pp.4001–4007.
42. Zahid S., Hector P.P., Salam A. & Ahmad J., Effect of different phase proportion of martensite on the mechanical properties of adual phase steel, Journal of Scientific Research, Vol. XXXIX (No. 2), Dec., 2009.
43. Borik F., and Chapman R.D., Trans.Am.Soc.Met., vol.53,1961.
44. Garwood M.F., Zurburg H.H., and Erickson M.A., Interpretation of tests and correlation with service, American society of metals park, Ohio, 1951.
45. Borik F., Chapman R.D., and Jominy W.E., Trans. Am. Soc. Met.,vol.50, 1958, pp.242-257,.
46. Deiter G.E., Mechanical metallurgy, Mc graw hill ltd.,UK, 1988, pp.375,378,379.
47. Metals Handbook., American society for metals, 8th ed., Metals park, Ohio, vol.10, 1975.
48. Khalifa T. A., Effect of Inclusions on the Fatigue Limit of a Heat-Treated Carbon Steel, Materials Science and Engineering A, vol.102, 1988, pp.175-180.
49. Chawla K. K., Mechanical Behavior of Materials, 4th ed., Prentic-Hall Inc., 1998.
50. Hayden H.W., Moffatt W.G., and Wu J., the Structure and Properties of Materials, John Wiley & Sons, vol. 3, 1965.
51. Ewing J.A. and Humfrey J.C.W., The fracture of metals under repeated alternations of stress. Phil Trans Roy Soc., vol.A200, 1903, pp.241–50.
52. Gough H.J., Am. Soc. Test. Mater. Proc., Vol.33, 1933, pp.3-114.
53. Peterson RE., Discussion of a century ago concerns the nature of fatigue, and review of some of the subsequent researches concerning the mechanism of fatigue, In: ASTM Bulletin, American Society for Testing and Materials, vol.164, 1950, pp. 28-36, 50–60.
54. Timoshenko S., Stress concentration in the history of strength of materials, The William M. Murray Lecture. Proc Soc Exp Stress Analysis (SESA), vol.12, 1954, pp.1–12.
55. Hete´nyi M. Handbook of experimental stress analysis, New York: John Wiley, 1950.
56. Mann J.Y., Aircraft fatigue—with particular emphasis on Australian operations and research. In: Proc 12th Symposium of the Int. Committee on Aeronautical Fatigue (ICAF). Centre d'Essais Ae´ronautique de Toulouse; 1983.
57. Schutz W., A history of fatigue, Engg. Fract. Mech., vol.54, 1996, pp.263–300.
58. Smith RA. Fatigue crack growth, 30 years of progress. Pergamon, 1986.
59. Sanfor RJ, editor. Selected papers on foundations of linear elastic fracture mechanics. SEM Classic papers, Vol. CP1, SPIE Milestone series, Vol. MS 137. 1997.

60. Hanewinckel D. and Zenner H., Fatigue strength, a collection of facsimile, Clausthal: Technical University, historical papers until 1950, 1989.
61. Schijve J. Fatigue of structures and materials. Dordrecht, Boston: Kluwer Academic Publ., 2001.
62. Ryder D.A. Some quantitative information obtained from the examination of fatigue fracture surfaces. Roy Aircraft Est., Tech. Note Met., 1958, pp.288.
63. Forsyth P.J.E.., The physical basis of metal fatigue, London, Blackie and Son, 1969.
64. Smith G.C., Proc. R.SOC., London, vol.242A, 1957, pp.189-196.
65. Frosyth P.J.E. and Stubbington C.A., journal inst. Met., vol.83, , 1955-1956, pp.395.
66. Wood W.A., Some basic studies of fatigue in metals, in "Fracture", John Wiley &Sons, Inc., Newyork, 1959.
67. Wood W.A., Bull.Inst.Met., vol.3, Sep.,1955, pp.5-6.
68. Plumbridge W.J. and D.A.Ryder, Metall, Rev., vol.14, 1969.
69. Laird C., Mechanism and Theories of Fatigue, in "Fatigue and microstructureAmerican society for metals, Metals Park, Ohio, 1979, pp.149-203.
70. Laird C., Fatigue Crack Propagation, ASTM Spec. tech. publ., vol.415, 1967, pp.131-168.
71. Bentachfine S., Notch effect in low cycle fatigue. International Journal of Fatigue, vol. 21, 1999, pp.421-430.
72. Ye D.Y., A new approach to the prediction of fatigue notch reduction factor Kf, International Journal of Fatigue, vol.18, 1996, pp.105-109.
73. Noda,N.A., Stress concentration formula useful for all notch shape in a round bar. International Journal of Fatigue, vol.18, 2005, pp.1-13.
74. Filippini,M., Stress gradient calculations at notches. International Journal of Fatigue, vol.22, 2000, pp.397-409.
75. Wang,X.S. and Fan,J.H., SEM online investigation of fatigue crack initiation and propagation in cast magnesium alloy. Journal of Materials Science, vol. 39(7), 2004, pp.2617-2620.
76. Wang,X.S., Feng,X.Q. and Guo,X.W., failure behavior of anodized coating-magnesium alloy substrate structures. Key Engineering Materials, vol.261-263, 2004, pp. 363-368.
77. Xiulin Z., on some basic problems of fatigue research in engineering, International Journal of Fatigue, vol.23, 2001, pp.751–766.
78. Uematsu Y., Akita M. and Nakajima M., Effect of temperature on high cycle fatigue behaviour in 18Cr–2Mo ferritic stainless steel, International Journal of Fatigue, vol.30, Issue 4, Apr., 2008, pp.642–648.

79. Hahnenberger F., Smaga M. and Eifler D., "Fatigue behavior and phase transformation in austenitic steels in the temperature range -60 °C ≤ T ≤ 25 °C", 11th International Conference on the Mechanical Behavior of Materials (ICM11), vol.10, 2011, pp.625–630.
80. Naito T., Ueda H., and Kikuchui M. Fatigue behavior of carburized steel with internal oxides and nonmartensitic micro-structure near the surface. Metal Trans., vol. 15A, 1984; pp.1431–6.
81. Asami K., and Sugiyama Y. Fatigue strength of various surface hardened steels. J Heat Treatment Technol Assoc., vol. 25, 1985; pp.147–50.
82. Murakami Y., Takada M., and Toriyama T., Super-long life tension compression fatigue properties of quenched and tempered 0.46% carbon steel. Int. J. Fatigue, vol.16 (9), 1998, pp.661–7.
83. Sakai T., Takeda M., Shiozawa K., Ochi Y., Nakajima M., Nakamura T., et al. Experimental evidence of duplex S–N characteristics in wide life region for high strength steels. Proceedings of the seventh international fatigue conference, Beijing, China, Beijing,China: Higher Education Press, vol.1, 1999. pp.573–8.
84. Shiozawa K., and Lu L., Very high-cycle fatigue behaviour of shot-peened high-carbon–chromium bearing steel. Fatigue Fract. Eng. Mater. Struct., vol.25, 2002, pp.813–22.
85. Tanaka K. and Akiniwa Y., Fatigue crack propagation behaviour derived from S–N data in very high cycle regime. Fatigue Fract Eng Mater Struct. vol.25, 2002, pp.775–84.
86. Ochi Y, Matsumura T, Masaki K. and Yoshida S., High-cycle rotating bending fatigue property in very long life regime of high-strength steel. Fatigue Fract. Eng. Mat. Struct., vol.25, 2002, pp.823–30.
87. Klesnil M. and Luka ´s P., Fatigue softening and hardening of annealed low-carbon steel. J Iron Steel Inst., vol.205, 1967, pp.746.
88. Mughrabi H., Herz K., Stark X., Cyclic deformation and fatigue behaviour of a-iron mono- and polycrystals. Int J Fract., vol.17 (2), 1981, pp.193–220.
89. Eifler D., and Macherauch E., Microstructure and cyclic deformation behaviour of plain carbon and low alloy steels. Int. J. Fatigue, vol.12 (3), 1990, pp.165–74.
90. Lukas P., and Kunz L., Specific features of high-cycle and ultra-high-cycle fatigue. Fatigue Fract Eng Mater Struct, vol.25, 2002, pp.747–53.
91. Alp T., and Wazzan A., The influence of microstructure on the tensile and fatigue behavior of SAE 6150 Steel, 2002, pp.351-359.
92. Bayram A., Uguz A., and Ula M., Effect of microstructure and notches on the mechanical properties of dual-phase steels, mater. Charact, vol.43, 1999, pp.259-269.

93. Durmus A., and Bayram A., An investigation on the tensile and abrasive wear properties of plain carbon dual-phase steels., 2004, pp.571-576.
94. Zheng X.L., Quantitative theory of metal fatigue. Xi'an: Publishing House of Northwestern Polytechnical University (NPU), 1994.
95. Tavernelli, J. F. and Coffin, L. F., Experimental support for generalized equation predicting low cycle fatigue, Journal of Basic Engineering, Transactions of the ASME, vol.84, 1962, pp.533-537.
96. Paris, P. C., A critical analysis of crack propagation laws. Journal of Basic Engineering, vol..85, 1963, pp.528-534.
97. Neuber, H., Theory of concentration for shear strained prismatical bodies with arbitrary nonlinear stressstrain law. Journal of Applied Mechanics, vol.28, 1961, pp.544-550.
98. Dowling,N.E., Fatigue at notches and the local strain fracture mechanics approaches. ASTM STP, vol. 677, 1979, pp. 247-273.
99. Zheng X.L., Quantitative theory of metal fatigue. Xi'an: Publishing House of Northwestern Polytechnical University (NPU), 1994.
100. Zhao MP., Handbook of strain fatigue analysis. Beijing: Publishing House of Science, 1988.
101. Kim Y.H., Speaker S.M., Gordon D.E, Manning S.D., Wei R.P., Development of fatigue and crack propagation design and analysis methodology in a corrosive environment for typical mechanically-fastened joints. In: Report NO. NADC-83126-60, vol.1 (AD-A136414), 1983.
102. Kim Y.H., Speaker S.M., Gordon D.E., Manning S.D., and Wei R.P., Development of fatigue and crack propagation design and analysis methodology in a corrosive environment for typical mechanically-fastened joints (assessment of art state). In: Report Nol NADC-83126-60, vol.2 (AD-A136415), 1983.
103. Wanhill R.J.H., De Luccia J.J., Russo M.T., The fatigue in aircraft corrosion testing (FACT) programme. In: AGARD Report No.713 (AD-A208-359), 1989.
104. Buch A. Prediction of fatigue life under aircraft loading with and without use of material memory rules. Int J Fatigue, vol.11 (2), 1989, pp.97–106.
105. Dupart D., Davy A., Boetsch R., and Boudet R., Fatigue damage calculation in stress concentration fields under uniaxial stress. Int. J Fatigue, vol.18 (4), 1996, pp.245–53.
106. Schutz W., The prediction of fatigue life in the crack initiation and propagation stages a state of the art survey. Eng. Fract. Mech., vol.11 (3), 1979, pp.405–21.
107. Laz P.J., Craig B.A., Rohrbaugh S.M., and Hillberry B.M., The development of a total fatigue life approach accounting for nucleation and propagation. In: Proceedings of the 7th International Fatigue Congress, FATIGUE '99, Beijing, High Education Press, EMAS, 1999, pp.833–8.

108. Nowack H. Development in variable amplitude prediction methods for light weight structures. In: Proceedings of the 7th International Fatigue Congress, FATIGUE '99, Beijing, High Education Press, EMAS, 1999, pp.991–1000.
109. Bannantine JA, Comer JJ, Handrock JL. Fundamentals of metal fatigue analysis. New Jersey: Prentice-Hall, 1990.
110. Murakami Y, Endo M. Effects of defects, inclusions and in homogeneities on fatigue-strength. Int J Fatigue, vol.16 (3), 1994, pp.163–82.
111. Murakami Y., Kodama S, Konuma S. Quantitative evaluation of effects of non-metallic inclusions on fatigue strength of high strength steels. I: Basic fatigue mechanism and evaluation of correlation between the fatigue fracture stress and the size and location of nonmetallic inclusions. Int J Fatigue, vol.11(5), 1989 , pp.291–8.
112. Li,Y.T., Rui,Z.Y. and Yan,C.F., The applied research of fracture for low carbon steel in extra-low cycle rotating bending fatigue. Key Engineering Materials, vol.271-272, 2004, pp.211-216.
113. Li,Y.T., The application of fracture for medium carbon steel in extra-low cycle inverse rotating bending fatigue loading. Key Engineering Materials, vol. 261-263, 2004, pp.1147-1152.
114. Li,Y.T., The application of fracture for medium carbon steel in extra-low cycle rotating bending fatigue loading. Key Engineering Materials, vol.261-263, 2004, pp.1153-1158.
115. Youtang Li, Shuai Tan, Hongyan Duan, Investigation of fracture design for medium carbon steel under extra-low cyclic fatigue inaxial loading, Acta Mechanica Solida Sinica, vol.21(4), Aug., 2008.
116. Pyttel B., Schwerdt D., Berge C., Very high cycle fatigue – Is there a fatigue limit?, International Journal of Fatigue xxx (2010) xxx–xxx.
117. Somer M. Nacy, Member, IAENG ,Effect of Heat Treatment on Fatigue Behavior of (A193-51T-B7) Alloy Steel, Proceedings of the World Congress on Engineering 2007 WCE 2007, July 2-4, London,U.K., vol.2, 2007.
118. Zettl B., Mayer H., Ede C., Stanzl-Tschegg S., Very high cycle fatigue of normalized carbon steels, International Journal of Fatigue, vol.28, 2006, pp.1583–1589.
119. De Los Rios ER, Mohamed HJ, Miller KJ. A micro-mechanics analysis for short fatigue crack growth. Fatigue Fract Eng Mater Struct., vol.8(1), 1985, pp.49–63.
120. Miller KJ, Mohamed HJ, De Los Rios ER. Fatigue damage accumulation above and below the fatigue limit. In: Miller KJ, De Los Rios ER, editors. The behaviour of short fatigue cracks. ECF Pub 1, Mech Eng Pub, London; 1986.
121. Miller KJ, O'Donnell WJ. The fatigue limit and its elimination. Fatigue Fract Eng Mater Struct., vol.22, 1999, pp.545–57.

122. Atanu Sahaa, Dipak Kumar Mondal, Joydeep Maity, Effect of cyclic heat treatment on microstructure and mechanical properties of 0.6wt% carbon steel. Materials Science and Engineering, vol.527(A), 2010, pp.4001–4007.
123. Chakraborti P.C., Mitra M.K., Microstructural response on the room temperature low cycle fatigue behavior of two high strength duplex ferritic- martensitic steels and a normalized ferrite-pearlite steel, international journal of fatigue, march 2006, pp.194-202.
124. Wagner V., Starke P., Kerscher E., Eifler D., Cyclic deformation behaviour of railway wheel steels in the very high cycle fatigue (VHCF) regime, International Journal of Fatigue January 2011,pp. 69–74.
125. Murakami Y., Miller K.J., What is fatigue damage? A view point from the observation of low cycle fatigue process, International Journal of Fatigue, vol.27, 2005, pp. 991–1005.
126. Ali.Rashidi M. and Moshrefi-Torbati M.; Effect of tempering conditions on the mechanical properties of ductile cast iron with dual matrix structure (DMS). Material Letters, vol. 45, Issue 3-4,Sep., 2000, pp. 203-207.
127. Olivera. E., Jovanovic M., et.al, The austempering study of alloyed ductile iron, Materials and Design, Vol.27, 2006, pp.617–622.
128. Putatunda Susil K., Kesani S., et.al.; Development of austenite free ADI (austempered ductile cast iron), Materials Science and Engineering A, July, 2006, pp. 112–122.